Robust and Resilient Control Design and Performance Analysis for Uncertain Systems with Finite Energy Disturbances

Fan Feng
Marquette University

ROBUST AND RESILIENT CONTROL DESIGN AND PERFORMANCE ANALYSIS FOR UNCERTAIN SYSTEMS WITH FINITE ENERGY DISTURBANCES

by

Fan Feng, B.S., M.S.

A Dissertation submitted to the Faculty of the Graduate School,
Marquette University,
in Partial Fulfillment of the Requirements for
the Degree of Doctor of Philosophy

Milwaukee, Wisconsin
August 2016

ABSTRACT
ROBUST AND RESILIENT CONTROL DESIGN AND PERFORMANCE ANALYSIS FOR UNCERTAIN SYSTEMS WITH FINITE ENERGY DISTURBANCES

Fan Feng

Marquette University, 2016

This dissertation addresses the problem of robust and resilient control design with additional performance analysis for uncertain systems with finite energy disturbances. The control design is robust and resilient in the sense of maintaining certain performance criteria in the presence of perturbations in both system parameters and feedback gains. The performance analysis evaluates resilience properties of state feedback and dynamic (state estimate) feedback controllers.

A resilient and robust state feedback controller is designed using linear matrix inequality (LMI) techniques for the characterization of solutions to the analysis and design problems posed in this work. Uncertainties are allowed in the linear and nonlinear parts of the system model and also in the feedback gain so that the designed controller is robust in addition to being resilient. The design of controllers for various performance criteria including asymptotic stability, H_2, H_∞, input strict passivity, output strict passivity and very strict passivity are presented.

In addition to the design problem, an approach is presented for performance analysis of the resilience property of perturbed controller and observer gains. The resilience property is defined in terms of both multiplicative and additive perturbations on the gains so that the closed loop eigenvalues do not leave a specified region in the complex plane, such as a vertical strip, disk, sector region, etc. The method presented allows maximum gain perturbation bounds to be obtained based on the designer's choices of controller eigenvalue region. The LMI technique is used also for the analysis process.

Both design and analysis problems are treated using Lyapunov functions. All work is conducted for both continuous- and discrete-time cases. Several illustrative simulation examples are included to show the effectiveness of the proposed design and analysis approaches.

ACKNOWLEDGEMENT

It is my great fortune to have Dr. Edwin Yaz and Dr. Susan Schneider as my co-advisers. All the work presented in this dissertation and in my academic career so far would not be possible without their help and support in the past a few years.

I would like to say “thank you” to my parents Dr. Jiansheng Feng and Nianhong Wan, for their love and care. I’m grateful for the spiritual and financial support they offered in years.

Besides my co-advisers, it is an honor to have Dr. James Heinen, Dr. Yvonne Yaz and Dr. Chung Seop Jeong on my committee. Dr. James Heinen gave me great advice and suggestions and Dr. Yvonne Yaz showed great support to me while we had papers published together. Dr. Chung Seop Jeong helped me to start from scratch working with LMIs and mathematical software, when I joined our research group.

I would like to thank my friend and research group-mate Dr. Jennifer Bonniwell for helping and giving suggestions on my dissertation and many of my publications. You are going to be a great professor.

I wish my paternal grandparents, who passed away during my study, to have a good life in heaven. And I wish my maternal grandparents to be healthy and happy. Unlike my mother, you never put any pressure on me, but the fact that all your graduate students seem smarter and working harder than me is like a hundred tons of load on me.

This is an end of an era, I wish I can have a good career, marry and have kids soon, and live a happy life with a fairy tale ending.

TABLE OF CONTENTS

LIST OF FIGURES

CHAPTER 1

INTRODUCTION

1.1 Statement of the Problem

This dissertation addresses the problems of robust and resilient control design for general performance criteria [1] and performance analysis for uncertain systems with finite energy disturbances. A robust controller is used to accommodate uncertainties in the system parameter while a resilient controller is used to tolerate perturbations in the feedback gain. The same resilient control design method can also be used in state estimate controller or observer design. Meanwhile, analysis work on the post-design controllers is important. System performance including settling time, rise time, percentage overshoot, etc., are some of the key factors of a design [2]. Therefore, analysis work of the system performance in the presence of the perturbations in the designed gain has been raised as a critical problem. Linear matrix inequality (LMI) techniques are used throughout the design and analysis process.

1.1.1 Background of Robust Control

For uncertainties or perturbations that may cause changes in system parameters, it is customary to use the approach of robust controller design. The controller is designed to work effectively with certain variables unknown but bounded, such as system parameter perturbations. The theory of robust control began in the late 1970s and early 1980s and soon became a popular topic [3]. Several results in the 90's and especially with applications to robust control and filtering can be found in [4]-[8]. Various of techniques for dealing with bounded system uncertainty were developed in the past a few years and the topic and its applications are still popular today. In particular, [9] and [10] are robust control of time-delay systems, [11] and [12] treat switched systems, [13] considers mixed criteria control and [14] and [15] address singular systems. Fault tolerant control for systems with time-varying delays is discussed in [16]; [17] focuses on the resilient control of networked systems and [18] on discrete-time sliding mode control. A mixed criteria finite time control design is presented in [19] and [20] considers H_2/H_∞ control for systems in the state-dependent nonlinear form.

1.1.2 Background of Resilient Control

A controller for which significant performance deterioration occurs due to a small perturbation in the controller gain is referred to as a "fragile" or "non-resilient" controller [21]. An example of such a perturbation would be numerical round off errors when computing the gains which might occur when implementing controllers and observers with microprocessors. In some other situations, manual tuning of the controller gains may be required to obtain the best performance. Thus, it is desirable to design a resilient controller that will have some tolerance to a change/readjustment and perturbations of the control gain.

The resilient control problem became a popular research topic in the 1990s. Some design methods, including LMIs, have been used in resilient control [22]-[24]. Additional work on resilient control or "non-fragile" systems can also be found in [25]-[32]. In particular, reference [25] focuses on resilient state-feedback with H_∞ using LMI. General criteria discrete-time resilient observer design is addressed in [26], while [27] considers the stochastic resilience problem for observers. Resilient control of networked systems is the focus of [28], while resilient control from a multi-agent dynamic systems perspective is considered in [29]. Resilient control theory is also applied to some cutting-edge technologies in practice in the past several years: [30] gives an overview of some examples and benchmark aspects, [31] integrates resilient control into nuclear power plants which requires significant precision and [32] uses resilient control in serial manufacturing networks.

1.2 Summary of the Main Contributions and Outline of the Dissertation

This dissertation is concerned with robust control design problems with a higher degree of uncertainty comparing to the existing problems in the sense of not only having the bounded uncertain or unknown variables but also having perturbations on the bounds themselves. In addition to the robust and resilient controller design problem, a procedure to analyze the resilience properties associated with system performance is proposed.

Chapter 1 presents the introduction, background information, notation and mathematical preliminaries. Chapter 2 presents a state feedback control design for continuous time nonlinear systems with conic type nonlinearities and finite energy disturbances in the case of uncertainties in the center and boundary of the sector in which the nonlinearity resides. General performance criteria including H_2, H_∞, output passivity, etc. are considered. Chapter 3 is the discrete counterpart of chapter 2. Chapter 4 presents a procedure for performance analysis of the resilience property of continuous- time systems with state feedback controllers. The resilience property is defined in terms of both multiplicative and additive perturbations on the controller gain that will maintain controller eigenvalues in a specified region in the complex plane. Chapter 5 is the discrete counterpart of chapter 4. Chapter 6 is an extension of Chapter 4 where a state estimate feedback controller is discussed. Therefore, the resilience property is considered on both the controller and the observer. Chapter 7 is the discrete counterpart of chapter 6. Conclusions and future work are given in Chapter 8.

1.3 Notation

The following notation is used in this work:

$\in$: Belongs to

$x \in R^n$: n-dimensional vector with real elements

$\|x\|$: The Euclidean norm of x, $(x^T x)^{1/2}$

$\dot{x} = \dfrac{dx}{dt}$: Derivative of vector x with respect to time

$A \in R^{n \times m}$: $n \times m$ matrix with real elements

$A > 0 (A < 0)$: A is a positive (negative) definite matrix

$A \geq 0 (A \leq 0)$: A is a positive (negative) semi-definite matrix

A^T : Transpose of matrix A

A^{-1}: Inverse of matrix A

I_m : Identity matrix of dimension m

$\lambda_{\min}(A)$ $(\lambda_{\max}(A))$: The minimum (maximum) eigenvalue of the symmetric matrix A

L_2 : The space of all real-valued continuous-time functions with finite energy, i.e. $w \in L_2$ means $\int_0^\infty \|w(t)\|^2 dt < \infty$

l_2 : The space of all real-valued discrete-time vector sequences with finite energy, i.e. $w \in l_2$ means $\sum_{k=0}^{\infty} \|w_k\|^2 < \infty$

$*$ in matrix $A = \begin{bmatrix} s_{11} & & s_{ij(i<j)} \\ & \ddots & \\ & & \ddots \\ * & & \\ & & s_{ii} \end{bmatrix}$ denotes the transpose of the upper triangular part, ${s_{ij(i<j)}}^T$, of the symmetric matrix A.

1.4 Mathematical Preliminaries

The following lemmas will be used in the derivation for the different problems considered in the dissertation:

Lemma 1. Schur complement.

The following are equivalent, for matrices *A, B, C* of appropriate dimensions:

(a) $\begin{bmatrix} A & B \\ B^T & C \end{bmatrix} > 0$

(b) $C > 0$ & $A - BC^{-1}B^T > 0$

(c) $A > 0$ & $C - B^T A^{-1} B > 0$

Lemma 2.

$-(A^T M^{-1} A + B^T M B) \le A^T B + B^T A \le A^T N^{-1} A + B^T N B$ is true for any positive definite symmetric matrices $M, N > 0$.

And for a scalar special case:

$-(\alpha^{-1} A^T A + \alpha B^T B) \le A^T B + B^T A \le \beta^{-1} A^T A + \beta B^T B$ is true for any scalar $\alpha, \beta > 0$.

Lemma 3. Rayleigh's inequality

For a symmetric matrix P, the following is true

$\lambda_{\min}(P)\|x\|^2 \le x^T P x \le \lambda_{\max}(P)\|x\|^2$

Lemma 4.

$\lambda_{\max}(A^T A) = \lambda_{\max}(A A^T)$ for any matrix A.

1.5 Performance Criteria Definitions

In this section, the continuous- and discrete-time performance criteria are introduced.

1.5.1 Continuous-time System Performance Criteria

For control and stability problems, it is common to start the design or analysis with the Lyapunov energy function $V = x^T P x$ where $P > 0$. In order to achieve stability, the energy of the system needs to be decreasing in time, which means

$$\dot{V} < 0 \tag{1.5-1}$$

By incorporating the additional terms in the Lyapunov equation as

$$-\dot{V} - \delta\|z\|^2 - \varepsilon\|w\|^2 + \beta z^T w > 0 \tag{1.5-2}$$

where *z* is the performance output and *w* is the finite energy disturbance, it is possible to design controllers for various performance criteria in a unified framework.

Notice that upon integration, inequality (1.5-2) yields

$$x(t)^T Px(t) < x(0)^T Px(0) - \int_0^t (\delta\|z(\tau)\|^2 + \varepsilon\|w(\tau)\|^2 - \beta z(\tau)^T w(\tau))d\tau \tag{1.5-3}$$

by using Lemma 3, we obtain,

$$\lambda_{\min}(P)\|x(t)\|^2 < \lambda_{\max}(P)\|x(0)\|^2 - \int_0^t (\delta\|z(\tau)\|^2 + \varepsilon\|w(\tau)\|^2 - \beta z(\tau)^T w(\tau))d\tau \tag{1.5-4}$$

that allows several design criteria to be addressed in a unified eigenvalue problem framework, so different controllers for a variety of performance criteria can be designed for this system.

First of all, in the absence of noise, $w(t) = 0$ for all $t \geq 0$, by taking $\delta = 0, \beta = 0, \varepsilon = 0$,we have

$$\lambda_{\min}(P)\|x(t)\|^2 < \lambda_{\max}(P)\|x(0)\|^2 \tag{1.5-5}$$

which means $\lim_{t\to\infty}\|x(t)\| = 0$, i.e. asymptotic stability.

By taking $\delta > 0, \beta = 0, \varepsilon = 0$ and assuming $x(t) = 0$ in steady state, will yield a bound on the energy of the performance output in terms of the initial value $x(0)$,

$$\int_0^t \|z(\tau)\|^2 d\tau < \delta^{-1}\lambda_{\max}(P)\|x(0)\|^2 \tag{1.5-6}$$

Minimizing $\lambda_{\max}(P)$ and maximizing δ will give us a smaller bound on the energy of the performance output. This is called H_2 control.

In the noisy case, $w(t) \neq 0$, by setting $\delta = 1, \beta = 0, \varepsilon < 0$, for $x_0 = 0$, gives the result

$$\int_0^t \|z(\tau)\|^2 d\tau < -\varepsilon \int_0^t \|w(\tau)\|^2) d\tau \tag{1.5-7}$$

which means a bound on the energy of the performance output of the controlled system or a H_∞ result.

When $x_0 = 0$, we can design several dissipative controllers by using different values of *δ, β* and *ε*.

If we set $\delta = 0, \beta = 1, \varepsilon > 0$, we get input strict passivity:

$$\int_0^t z(\tau)^T w(\tau) d\tau > \varepsilon \int_0^t \|w(\tau)\|^2 d\tau \tag{1.5-8}$$

If we set $\delta > 1, \beta = 1, \varepsilon = 0$, we get output strict passivity:

$$\int_0^t z(\tau)^T w(\tau) d\tau > \delta \int_0^t \|z(\tau)\|^2 d\tau \tag{1.5-9}$$

Very strict passivity, which is the strict passivity both in the terms of the input and the output, can be obtained if we set $\delta > 0, \beta = 1, \varepsilon > 0$.

$$\int_0^t z(\tau)^T w(\tau) d\tau > \delta \int_0^t \|z(\tau)\|^2 d\tau + \varepsilon \int_0^t \|w(\tau)\|^2 d\tau \tag{1.5-10}$$

As described above, this formulation enables us to design various controllers according to different performance criteria in a common framework. A criteria summary is given in Table 1-1.

Table 1-1 Continuous-time general performance criteria

	Performance Criteria	δ	β	ε	Inequality Conditions
Non-noisy case	Asymptotic stability	0	0	0	$\lambda_{\min}(P)\|x(t)\|^2 < \lambda_{\max}(P)\|x(0)\|^2$
	H_2 controller	>0	0	0	$\int_0^t \|z(\tau)\|^2 d\tau < \delta^{-1}\lambda_{\max}(P)\|x(0)\|^2$

Noisy case	H_∞ controller	1	0	<0	$\int_0^t \lVert z(\tau)\rVert^2 d\tau < -\varepsilon \int_0^t \lVert w(\tau)\rVert^2) d\tau$
	Input strict Passivity	0	1	>0	$\int_0^t z(\tau)^T w(\tau) d\tau > \varepsilon \int_0^t \lVert w(\tau)\rVert^2 d\tau$
	Output strict Passivity	>0	1	0	$\int_0^t z(\tau)^T w(\tau) d\tau > \delta \int_0^t \lVert z(\tau)\rVert^2 d\tau$
	Very strict Passivity	>0	1	>0	$\int_0^t z(\tau)^T w(\tau) d\tau > \delta \int_0^t \lVert z(\tau)\rVert^2 d\tau + \varepsilon \int_0^t \lVert w(\tau)\rVert^2 d\tau$

1.5.2 Discrete-time System Performance Criteria

For discrete-time systems, compared to the condition (1.5-1), we have

$$V_{k+1} - V_k < 0 \tag{1.5-11}$$

By incorporating additional terms in the Lyapunov inequality as

$$V_k - V_{k+1} - \delta \lVert z_k \rVert^2 - \varepsilon \lVert w_k \rVert^2 + \beta z_k{}^T w_k > 0 \tag{1.5-12}$$

where z_k is the performance output and w_k is the finite energy disturbance, it is possible to design controllers for various performance criteria in a unified framework.

Notice that upon summation, inequality (1.5-12) yields

$$x_k{}^T P x_k < x_0{}^T P x_0 - \sum_{i=0}^{k-1} (\delta \lVert z_i \rVert^2 + \varepsilon \lVert w_i \rVert^2 - \beta z_i{}^T w_i) \tag{1.5-13}$$

by using Lemma 3, we obtain,

$$\lambda_{\min}(P) \lVert x_k \rVert^2 < \lambda_{\max}(P) \lVert x_0 \rVert^2 - \sum_i (\delta \lVert z_i \rVert^2 + \varepsilon \lVert w_i \rVert^2 - \beta z_i{}^T w_i) \tag{1.5-14}$$

that allows several design criteria to be addressed in a unified eigenvalue problem framework, so we can design different controllers for a variety of performance criteria for this system.

First of all, in the absence of noise, $w_k = 0$, by taking $\delta = 0, \beta = 0, \varepsilon = 0$,we have asymptotic stability.

$$\lambda_{\min}(P)\|x_k\|^2 < \lambda_{\max}(P)\|x_0\|^2 \tag{1.5-15}$$

By taking $\delta > 0, \beta = 0, \varepsilon = 0$ and assuming $x_k = 0$ in steady state, will yield a bound on the energy of the performance output in terms of the initial value x_0 ,

$$\sum_i \|z_i\|^2 < \frac{1}{\delta}\lambda_{\max}(P)\|x_0\|^2 \tag{1.5-16}$$

Minimizing $\lambda_{\max}(P)$ and maximizing δ will give us a smaller bound on the energy of the performance output. This is called sub-optimal H_2 control.

In the noisy case, $w_k \neq 0$, by setting $\delta = 1, \beta = 0, \varepsilon < 0$, for $x_0 = 0$, gives the result

$$\sum_i \|z_i\|^2 < -\varepsilon \sum_i \|w_i\|^2 \tag{1.5-17}$$

which means a bound on the l_2 to l_2 gain of the controlled system or a suboptimal H_∞ result.

When $x_0 = 0$, we can design several dissipative controllers by using different values of δ, β and ε.

If we set $\delta = 0, \beta = 1, \varepsilon > 0$, we get input strict passivity:

$$\sum_i z_i^T w_i > \varepsilon \sum_i \|w_i\|^2 \tag{1.5-18}$$

If we set $\delta > 1, \beta = 1, \varepsilon = 0$, we get output strict passivity:

$$\sum_i z_i^T w_i > \delta \sum_i \|z_i\|^2 \tag{1.5-19}$$

Very strict passivity, which is the strict passivity both in terms of the input and the output, can be obtained if we set $\delta > 0, \beta = 1, \varepsilon > 0$.

$$\sum_i z_i^T w_i > \delta \sum_i \|z_i\|^2 + \varepsilon \sum_i \|w_i\|^2 \tag{1.5-20}$$

As described above, this formulation enables us to design various controllers according to different performance criteria in a common framework. A criteria summary is given in Table 1-2.

Table 1-2 Discrete-time general performance criteria

	Performance Criteria	δ	β	ε	Inequality Conditions
Non-noisy case	Asymptotic stability	0	0	0	$\lambda_{\min}(P)\|x_k\|^2 < \lambda_{\max}(P)\|x_0\|^2$
	H_2 controller	>0	0	0	$\sum_i \|z_i\|^2 < \frac{1}{\delta}\lambda_{\max}(P)\|x_0\|^2$
Noisy case	H_∞ controller	1	0	<0	$\sum_i \|z_i\|^2 < -\varepsilon \sum_i \|w_i\|^2$
	Input strict Passivity	0	1	>0	$\sum_i z_i^T w_i > \varepsilon \sum_i \|w_i\|^2$
	Output strict Passivity	>0	1	0	$\sum_i z_i^T w_i > \delta \sum_i \|z_i\|^2$
	Very strict Passivity	>0	1	>0	$\sum_i z_i^T w_i > \delta \sum_i \|z_i\|^2 + \varepsilon \sum_i \|w_i\|^2$

1.6 Class of Nonlinear System Considered

For the problem of the robust and resilient controller design, a class of nonlinear systems with unknown nonlinearities lying within a conic bound and with known finite energy disturbances is considered in continuous- and discrete-time. For the purpose of illustrating the significance of such a class of nonlinearities, the continuous-time model of the system is introduced in this section.

The nonlinear system is described by the following model in the continuous-time case

$$\dot{x} = f(x,u,w) \tag{1.6-1}$$

where x is the state, u is the input and w is a L_2 disturbance.

The nonlinear function satisfies a conic sector condition given by

$$\left\| f(x,u,w) - (Ax + Bu + Fw) \right\|^2 \le (C_f x + D_f u + E_f w)^T (C_f x + D_f u + E_f w) \tag{1.6-2}$$

The center and the radius of the cone are described by $Ax + Bu + Fw$ and the right-hand side of (1.6-2), respectively. To show it graphically, considering a second order case, the conic nonlinearity is shown in the following figure.

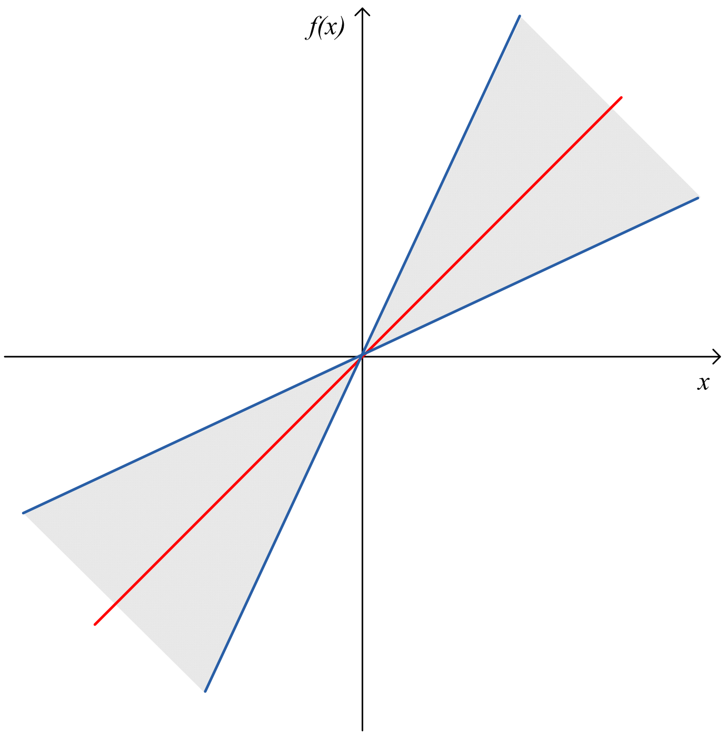

Figure 1.6-1 An example of second order conic nonlinearity

This type of nonlinear is very common in science and engineering problems, such as example systems introduced in Section 1.8 and other nonlinear systems including:

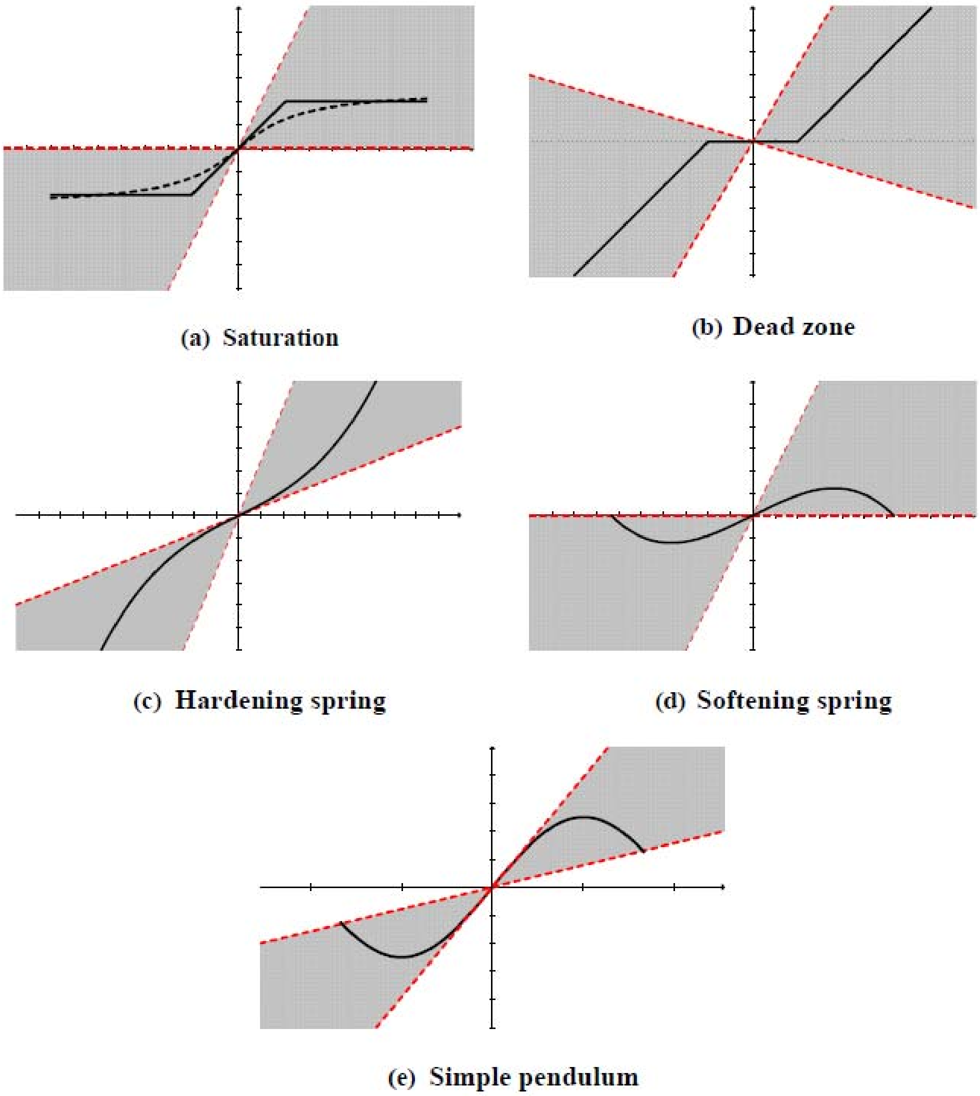

Figure 1.6-2 Example applications of conic nonlinearities

- Saturation nonlinearity (Fig. 1.6-2-a) may arise in electrical amplifiers, motors, etc.,
- Dead zone nonlinearity (Fig. 1.6-2-b) may arise in amplifier circuits at low input frequencies and in mechanical systems,
- Nonlinearities of a hardening spring(Fig. 1.6-2-c) and a softening spring(Fig. 1.6-2-d)

- Sinusoidal nonlinearities (Fig. 1.6-2-e) which appear in systems of simple pendulum, inverted pendulum, etc. [33]

1.7 Introduction to Linear Matrix Inequalities

Linear matrix inequality is the major mathematical technique used in this dissertation [34]. One of its most powerful functions is to reduce a very variety of control system problems to a few standard optimization problems, which can be relatively easily solved by efficient software. The following is a brief introduction to LMIs:

The first LMI known goes back more than 100 years ago when Lyapunov showed that the solution, *x(t)*, for differential equation

$$\frac{d}{dt}x(t) = Ax(t) \tag{1.7-1}$$

is stable if and only if there exists a positive definite matrix P such that

$$A^T P + PA < 0 \tag{1.7-2}$$

This is the well-known Lyapunov inequality, which is an LMI. It can be solved as a linear equation in the following by picking any positive definite matrix Q,

$$A^T P + PA = -Q \tag{1.7-3}$$

In the past decades, a lot of scientists and engineers have made great efforts toward the development of efficient computational methods to solve LMI and using LMI to formulate solutions to systems and control problems.

A linear matrix inequality has the general form

$$F(x) = F_0 + \sum_{i=1}^{m} x_i F_i > 0 \tag{1.7-4}$$

where $x \in R^m$ is the variable. The symmetric matrices $F_i = F_i^T \in R^{n\times n}$, $i = 0,\cdots,m$, are given.

Multiple LMIs $F_1(x) > 0, F_2(x) > 0,\cdots, F_n(x) > 0$ can be expressed as a single LMI

$$\begin{bmatrix} F_1(x) & & & 0 \\ & F_2(x) & & \\ & & \ddots & \\ 0 & & & F_n(x) \end{bmatrix} > 0 \qquad (1.7\text{-}5)$$

Notice that the matrix in (1.7-5) is a block diagonal matrix, which means for this condition to hold, each element on the diagonal must be positive definite, $F_i(x) > 0$.

For nonlinear inequalities, we can use lemma 1, Schur complement, which is a powerful tool to convert nonlinear problems to linear problems.

<u>Example 1-1</u>

Let us discuss a simple example of positive scalar unknown variables x and y in the following,

$$x - x^{-1}y^2 > 0 \qquad (1.7\text{-}6)$$

There are nonlinearities x^{-1} and y^2 in (1.7-6), which may cause difficulties and complications. Applying Lemma 1 to (1.7-6), will give us,

$$\begin{bmatrix} x & y \\ y & x \end{bmatrix} > 0 \qquad (1.7\text{-}7)$$

where every element of the matrix is linear in the solution x and y, so that we get a linear matrix inequality.

1.8 Selected Example Systems for Simulation Studies

The following systems will be used as examples throughout the dissertation.

1.8.1 Simple pendulum

The simple pendulum with damping in Figure 1.8-1 is assumed to satisfy the following equation

$$m\ddot{\theta} = -b\dot{\theta} - \frac{mg}{L}\sin\theta \qquad (1.8\text{-}1)$$

where θ denotes the angle from the vertical axis, m is the mass of the ball, L is the length of the massless string, b is the friction coefficient and *g* is gravity.

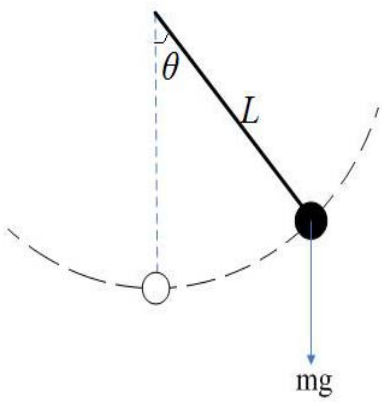

Figure 1.8-1 Simple pendulum

Writing the state space model of (1.8-1) for $x_1 = \theta, x_2 = \dot{\theta}$, we have

$$\begin{bmatrix} \dot{x}_1 \\ \dot{x}_2 \end{bmatrix} = \begin{bmatrix} 0 & 1 \\ -\frac{b}{m} & 0 \end{bmatrix} \begin{bmatrix} x_1 \\ x_2 \end{bmatrix} + \begin{bmatrix} 0 \\ -\frac{g}{L}\sin x_1 \end{bmatrix} \qquad (1.8\text{-}2)$$

In order to illustrate certain controller properties, in some examples we make some minor changes in the system (1.8-2) for it to be unstable or with disturbances. The modified systems will be introduced in relevant examples.

1.8.2 Chua's Circuit

A chaotic synchronization example involving Chua's circuit is also used in this dissertation. Chua's circuit is shown in Figure 1.8-2.

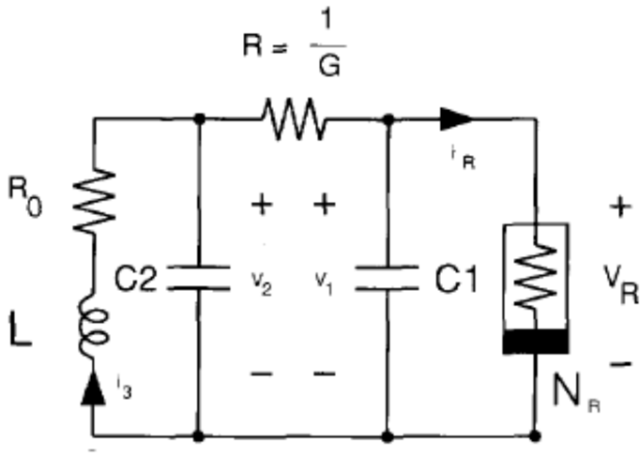

Figure 1.8-2 Chua's circuit diagram

The differential equations of the Chua's circuit are given in the following:

$$\begin{aligned}
\frac{dv_1}{dt} &= \frac{1}{C_1}[G(v_2 - v_1) - f(v_1)] \\
\frac{dv_2}{dt} &= \frac{1}{C_2}[G(v_1 - v_2) + i_3] \\
\frac{di_3}{dt} &= -\frac{1}{L}(v_2 + R_0 i_3)
\end{aligned} \tag{1.8-3}$$

where $G = \frac{1}{R}$ and $f(v_1) = G_b v_1 + \frac{1}{2}(G_a - G_b)(|v_1 + E| - |v_1 - E|)$

E is the breakpoint voltage of the nonlinear resistor in the Chua's circuit. $f(v_1)$ is the V-I characteristic of the nonlinear resistor with a slope of G_a and G_b in the inner and outer region respectively.

We define the state variables and parameters for this circuit as

$$\begin{aligned} &x_1 = \frac{v_1}{E}, x_2 = \frac{v_2}{E}, x_3 = \frac{i_3}{GE}, \\ &\alpha_c = \frac{C_2}{C_1}, \beta_c = \frac{C_2}{LG^2}, a = \frac{G_a}{G}, b = \frac{G_b}{G} \end{aligned} \tag{1.8-4}$$

Then, we have the state space model as

$$\begin{aligned} &\begin{bmatrix} \dot{x}_1 \\ \dot{x}_2 \\ \dot{x}_3 \end{bmatrix} = \begin{bmatrix} -\alpha_c & \alpha_c & 0 \\ 1 & -1 & 1 \\ 0 & \beta_c & -\mu \end{bmatrix} \begin{bmatrix} x_1 \\ x_2 \\ x_3 \end{bmatrix} - \begin{bmatrix} \alpha_c f(x_1) \\ 0 \\ 0 \end{bmatrix} + \begin{bmatrix} 7 \\ 1 \\ 1 \end{bmatrix} u \\ &y = \begin{bmatrix} 1 & 0 & 0 \end{bmatrix} \begin{bmatrix} x_1 \\ x_2 \\ x_3 \end{bmatrix} \end{aligned} \tag{1.8-5}$$

where $f(x_1) = bx_1 + 0.5(a+b)(|x_1+1| - |x_1-1|)$.

CHAPTER 2

CONTINUOUS TIME ROBUST AND RESILIENT CONTROLLER DESIGN WITH GENERAL CRITERIA FOR UNCERTAIN CONIC NONLINEAR SYSTEMS WITH DISTURBANCES

2.0 Introduction

In this chapter, we present a state feedback control design procedure for continuous time nonlinear systems with conic type nonlinearities and finite energy disturbances in the case of uncertainties in the center and boundary of the sector in which the nonlinearity resides. Uncertainties are allowed in both the system model and the conic bound of the nonlinearities in the form of perturbed parameters with known bounds on the perturbations. The robust controller that is designed will be tolerant to perturbations in both the center line and the boundary of the cone. Additionally, the controller is resilient in the sense of having some tolerance to a readjustment or perturbations of the feedback gain. LMI techniques are used to obtain the controller design for various performance criteria such as H_2 , H_∞, etc. Some illustrative examples and discussion are included to show the effectiveness of the proposed methodology.

In Section 2.1, the system model and the uncertain nonlinearities are introduced and in Section 2.2, LMI formulations are derived for several cases and the main theorem is given. Section 2.3 contains two simulations studies of two different types of system.

Two special cases of the design method proposed in this chapter are discussed in Section 2.4 and 2.5.

2.1 Problem Formulation

Let us consider a continuous time nonlinear system,

$$\dot{x} = f(x,u,w) \tag{2.1-1}$$

where $x \in R^n$ is the state, $u \in R^m$ is the input, and $w \in R^w$ is an L_2 disturbance input.

A linear state feedback control is used in this system

$$u = \tilde{K}x \tag{2.1-2}$$

where the feedback gain is perturbed as $\tilde{K} = K + \Delta_K$, with the perturbation bounded as

$$\Delta_K M \Delta_K{}^T \leq N \tag{2.1-3}$$

A resilient control design is used to accommodate the perturbations, Δ_K, on the feedback gain based on the knowledge of the bounds, *M* and *N*, given in (2.1-3).

The performance output is given as

$$z = C_z x + D_z u + E_z w \tag{2.1-4}$$

It is assumed that the nonlinear function is analytic and can be expanded into a linear component,

$$\dot{x}_{lin} = \tilde{A}x + \tilde{B}u + \tilde{F}w \tag{2.1-5}$$

and a nonlinear component $\mathfrak{F}$

$$\mathfrak{F} = f(x,u,w) - (\tilde{A}x + \tilde{B}u + \tilde{F}w) \tag{2.1-6}$$

It is assumed that there is uncertainty in the linear part, so that the system parameters are perturbed where

$$\tilde{A} = A + \Delta_A, \tilde{B} = B + \Delta_B, \tilde{F} = F + \Delta_F \tag{2.1-7}$$

It is also assumed that the nonlinear part of the system satisfies

$$\mathfrak{F}^T \mathfrak{F} = \left\| f(x,u,w) - (\tilde{A}x + \tilde{B}u + \tilde{F}w) \right\|^2 \le (\tilde{C}_f x + \tilde{D}_f u + \tilde{E}_f w)^T (\tilde{C}_f x + \tilde{D}_f u + \tilde{E}_f w) \tag{2.1-8}$$

There is also uncertainty regarding the maximum deviation from the linear part, so that the boundary parameters are perturbed where

$$\tilde{C}_f = C_f + \Delta_{C_f}, \tilde{D}_f = D_f + \Delta_{D_f}, \tilde{E}_f = E_f + \Delta_{E_f} \tag{2.1-9}$$

Therefore uncertainties about the maximum deviation from the linear part are also considered in this work. A robust controller is used to accommodate uncertainties or perturbations in the system dynamics, such as given in (2.1-7) - (2.1-9).

By having perturbations on all the parameters of the cone as given in (2.1-7) and (2.1-9), we will have robustness on both the center line and the radius of the cone, i.e., we can accommodate uncertainties in both the linear and nonlinear parts of the system.

Equations (2.1-6)-(2.1-9) describe a locally conic nonlinearity with perturbation. To show this graphically for the scalar case with no noise, the cone in which the nonlinearity resides is shown as the shaded region in Figure 2.1-1 with solid center and boundary lines. The uncertainties for the center and boundaries of the nonlinear region are shown as the dashed lines in the figure. The design methodology described in this paper allows us to incorporate such center/radius uncertainties.

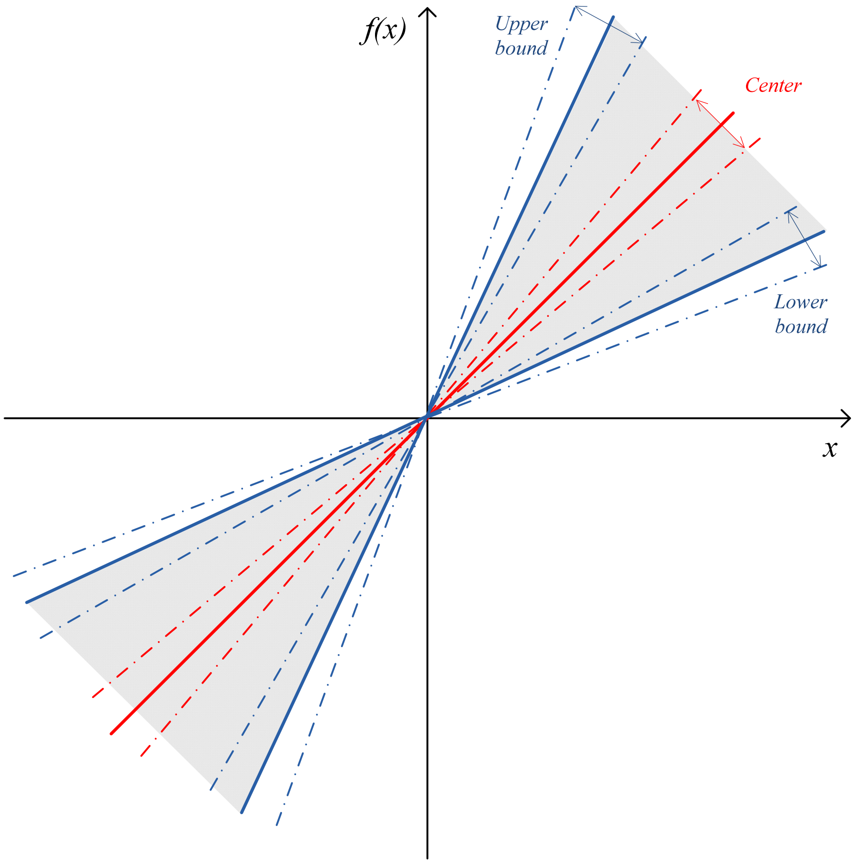

Figure 2.1-1 Center and boundaries of a conic nonlinearity with uncertainty

The perturbations $\Delta_A, \Delta_B, \Delta_F, \Delta_{C_f}, \Delta_{D_f}, \Delta_{E_f}$ are bounded as follows,

$$\begin{bmatrix} \Delta_A & \Delta_B & \Delta_F \\ \Delta_{C_f} & \Delta_{D_f} & \Delta_{E_f} \end{bmatrix} \Phi \begin{bmatrix} \Delta_A{}^T & \Delta_{C_f}{}^T \\ \Delta_B{}^T & \Delta_{D_f}{}^T \\ \Delta_F{}^T & \Delta_{E_f}{}^T \end{bmatrix} \leq \Psi \tag{2.1-10}$$

where $\Phi = \begin{bmatrix} \Phi_{11} & \Phi_{12} & \Phi_{13} \\ & \Phi_{22} & \Phi_{23} \\ * & & \Phi_{33} \end{bmatrix}, \Psi = \begin{bmatrix} \Psi_{11} & \Psi_{12} \\ * & \Psi_{22} \end{bmatrix}$ are positive definite symmetric block matrices.

The design starts with following inequality

$$-\dot{V} - \delta\|z\|^2 - \varepsilon\|w\|^2 + \beta z^T w > 0 \tag{2.1-11}$$

as introduced in Section 1.5. The continuous time performance criteria given in Table 1-1 are used in this design.

2.2 LMI Formulations and Main Result

In this section, the main theorem of the controller is given and the proof of the theorem for various cases is conducted.

2.2.1 Main Theorem

Theorem 2-1. There exists a resilient and robust state feedback controller (2.1-2) for systems with conic-type nonlinearity (2.1-8) and performance output (2.1-4), if the LMI (2.2-1) is feasible for some Y, and the positive definite matrices Q, M, N, Φ, Ψ and α. The control gain is found by $K = YQ^{-1}$. In addition, for design parameters $\delta > 0$, $\beta = 1, \varepsilon > 0$, the very strict passivity criterion is satisfied.

$$S_1 = \begin{bmatrix} s_{11} & s_{12} & s_{13} & s_{14} & s_{15} & s_{16} & s_{17} & s_{18} \\ & s_{22} & s_{23} & s_{24} & s_{25} & s_{26} & s_{27} & s_{28} \\ & & s_{33} & s_{34} & s_{35} & s_{36} & s_{37} & s_{38} \\ & & & s_{44} & s_{45} & s_{46} & s_{47} & s_{48} \\ & & & & s_{55} & s_{56} & s_{57} & s_{58} \\ & * & & & & s_{66} & s_{67} & s_{68} \\ & & & & & & s_{77} & s_{78} \\ & & & & & & & s_{88} \end{bmatrix} > 0 \qquad (2.2\text{-}1)$$

where the matrices elements, S_{ij}, are given as,

$$s_{11} = -AQ - BY - QA^T - Y^T B^T - \alpha I - \Psi_{11} - BNB^T,$$
$$s_{12} = \frac{\beta}{2}(QC_z^T + Y^T D_z^T) - F + \frac{\beta}{2} BND_z^T,$$
$$s_{13} = QC_f^T + Y^T D_f^T + \Psi_{12} + BND_f^T,$$

$$s_{14} = \sqrt{\delta}(QC_z^{\ T} + Y^T D_z^{\ T} + BND_z^{\ T}),$$
$$s_{15} = Q,$$
$$s_{16} = Y^T + BN,$$
$$s_{17} = 0,$$
$$s_{18} = Q,$$
$$s_{22} = \frac{\beta}{2}(E_z^{\ T} + E_z) - \varepsilon I - \frac{\beta^2}{4} D_z N D_z^{\ T},$$
$$s_{23} = E_f - \frac{\beta}{2} D_z N D_f^{\ T},$$
$$s_{24} = \sqrt{\delta}(E_z - \frac{\beta}{2} D_z N D_z^{\ T}),$$
$$s_{25} = 0,$$
$$s_{26} = -\frac{\beta}{2} D_z N,$$
$$s_{27} = I - \frac{\beta}{2} D_z N,$$
$$s_{28} = 0,$$
$$s_{33} = \alpha I - \Psi_{22} - D_f N D_f^{\ T},$$
$$s_{34} = -\sqrt{\delta} D_f N D_z^{\ T},$$
$$s_{36} = -D_f N,$$
$$s_{35} = s_{37} = s_{38} = 0,$$
$$s_{44} = I - \delta D_z N D_z^{\ T},$$
$$s_{46} = -\sqrt{\delta} D_z N,$$
$$s_{45} = s_{47} = s_{48} = 0,$$
$$s_{55} = \Phi_{11},$$
$$s_{56} = \Phi_{12},$$
$$s_{57} = \Phi_{13},$$
$$s_{58} = 0,$$
$$s_{66} = \Phi_{22} - N,$$
$$s_{67} = \Phi_{23},$$
$$s_{68} = 0,$$
$$s_{77} = \Phi_{33},$$
$$s_{78} = 0,$$
$$s_{88} = M$$

Comments: In the above LMI, system parameters A, B, C_z, D_z, E_z, nonlinear bound parameters C_f, D_f, E_f for the system nonlinearity and performance parameters δ, β, ε are all known. The unknowns are Q, Y, intermediate (slack) variable J, and the perturbation bound parameters M, N, Φ and Ψ. All unknowns are in linear form in the above LMI.

Corollary 2-1. For design parameters $\delta > 0, \beta = 1, \varepsilon = 0$, Theorem 2-1 holds for the output strict passivity criterion.

Corollary 2-2. For design parameters $\delta = 1, \beta = 0, \varepsilon < 0$, Theorem 2-1 holds for the H_∞ controller criterion.

Corollary 2-3. For design parameters $\delta = 0, \beta = 1, \varepsilon > 0$, Theorem 2-1 holds for the input strict passivity criterion.

Corollary 2-4. For design parameters $\delta > 0, \beta = 0, \varepsilon = 0$, and replacing LMI (2.2-1) with LMI (2.2-2), then Theorem 2-1 holds for the H_2 controller criterion.

$$S_2 = \begin{bmatrix} s_{11} & s_{13} & s_{14} & s_{15} & s_{16} & s_{18} \\ & s_{33} & s_{34} & s_{35} & s_{36} & s_{38} \\ & & s_{44} & s_{45} & s_{46} & s_{48} \\ & * & & s_{55} & s_{56} & s_{58} \\ & & & & s_{66} & s_{68} \\ & & & & & s_{88} \end{bmatrix} > 0 \qquad (2.2\text{-}2)$$

Corollary 2-5. For design parameters $\delta = 0, \beta = 0, \varepsilon = 0$, and replacing LMI (2.2-1) with LMI (2.2-2), then Theorem 2-1 holds for asymptotic stability.

The proof of the theorem is given for several cases in the next a few sections.

2.2.2 General Form

The development leading to an LMI framework is given below.

From (2.1-11), using the definition of $V = x^T Px$, we have

$$\dot{V} = x^T P[(\tilde{A} + \tilde{B}\tilde{K})x + \tilde{F}w + \mathfrak{F}] + [(\tilde{A} + \tilde{B}\tilde{K})x + \tilde{F}w + \mathfrak{F}]^T Px \tag{2.2-3}$$

Using Lemma 2 and a slack variable α, and applying nonlinear bound (2.1-8), we can bound the term $x^T P\mathfrak{F} + \mathfrak{F}^T Px$ as,

$$\begin{aligned} x^T P\mathfrak{F} + \mathfrak{F}^T Px &\leq \alpha x^T P^2 x + \alpha^{-1}\mathfrak{F}^T \mathfrak{F} \\ &\leq \alpha x^T P^2 x + \alpha^{-1}(\tilde{C}_f x + \tilde{D}_f u + \tilde{E}_f w)^T (\tilde{C}_f x + \tilde{D}_f u + \tilde{E}_f w) \end{aligned} \tag{2.2-4}$$

Substituting (2.2-4) into (2.2-3), we have

$$\begin{aligned} \dot{V} \leq\ & x^T P[(\tilde{A} + \tilde{B}\tilde{K})x + \tilde{F}w] + [(\tilde{A} + \tilde{B}\tilde{K})x + \tilde{F}w]^T Px \\ & + \alpha x^T P^2 x + \alpha^{-1}(\tilde{C}_f x + \tilde{D}_f u + \tilde{E}_f w)^T (\tilde{C}_f x + \tilde{D}_f u + \tilde{E}_f w) \end{aligned} \tag{2.2-5}$$

Substituting (2.2-5) into (2.1-11), we obtain,

$$\begin{aligned} & x^T P[(\tilde{A} + \tilde{B}\tilde{K})x + \tilde{F}w] + [(\tilde{A} + \tilde{B}\tilde{K})x + \tilde{F}w]^T Px \\ & + \alpha x^T P^2 x + \alpha^{-1}[(\tilde{C}_f + \tilde{D}_f\tilde{K})x + \tilde{E}_f w]^T [(\tilde{C}_f + \tilde{D}_f\tilde{K})x + \tilde{E}_f w] \\ & \leq -\delta \|z\|^2 - \varepsilon \|w\|^2 + \beta z^T w \end{aligned} \tag{2.2-6}$$

Inequality (2.2-6) is a sufficient condition for (2.1-11) and can be rewritten in a quadratic form as,

$$\begin{bmatrix} x^T & w^T \end{bmatrix} H \begin{bmatrix} x \\ w \end{bmatrix} \geq 0 \tag{2.2-7}$$

where $H = \begin{bmatrix} h_{11} & h_{12} \\ h_{12}^T & h_{22} \end{bmatrix} > 0$

with

$$h_{11} = -P(\tilde{A}+\tilde{B}\tilde{K}) - (\tilde{A}+\tilde{B}\tilde{K})^T P - \alpha P^2$$
$$-\alpha^{-1}(\tilde{C}_f + \tilde{D}_f\tilde{K})^T(\tilde{C}_f + \tilde{D}_f\tilde{K}) - \delta(C_z + D_z\tilde{K})^T(C_z + D_z\tilde{K})$$
$$h_{12} = -P\tilde{F} - \alpha^{-1}(\tilde{C}_f + \tilde{D}_f\tilde{K})^T\tilde{E}_f - \delta(C_z + D_z\tilde{K})^T E_z + \frac{\beta}{2}(C_z + D_z\tilde{K})^T$$
$$h_{22} = -\alpha^{-1}\tilde{E}_f{}^T\tilde{E}_f - \delta E_z{}^T E_z - \varepsilon I + \frac{\beta}{2}(E_z{}^T + E_z)$$

2.2.3 Case When Noise Is Present

By pre- and post-multiplying H by $\begin{bmatrix} Q & 0 \\ 0 & I \end{bmatrix}$ where $Q = P^{-1}$ and using $\tilde{Y} = \tilde{K}Q = (K + \Delta_K)Q$, we obtain,

$$\begin{bmatrix} Q & 0 \\ 0 & I \end{bmatrix} H \begin{bmatrix} Q & 0 \\ 0 & I \end{bmatrix} = \begin{bmatrix} h'_{11} & h'_{12} \\ h'^T_{12} & h'_{22} \end{bmatrix} > 0 \qquad (2.2\text{-}8)$$

where

$$h_{11}' = -\tilde{A}Q - \tilde{B}\tilde{Y} - Q\tilde{A}^T - \tilde{Y}^T\tilde{B}^T - \alpha I - \alpha^{-1}(Q\tilde{C}_f{}^T + \tilde{Y}^T\tilde{D}_f{}^T)(\tilde{C}_f Q + \tilde{D}_f\tilde{Y})$$
$$-\delta(QC_z{}^T + \tilde{Y}^T D_z)(C_z Q + D_z\tilde{Y})$$
$$h_{12}' = -\tilde{F} - \alpha^{-1}(Q\tilde{C}_f{}^T + \tilde{Y}^T\tilde{D}_f{}^T)\tilde{E}_f - \delta(QC_z{}^T + \tilde{Y}^T D_z)E_z + \frac{\beta}{2}(QC_z{}^T + \tilde{Y}^T D_z)$$
$$h_{22}' = -\alpha^{-1}\tilde{E}_f{}^T\tilde{E}_f - \delta E_z{}^T E_z - \varepsilon I + \frac{\beta}{2}(E_z{}^T + E_z)$$

Inequality (2.2-8) must be true in order to satisfy (2.1-11). Applying Lemma 1 to (2.2-8) yields

$$\left[\begin{array}{c|c|c} \begin{array}{c} -\tilde{A}Q - \tilde{B}\tilde{Y} - Q\tilde{A}^T - \tilde{Y}^T\tilde{B}^T - \alpha I \\ -\delta(QC_z{}^T + \tilde{Y}^T D_z)(C_z Q + D_z\tilde{Y}) \end{array} & \begin{array}{c} \frac{\beta}{2}(QC_z{}^T + \tilde{Y}^T D_z{}^T) - \tilde{F} \\ -\delta(QC_z{}^T + \tilde{Y}^T D_z)E_z \end{array} & Q\tilde{C}_f{}^T + \tilde{Y}^T\tilde{D}_f{}^T \\ \hline * & \begin{array}{c} -\varepsilon I - \delta E_z{}^T E_z \\ + \frac{\beta}{2}(E_z{}^T + E_z) \end{array} & \tilde{E}_f \\ \hline * & * & \alpha I \end{array}\right] > 0 \quad (2.2\text{-}9)$$

Moving terms with $\Delta_A, \Delta_B, \Delta_F, \Delta_{C_f}, \Delta_{D_f}, \Delta_{E_f}$ to the right side of the inequality, we have

$$\left[\begin{array}{c:c:c} \begin{matrix} -AQ - B\tilde{Y} - Q\tilde{A}^T - \tilde{Y}^T B^T - \alpha I \\ -\delta(QC_z{}^T + \tilde{Y}^T D_z)(C_z Q + D_z \tilde{Y}) \end{matrix} & \begin{matrix} \frac{\beta}{2}(QC_z{}^T + \tilde{Y}^T D_z{}^T) - \tilde{F} \\ -\delta(QC_z{}^T + \tilde{Y}^T D_z)E_z \end{matrix} & QC_f{}^T + \tilde{Y}^T D_f{}^T \\ \hdashline * & \begin{matrix} -\varepsilon I - \delta E_z{}^T E_z \\ +\frac{\beta}{2}(E_z{}^T + E_z) \end{matrix} & E_f \\ \hdashline * & * & \alpha I \end{array}\right] \qquad (2.2\text{-}10)$$

$$> \begin{bmatrix} \Delta_A Q + \Delta_B \tilde{Y} + Q\Delta_A{}^T + \tilde{Y}^T \Delta_B{}^T & \Delta_F & -Q\Delta_{C_f}{}^T - \tilde{Y}^T \Delta_{D_f}{}^T \\ \Delta_F{}^T & 0 & -\Delta_{E_f} \\ -\Delta_{C_f} Q - \Delta_{D_f} \tilde{Y} & -\Delta_{E_f}{}^T & 0 \end{bmatrix}$$

The right side (2.2-10) of can be rewritten and can then be bounded by using Lemma 2 as

$$\begin{aligned} &\begin{bmatrix} \Delta_A Q + \Delta_B \tilde{Y} + Q\Delta_A{}^T + \tilde{Y}^T \Delta_B{}^T & \Delta_F & -Q\Delta_{C_f}{}^T - \tilde{Y}^T \Delta_{D_f}{}^T \\ \Delta_F{}^T & 0 & -\Delta_{E_f} \\ -\Delta_{C_f} Q - \Delta_{D_f} \tilde{Y} & -\Delta_{E_f}{}^T & 0 \end{bmatrix} \\ &= \begin{bmatrix} \Delta_A & \Delta_B & \Delta_F \\ 0 & 0 & 0 \\ -\Delta_{C_f} & -\Delta_{D_f} & -\Delta_{E_f} \end{bmatrix} \begin{bmatrix} Q & 0 & 0 \\ \tilde{Y} & 0 & 0 \\ 0 & I & 0 \end{bmatrix} + \begin{bmatrix} Q & \tilde{Y}^T & 0 \\ 0 & 0 & I \\ 0 & 0 & 0 \end{bmatrix} \begin{bmatrix} \Delta_A{}^T & 0 & -\Delta_{C_f}{}^T \\ \Delta_B{}^T & 0 & -\Delta_{D_f}{}^T \\ \Delta_F{}^T & 0 & -\Delta_{E_f} \end{bmatrix} \qquad (2.2\text{-}11) \\ &\le \begin{bmatrix} \Delta_A & \Delta_B & \Delta_F \\ 0 & 0 & 0 \\ -\Delta_{C_f} & -\Delta_{D_f} & -\Delta_{E_f} \end{bmatrix} \Phi \begin{bmatrix} \Delta_A{}^T & 0 & -\Delta_{C_f}{}^T \\ \Delta_B{}^T & 0 & -\Delta_{D_f}{}^T \\ \Delta_F{}^T & 0 & -\Delta_{E_f} \end{bmatrix} + \begin{bmatrix} Q & \tilde{Y}^T & 0 \\ 0 & 0 & I \\ 0 & 0 & 0 \end{bmatrix} \Phi^{-1} \begin{bmatrix} Q & 0 & 0 \\ \tilde{Y} & 0 & 0 \\ 0 & I & 0 \end{bmatrix} \end{aligned}$$

The left term in the third line of (2.2-11) can be rewritten and by using bound condition (2.1-10), we have

$$\begin{bmatrix} \Delta_A & \Delta_B & \Delta_F \\ 0 & 0 & 0 \\ -\Delta_{C_f} & -\Delta_{D_f} & -\Delta_{E_f} \end{bmatrix} \Phi \begin{bmatrix} \Delta_A{}^T & 0 & -\Delta_{C_f}{}^T \\ \Delta_B{}^T & 0 & -\Delta_{D_f}{}^T \\ \Delta_F{}^T & 0 & -\Delta_{E_f}{}^T \end{bmatrix}$$

$$= \begin{bmatrix} I & 0 \\ 0 & 0 \\ 0 & -I \end{bmatrix} \begin{bmatrix} \Delta_A & \Delta_B & \Delta_F \\ \Delta_{C_f} & \Delta_{D_f} & \Delta_{E_f} \end{bmatrix} \Phi \begin{bmatrix} \Delta_A{}^T & \Delta_{C_f}{}^T \\ \Delta_B{}^T & \Delta_{D_f}{}^T \\ \Delta_F{}^T & \Delta_{E_f}{}^T \end{bmatrix} \begin{bmatrix} I & 0 & 0 \\ 0 & 0 & -I \end{bmatrix} \qquad (2.2\text{-}12)$$

$$= \begin{bmatrix} I & 0 \\ 0 & 0 \\ 0 & -I \end{bmatrix} \Psi \begin{bmatrix} I & 0 & 0 \\ 0 & 0 & -I \end{bmatrix} = \begin{bmatrix} \Psi_{11} & 0 & -\Psi_{12} \\ & 0 & 0 \\ * & & \Psi_{22} \end{bmatrix}$$

Substituting (2.2-11) and (2.2-12) into (2.2-10), we have (2.2-13) a sufficient condition for (2.2-10) to hold.

$$\left[\begin{array}{c:c:c} -AQ - B\tilde{Y} - QA^T - \tilde{Y}^T B^T - \alpha I & \frac{\beta}{2}(QC_z{}^T + \tilde{Y}^T D_z{}^T) - \tilde{F} & QC_f{}^T + \tilde{Y}^T D_f{}^T \\ -\delta(QC_z{}^T + \tilde{Y}^T D_z)(C_z Q + D_z \tilde{Y}) - \Psi_{11} & -\delta(QC_z{}^T + \tilde{Y}^T D_z)E_z & +\Psi_{12} \\ \hdashline & -\varepsilon I - \delta E_z{}^T E_z & \\ * & & E_f \\ & +\frac{\beta}{2}(E_z{}^T + E_z) & \\ \hdashline * & * & \alpha I - \Psi_{22} \end{array}\right] \qquad (2.2\text{-}13)$$

$$- \begin{bmatrix} Q & \tilde{Y}^T & 0 \\ 0 & 0 & I \\ 0 & 0 & 0 \end{bmatrix} \Phi^{-1} \begin{bmatrix} Q & 0 & 0 \\ \tilde{Y} & 0 & 0 \\ 0 & I & 0 \end{bmatrix} > 0$$

Applying Lemma 1 to (2.2-13) twice, we have

$$\left[\begin{array}{c:c:c:c:c:c:c}
\begin{array}{l}-AQ-B\tilde{Y}\\-QA-\tilde{Y}^TB\\-\alpha I-\Psi_{11}\end{array} & \begin{array}{l}\frac{\beta}{2}(QC_z{}^T+\tilde{Y}^TD_z{}^T)\\-F\end{array} & \begin{array}{l}QC_f{}^T\\+\tilde{Y}^TD_f{}^T\\+\Psi_{12}\end{array} & \begin{array}{l}\sqrt{\delta}(QC_z{}^T\\+\tilde{Y}^TD_z{}^T)\end{array} & Q & \tilde{Y}^T & 0\\ \hdashline
* & \begin{array}{l}\frac{\beta}{2}(E_z{}^T+E_z)\\-\varepsilon I\end{array} & E_f & \sqrt{\delta}E_z & 0 & 0 & I\\ \hdashline
* & * & \alpha I-\Psi_{22} & 0 & 0 & 0 & 0\\ \hdashline
* & * & * & I & 0 & 0 & 0\\ \hdashline
* & * & * & * & \Phi_{11} & \Phi_{12} & \Phi_{13}\\ \hdashline
* & * & * & * & * & \Phi_{22} & \Phi_{23}\\ \hdashline
* & * & * & * & * & * & \Phi_{33}
\end{array}\right] > 0 \quad (2.2\text{-}14)$$

Moving the terms with Δ_K to the right side of (2.2-14), we have

$$\left[\begin{array}{c:c:c:c:c:c:c}
\begin{array}{l}-AQ-BY\\-QA-Y^TB\\-\alpha I-\Psi_{11}\end{array} & \begin{array}{l}\frac{\beta}{2}(QC_z{}^T+Y^TD_z{}^T)\\-F\end{array} & \begin{array}{l}QC_f{}^T\\+Y^TD_f{}^T\\+\Psi_{12}\end{array} & \begin{array}{l}\sqrt{\delta}(QC_z{}^T\\+Y^TD_z{}^T)\end{array} & Q & Y^T & 0\\ \hdashline
* & \begin{array}{l}\frac{\beta}{2}(E_z{}^T+E_z)\\-\varepsilon I\end{array} & E_f & \sqrt{\delta}E_z & 0 & 0 & I\\ \hdashline
* & * & \alpha I-\Psi_{22} & 0 & 0 & 0 & 0\\ \hdashline
* & * & * & I & 0 & 0 & 0\\ \hdashline
* & * & * & * & \Phi_{11} & \Phi_{12} & \Phi_{13}\\ \hdashline
* & * & * & * & * & \Phi_{22} & \Phi_{23}\\ \hdashline
* & * & * & * & * & * & \Phi_{33}
\end{array}\right] \quad (2.2\text{-}15)$$

$$> \left[\begin{array}{c:c:c:c:c:c:c}
\begin{array}{l}B\Delta_kQ\\+Q\Delta_k{}^TB^T\end{array} & -\frac{\beta}{2}Q\Delta_k{}^TD_z{}^T & -Q\Delta_k{}^TD_f{}^T & -\sqrt{\delta}Q\Delta_k{}^TD_z{}^T & 0 & -Q\Delta_k{}^T & 0\\ \hdashline
* & 0 & 0 & 0 & 0 & 0 & 0\\ \hdashline
* & * & 0 & 0 & 0 & 0 & 0\\ \hdashline
* & * & * & 0 & 0 & 0 & 0\\ \hdashline
* & * & * & * & 0 & 0 & 0\\ \hdashline
* & * & * & * & * & 0 & 0\\ \hdashline
* & * & * & * & * & * & 0
\end{array}\right]$$

A bound for the right side of (2.2-15) is found by applying Lemma 2 as

$$\begin{bmatrix} B \\ -\frac{\beta}{2}D_z \\ -D_f \\ -\sqrt{\delta}D_z \\ 0 \\ -I \\ 0 \end{bmatrix} \Delta_k \begin{bmatrix} Q & 0 & 0 & 0 & 0 & 0 & 0 \end{bmatrix} + \begin{bmatrix} Q \\ 0 \\ 0 \\ 0 \\ 0 \\ 0 \\ 0 \end{bmatrix} \Delta_k{}^T \begin{bmatrix} B^T & -\frac{\beta}{2}D_z{}^T & -D_f{}^T & -\sqrt{\delta}D_z{}^T & 0 & -I & 0 \end{bmatrix}$$

$$\leq \begin{bmatrix} B \\ -\frac{\beta}{2}D_z \\ -D_f \\ -\sqrt{\delta}D_z \\ 0 \\ -I \\ 0 \end{bmatrix} \Delta_k M \Delta_k{}^T \begin{bmatrix} B^T & -\frac{\beta}{2}D_z{}^T & -D_f{}^T & -\sqrt{\delta}D_z{}^T & 0 & -I & 0 \end{bmatrix} + \begin{bmatrix} Q \\ 0 \\ 0 \\ 0 \\ 0 \\ 0 \\ 0 \end{bmatrix} M^{-1} \begin{bmatrix} Q & 0 & 0 & 0 & 0 & 0 & 0 \end{bmatrix} \tag{2.2-16}$$

Using the bound (2.1-3), the right side of (2.2-16) can be rewritten as

$$\begin{bmatrix} BNB^T & -\frac{\beta}{2}BND_z{}^T & -BND_f{}^T & -\sqrt{\delta}BND_z{}^T & 0 & -BN & 0 \\ * & \frac{\beta^2}{4}D_zND_z{}^T & \frac{\beta}{2}D_zND_f{}^T & \frac{\beta}{2}\sqrt{\delta}D_zND_z{}^T & 0 & \frac{\beta}{2}D_zN & 0 \\ * & * & D_fND_f{}^T & \sqrt{\delta}D_fND_z{}^T & 0 & D_fN & 0 \\ * & * & * & \delta D_zND_z{}^T & 0 & \sqrt{\delta}D_zN & 0 \\ * & * & * & * & 0 & 0 & 0 \\ * & * & * & * & * & N & 0 \\ * & * & * & * & * & * & 0 \end{bmatrix} + \begin{bmatrix} Q \\ 0 \\ 0 \\ 0 \\ 0 \\ 0 \end{bmatrix} M^{-1} \begin{bmatrix} Q \\ 0 \\ 0 \\ 0 \\ 0 \\ 0 \end{bmatrix}^T \tag{2.2-17}$$

Substituting (2.2-16) and (2.2-17) into (2.2-15) and use Lemma 1, we have

$$
\left[\begin{array}{c:c:c:c:c:c:c:c}
\begin{array}{l}-AQ-BY\\-QA-Y^TB\\-\alpha I-\Psi_{11}\\-BNB^T\end{array} & \begin{array}{l}\frac{\beta}{2}(QC_z^T+Y^TD_z^T)\\+\frac{\beta}{2}BND_z^T-F\end{array} & \begin{array}{l}QC_f^T\\+Y^TD_f^T\\+\Psi_{12}\\+BND_f^T\end{array} & \begin{array}{l}\sqrt{\delta}(QC_z^T\\+Y^TD_z^T\\+BND_z^T)\end{array} & Q & Y^T+BN & 0 & Q \\ \hdashline
* & \begin{array}{l}\frac{\beta}{2}(E_z^T+E_z)-\varepsilon I\\-\frac{\beta^2}{4}D_zND_z^T\end{array} & \begin{array}{l}E_f\\-\frac{\beta}{2}D_zND_f^T\end{array} & \begin{array}{l}\sqrt{\delta}(E_z\\-\frac{\beta}{2}D_zND_z^T)\end{array} & 0 & -\frac{\beta}{2}D_zN & \begin{array}{l}I\\-\frac{\beta}{2}D_zN\end{array} & 0 \\ \hdashline
* & * & \begin{array}{l}\alpha I-\Psi_{22}\\-D_fND_f^T\end{array} & -\sqrt{\delta}D_fND_z^T & 0 & -D_fN & 0 & 0 \\ \hdashline
* & * & * & I-\delta D_zND_z^T & 0 & -\sqrt{\delta}D_zN & 0 & 0 \\ \hdashline
* & * & * & * & \Phi_{11} & \Phi_{12} & \Phi_{13} & 0 \\ \hdashline
* & * & * & * & * & \Phi_{22}-N & \Phi_{23} & 0 \\ \hdashline
* & * & * & * & * & * & \Phi_{33} & 0 \\ \hdashline
* & * & * & * & * & * & * & M
\end{array}\right] > 0
$$

(2.2-18)

2.2.4 Case When Noise Is Not Present

This is a special case. When $w(t) = 0$, from (2.2-7) we only have

$$x^T h_{11} x > 0 \tag{2.2-19}$$

We want $h_{11} > 0$, which is

$$
\begin{aligned}
&-P(\tilde{A}+\tilde{B}\tilde{K})-(\tilde{A}+\tilde{B}\tilde{K})^T P-\alpha P^2\\
&-\alpha^{-1}(\tilde{C}_f+\tilde{D}_f\tilde{K})^T(\tilde{C}_f+\tilde{D}_f\tilde{K})-\delta(C_z+D_z\tilde{K})^T(C_z+D_z\tilde{K})>0
\end{aligned} \tag{2.2-20}
$$

By pre- and post-multiplying (2.2-20) by Q where $Q = P^{-1}$ and using

$\tilde{Y} = \tilde{K}Q = (K+\Delta_K)Q$, we obtain,

$$
\begin{aligned}
&-\tilde{A}Q-\tilde{B}\tilde{Y}-Q\tilde{A}^T-\tilde{Y}^T\tilde{B}^T-\alpha I-\alpha^{-1}(Q\tilde{C}_f^{\,T}+\tilde{Y}^T\tilde{D}_f^{\,T})(\tilde{C}_fQ+\tilde{D}_f\tilde{Y})\\
&-\delta(QC_z^T+\tilde{Y}^TD_z)(C_zQ+D_z\tilde{Y})>0
\end{aligned} \tag{2.2-21}
$$

Inequality (2.2-21) must be true in order to satisfy (2.1-11). Applying Lemma 1 to (2.2-21) results in

$$\left[\begin{array}{c|c} -\tilde{A}Q-\tilde{B}\tilde{Y}-Q\tilde{A}^{T}-\tilde{Y}^{T}\tilde{B}^{T}-\alpha I & \\ -\delta(QC_{z}^{T}+\tilde{Y}^{T}D_{z})(C_{z}Q+D_{z}\tilde{Y}) & Q\tilde{C}_{f}^{\ T}+\tilde{Y}^{T}\tilde{D}_{f}^{\ T} \\ \hline * & \alpha I \end{array}\right]>0 \tag{2.2-22}$$

Moving terms with $\Delta_A,\Delta_B,\Delta_F,\Delta_{C_f},\Delta_{D_f},\Delta_{E_f}$ to the right side of the inequality, we have

$$\begin{aligned} &\left[\begin{array}{c|c} -AQ-B\tilde{Y}-QA^{T}-\tilde{Y}^{T}B^{T}-\alpha I & \\ -\delta(QC_{z}^{T}+\tilde{Y}^{T}D_{z})(C_{z}Q+D_{z}\tilde{Y}) & QC_{f}^{\ T}+\tilde{Y}^{T}D_{f}^{\ T} \\ \hline * & \alpha I \end{array}\right] \\ &>\begin{bmatrix} \Delta_A Q+\Delta_B\tilde{Y}+Q\Delta_A^{\ T}+\tilde{Y}^T\Delta_B^{\ T} & -Q\Delta_{C_f}^{\ T}-\tilde{Y}^T\Delta_{D_f}^{\ T} \\ -\Delta_{C_f}Q-\Delta_{D_f}\tilde{Y} & 0 \end{bmatrix} \end{aligned} \tag{2.2-23}$$

The right side (2.2-23) of can be rewritten and can then be bounded by using Lemma 2 as

$$\begin{aligned} &\begin{bmatrix} \Delta_A Q+\Delta_B\tilde{Y}+Q\Delta_A^{\ T}+\tilde{Y}^T\Delta_B^{\ T} & -Q\Delta_{C_f}^{\ T}-\tilde{Y}^T\Delta_{D_f}^{\ T} \\ -\Delta_{C_f}Q-\Delta_{D_f}\tilde{Y} & 0 \end{bmatrix} \\ &=\begin{bmatrix} \Delta_A & \Delta_B \\ -\Delta_{C_f} & -\Delta_{D_f} \end{bmatrix}\begin{bmatrix} Q & 0 \\ \tilde{Y} & 0 \end{bmatrix}+\begin{bmatrix} Q & \tilde{Y}^T \\ 0 & 0 \end{bmatrix}\begin{bmatrix} \Delta_A^{\ T} & -\Delta_{C_f}^{\ T} \\ \Delta_B^{\ T} & -\Delta_{D_f}^{\ T} \end{bmatrix} \\ &\le\begin{bmatrix} I & 0 \\ 0 & -I \end{bmatrix}\begin{bmatrix} \Delta_A & \Delta_B \\ \Delta_{C_f} & \Delta_{D_f} \end{bmatrix}\begin{bmatrix} \Phi_{11} & \Phi_{12} \\ * & \Phi_{22} \end{bmatrix}\begin{bmatrix} \Delta_A^{\ T} & \Delta_{C_f}^{\ T} \\ \Delta_B^{\ T} & \Delta_{D_f}^{\ T} \end{bmatrix}\begin{bmatrix} I & 0 \\ 0 & -I \end{bmatrix}+\begin{bmatrix} Q & \tilde{Y}^T \\ 0 & 0 \end{bmatrix}\begin{bmatrix} \Phi_{11} & \Phi_{12} \\ * & \Phi_{22} \end{bmatrix}^{-1}\begin{bmatrix} Q & 0 \\ \tilde{Y} & 0 \end{bmatrix} \end{aligned} \tag{2.2-24}$$

Applying bound condition (2.1-10) to (2.2-24), we have

$$\begin{aligned} &\begin{bmatrix} \Delta_A Q+\Delta_B\tilde{Y}+Q\Delta_A^{\ T}+\tilde{Y}^T\Delta_B^{\ T} & -Q\Delta_{C_f}^{\ T}-\tilde{Y}^T\Delta_{D_f}^{\ T} \\ -\Delta_{C_f}Q-\Delta_{D_f}\tilde{Y} & 0 \end{bmatrix} \\ &>\begin{bmatrix} \Psi_{11} & -\Psi_{12} \\ * & \Psi_{22} \end{bmatrix}+\begin{bmatrix} Q & \tilde{Y}^T \\ 0 & 0 \end{bmatrix}\begin{bmatrix} \Phi_{11} & \Phi_{12} \\ * & \Phi_{22} \end{bmatrix}^{-1}\begin{bmatrix} Q & 0 \\ \tilde{Y} & 0 \end{bmatrix} \end{aligned} \tag{2.2-25}$$

Substituting (2.2-25) into (2.2-23) and applying Lemma 1, we have

$$\begin{bmatrix} -AQ-B\tilde{Y}-QA^T \\ -\tilde{Y}^T B^T-\alpha I-\Psi_{11} & QC_f^{\ T}+\tilde{Y}^T D_f^{\ T}+\Psi_{12} & \sqrt{\delta}(QC_z^{\ T}+\tilde{Y}^T D_z^{\ T}) & Q & \tilde{Y}^T \\ * & \alpha I-\Psi_{22} & 0 & 0 & 0 \\ * & * & I & 0 & 0 \\ * & * & * & \Phi_{11} & \Phi_{12} \\ * & * & * & * & \Phi_{22} \end{bmatrix} > 0 \quad (2.2\text{-}26)$$

Moving the terms with Δ_K to the right side of (2.2-26), we have

$$\left[\begin{array}{c:c:c:c:c} -AQ-BY-QA^T-Y^T B^T & QC_f^{\ T}+Y^T D_f^{\ T} & \sqrt{\delta}(QC_z^{\ T}+Y^T D_z^{\ T}) & Q & Y^T \\ -\alpha I-\Psi_{11} & +\Psi_{12} & & & \\ \hdashline * & \alpha I-\Psi_{22} & 0 & 0 & 0 \\ \hdashline * & * & I & 0 & 0 \\ \hdashline * & * & * & \Phi_{11} & \Phi_{12} \\ \hdashline * & * & * & * & \Phi_{22} \end{array}\right] \quad (2.2\text{-}27)$$

$$> \left[\begin{array}{c:c:c:c:c} B\Delta_k Q+Q\Delta_k^{\ T}B^T & -Q\Delta_k^{\ T}D_f^{\ T} & -\sqrt{\delta}Q\Delta_k^{\ T}D_z^{\ T} & 0 & -Q\Delta_k^{\ T} \\ \hdashline * & 0 & 0 & 0 & 0 \\ \hdashline * & * & 0 & 0 & 0 \\ \hdashline * & * & * & 0 & 0 \\ \hdashline * & * & * & * & 0 \end{array}\right]$$

A bound for the right side of (2.2-27) is found by applying Lemma 2 as

$$\begin{bmatrix} B \\ -D_f \\ -\sqrt{\delta}D_z \\ 0 \\ -I \end{bmatrix}\Delta_k\begin{bmatrix} Q & 0 & 0 & 0 & 0 \end{bmatrix}+\begin{bmatrix} Q \\ 0 \\ 0 \\ 0 \\ 0 \end{bmatrix}\Delta_k^{\ T}\begin{bmatrix} B^T & -D_f^{\ T} & -\sqrt{\delta}D_z^{\ T} & 0 & -I \end{bmatrix}$$

$$\leq \begin{bmatrix} B \\ -D_f \\ -\sqrt{\delta}D_z \\ 0 \\ -I \end{bmatrix}\Delta_k M\Delta_k^{\ T}\begin{bmatrix} B^T & -D_f^{\ T} & -\sqrt{\delta}D_z^{\ T} & 0 & -I \end{bmatrix}+\sigma\begin{bmatrix} Q \\ 0 \\ 0 \\ 0 \\ 0 \end{bmatrix}M^{-1}\begin{bmatrix} Q & 0 & 0 & 0 & 0 \end{bmatrix} \quad (2.2\text{-}28)$$

Using the bound (2.1-3), the right side of (2.2-28) can be rewritten as

$$\begin{bmatrix} BNB^T & -BND_f^{\ T} & -\sqrt{\delta}BND_z^{\ T} & 0 & -BN \\ * & D_f ND_f^{\ T} & \sqrt{\delta}D_f ND_z^{\ T} & 0 & D_f N \\ * & * & \delta D_z ND_z^{\ T} & 0 & \sqrt{\delta}D_z N \\ * & * & * & 0 & 0 \\ * & * & * & * & N \end{bmatrix} + \begin{bmatrix} Q \\ 0 \\ 0 \\ 0 \\ 0 \end{bmatrix} M^{-1} \begin{bmatrix} Q & 0 & 0 & 0 & 0 \end{bmatrix} \quad (2.2\text{-}29)$$

Substituting (2.2-28) and (2.2-29) into (2.2-27) and use Lemma 1, we have

$$\left[\begin{array}{c|c|c|c|c|c} \begin{matrix} -AQ - BY - QA^T - Y^T B^T \\ -\alpha I - \Psi_{11} - BNB^T \end{matrix} & \begin{matrix} QC_f^{\ T} + Y^T D_f^{\ T} \\ +\Psi_{12} + BND_f^{\ T} \end{matrix} & \begin{matrix} (QC_z^{\ T} + Y^T D_z^{\ T} \\ +BND_z^{\ T})\sqrt{\delta} \end{matrix} & Q & Y^T + BN & Q \\ \hline * & \begin{matrix} \alpha I - \Psi_{22} \\ -D_f ND_f^{\ T} \end{matrix} & -\sqrt{\delta}D_f ND_z^{\ T} & 0 & -D_f N & 0 \\ \hline * & * & I - \delta D_z ND_z^{\ T} & 0 & -\sqrt{\delta}D_z N & 0 \\ \hline * & * & * & \Phi_{11} & \Phi_{12} & 0 \\ \hline * & * & * & * & \Phi_{22} - N & 0 \\ \hline * & * & * & * & * & M \end{array}\right] > 0 \quad (2.2\text{-}30)$$

This completes the theorem and corollaries.

2.3 Simulation Studies

This section contains some simulation results of controller designs proposed in this chapter. The controllers for two different systems – one with unstable behavior and a second with chaotic behavior – are designed to demonstrate possible applications of the proposed design procedure.

In the following examples, we choose $M=I$ and N as a scalar σ in (2.1-3), similarly for Φ, Ψ in (2.1-10). So (2.1-3) and (2.1-10) become:

$$\Delta_K \Delta_K^{\ T} \le \sigma I \quad (2.3\text{-}1)$$

$$\begin{bmatrix} \Delta_A & \Delta_B & \Delta_F \\ \Delta_{C_f} & \Delta_{D_f} & \Delta_{E_f} \end{bmatrix} \begin{bmatrix} \Delta_A{}^T & \Delta_{C_f}{}^T \\ \Delta_B{}^T & \Delta_{D_f}{}^T \\ \Delta_F{}^T & \Delta_{E_f}{}^T \end{bmatrix} \le \gamma I \tag{2.3-2}$$

Example 2-1. The state space model of an unstable system is given by:

$$\begin{bmatrix} \dot{x}_1 \\ \dot{x}_2 \end{bmatrix} = \begin{bmatrix} -0.3 & 1 \\ -1 & 1 \end{bmatrix} \begin{bmatrix} x_1 \\ x_2 \end{bmatrix} + \begin{bmatrix} 0 \\ -\sin x_1 \end{bmatrix} + \begin{bmatrix} 1 \\ 1 \end{bmatrix} u + \begin{bmatrix} 1 \\ 1 \end{bmatrix} w \tag{2.3-3}$$

The finite energy disturbance w is chosen to be a sinusoidal wave $5\sin(0.3t)$ only added from 1 to 3 second showing in Figure 2.3-1.

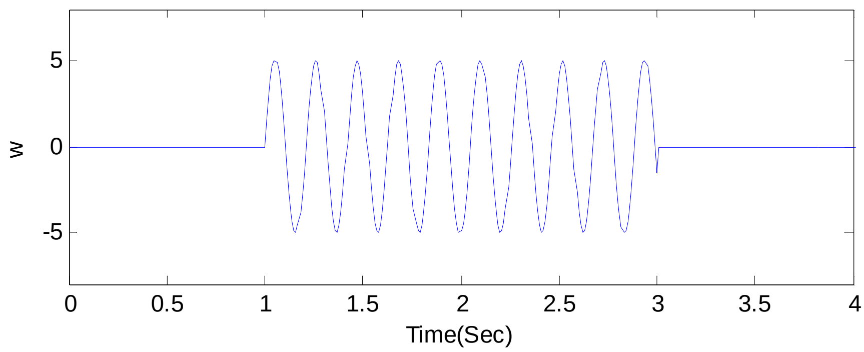

Figure 2.3-1 Finite disturbance used in example 2-1

The objective of this example is H_∞ control. The performance parameters are chosen to be $\delta = 1, \beta = 0, \varepsilon = -1$. And other system parameters are given in Table 2-1.

Table 2-1 Design parameters of the example 2-1

C_z	D_z	E_z	C_f	D_f	E_f
$0.1*I_2$	[0.1; 0.1]	$0.1*I_2$	$0.1*I_2$	[0.1; 0.1]	$0.1*I_2$

The time responses of the state variables of the open loop system which shows fast divergence are given in Figure 2.3-2.

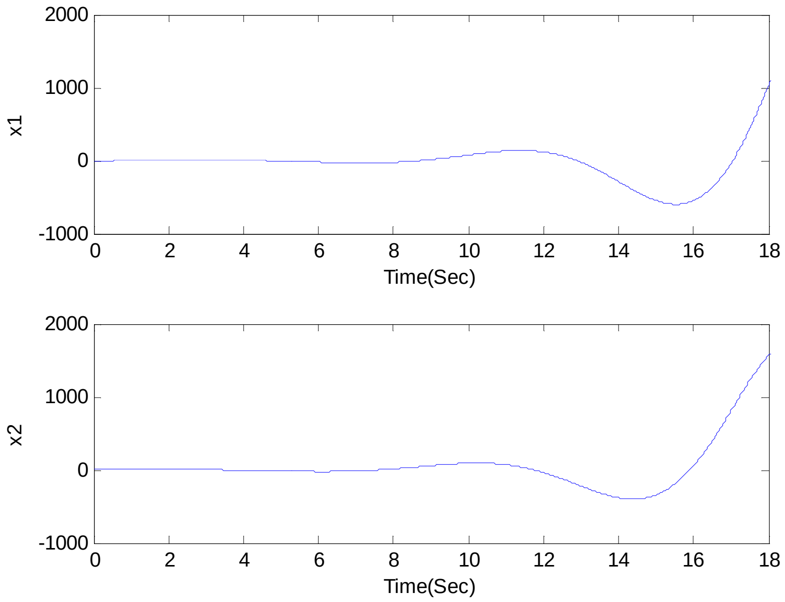

Figure 2.3-2 The state variables of the open loop system

For the given system and the performance criteria chosen, the controller gain from LMI (2.2-1) is found to be K=[-7.39, 2.40] with a maximum σ value of 0.68 solve form the LMI.

To test the feedback gain perturbation bound of σ, we choose a perturbed gain K_p=[-7, 2.8], whose σ_p value is calculated to be 0.56, within the bound of 0.68. A co-plot of the states of perturbed and unperturbed gains is given in Figure 2.3-3 showing that the perturbed gain is able to stabilize the system.

Recalling the H_∞ criterion formula $\int_0^t \|z(\tau)\|^2 d\tau < -\varepsilon \int_0^t \|w(\tau)\|^2)d\tau$. Calculations are done via the data from perturbed system simulation to validate the criterion in the following:

$$\begin{aligned} &\int_0^t \|z(\tau)\|^2 d\tau = 88.66 \\ -\varepsilon &\int_0^t \|w(\tau)\|^2 = 4979 \end{aligned} \tag{2.3-4}$$

which shows that the H_∞ criterion is achieved with the perturbed feedback gain K_p, also showing the effectiveness of the proposed control design method.

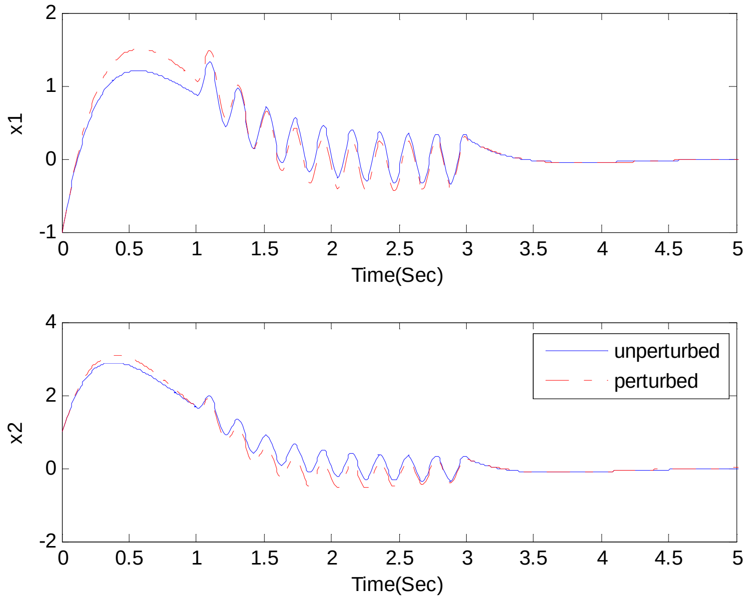

Figure 2.3-3 The co-plot of the state variables of the controlled system with unperturbed and perturbed gain

Example 2-2. This example contains the comparison of simulation results for all the controller designs proposed in this work using Chua's circuit with chaotic behavior. The state space model is given as follows,

$$\begin{bmatrix} \dot{x}_1 \\ \dot{x}_2 \\ \dot{x}_3 \end{bmatrix} = \begin{bmatrix} -\alpha_c & \alpha_c & 0 \\ 1 & -1 & 1 \\ 0 & -\beta_c & -\mu \end{bmatrix} \begin{bmatrix} x_1 \\ x_2 \\ x_3 \end{bmatrix} - \begin{bmatrix} \alpha_c f(x_1) \\ 0 \\ 0 \end{bmatrix} + \begin{bmatrix} 7 \\ 1 \\ 1 \end{bmatrix} u + \begin{bmatrix} 1 \\ 0 \\ 0 \end{bmatrix} w \tag{2.3-5}$$

where $w = e^{-t}$, $f(x_1) = bx_1 + 0.5(a-b)(|x_1+1| - |x_1-1|)$, with the parameters

$\alpha_c = 9.1,\ \beta_c = 16.5811,\ \mu = 0.138083,\ a = -1.3659,\ b = -0.7408$.

The design criteria parameters are given in Table 2-2.

Table 2-2 Design parameters of Example 2-2

	Asy. Stb.	H_2 Ctrl.	H_∞ Ctrl.	Input S. P.	Output S. P.	Very S. P.
δ	0	1	1	0	1	1
β	0	0	0	1	1	1
ε	0	0	-1	0.05	0	0.05

For all cases, C_f, C_z and D_f, D_z are chosen to be 0.1*I_3 and [0.1; 0.1; 0.1], respectively. E_f, E_z are chosen to be 0.1*I_3 for the noisy cases and the zero matrix for non-noisy cases.

The time evolution of the state variables of the open loop chaotic Chua's circuit is shown in Figure 2.3-4. The initial values of the state variables were chosen to be [1;1;1].

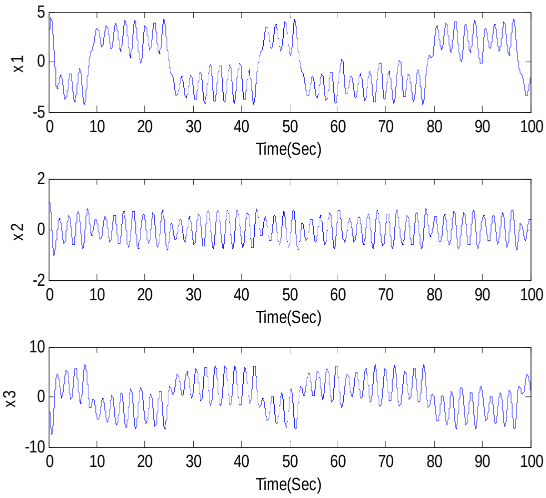

Figure 2.3-4 The state variables of open loop Chua's circuit

For each type of controller design, the feedback gain K for the unperturbed system, and $\sigma_{\max}$, the bound on the gain perturbation which results from the solution of the LMI, are shown in Table 2-3. For the simulation studies, the feedback gains are perturbed as shown in Table 2-3. The value of σ_P is also shown in Table 2-3, which results for this SISO system by applying (2.1-3) using $\Delta_K = K - K_p$.

Table 2-3 Feedback gain K , perturbed gain K_p and their corresponding $\sigma_{\max}$, σ_P

	Feedback Gain K	Perturbed Gain K_p	$\sigma_{\max}$	σ_P
Asy. Stb.	[-1.15 -13.61 1]	[-0.9 -13.3 0.8]	0.56	0.45
***H₂* Ctrl.**	[-2.3 -15.52 1.19]	[-2.1 -15.3 1.3]	0.36	0.31
H_∞ Ctrl.	[-1.72 -12.15 0.91]	[-1.6 -12 1]	0.23	0.21
Input S. P.	[-0.91 -5.99 0.036]	[-0.8 -6 0.1]	0.15	0.13
Output S. P.	[-0.599 -5.69 0.05]	[-0.7 -5.6 0.1]	0.18	0.14
Very S. P.	[-0.77 -5.02 -0.94]	[-0.8 -5.1 -1]	0.12	0.1

To verify the robustness and resilience property of the controller, the system matrix and coefficients of the nonlinearity are perturbed as follows

$$\alpha_c = 8.9,\ \beta_c = 17\ \mu = 0.15,\ a = -1.4, b = -0.76$$

and the feedback gain K is perturbed as shown in Table 2-3. After the proposed control is applied, we see the controlled perturbed system in Figure 2.3-5 for non-noisy cases and in Figure 2.3-6 for noisy cases. Since the feedback gains are perturbed within the bound of $\sigma_{\max}$ given in Table 2-3, the systems are still controlled and the desired performance criteria are still achieved, demonstrating the effectiveness of the design method of this paper.

The validation of all the performance criteria is given in the following table. Values in the left columns are values can be calculated before running the simulation while values in the right columns are calculated from simulation results.

Table 2-4 Validation of the performance criteria

Criteria	Pre-calculated Values		Simulation Results
Input S. P.	$\varepsilon \sum_i \lVert w_i \rVert^2$		$\sum_i z_i^T w_i$
	2.475	<	3.65
H_2 Ctrl.	$\delta^{-1} \lVert x_0 \rVert^2$		$\sum_i \lVert z_i \rVert^2 \Big/ \lambda_{\max}(P)$
	3	>	2.54
H_∞ Ctrl.	$-\varepsilon \sum_i \lVert w_i \rVert^2$		$\sum_i \lVert z_i \rVert^2$
	49.5	>	36.24
Output S. P.	0		$\sum_i z_i^T w_i - \delta \sum_i \lVert z_i \rVert^2$
	0	<	2.43
Very S. P.	$\varepsilon \sum_i \lVert w_i \rVert^2$		$\sum_i z_i^T w_i - \delta \sum_i \lVert z_i \rVert^2$
	2.475	<	3.95

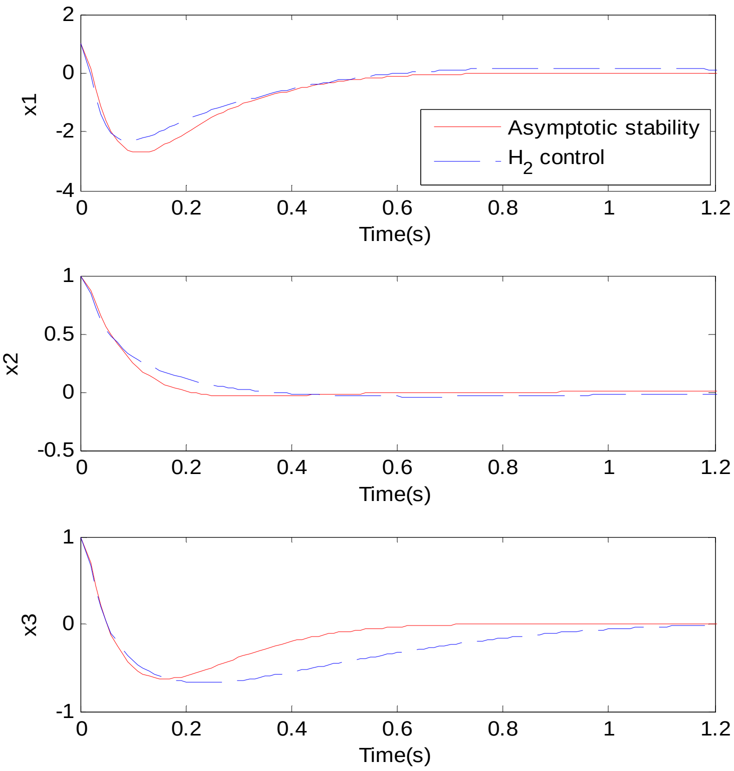

Figure 2.3-5 The state variables of Chua's circuit with the controller having perturbed control gain for non-noisy cases.

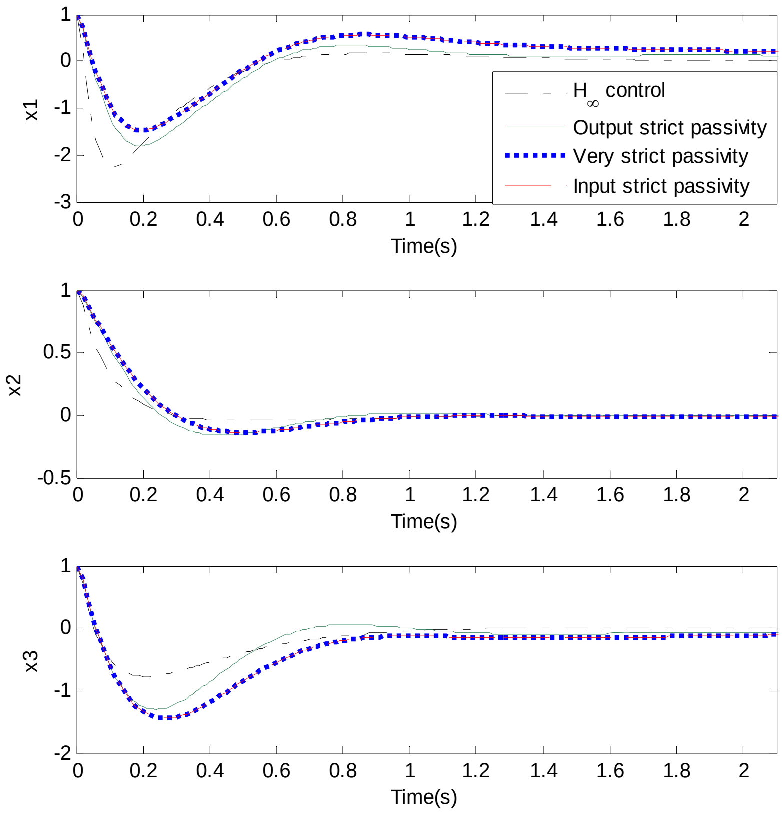

Figure 2.3-6 The state variables of Chua's circuit with the controller having perturbed control gain for noisy cases.

2.4 Robust Controller design, Special Case I

In this section, we discuss a special case of the robust controller design with only perturbations in the system parameters and no perturbation in the feedback gain.

2.4.1 System Model and Performance Criteria

System model is described as (2.1-1) and (2.1-8) and its perturbations as (2.1-7), (2.1-9) and (2.1-10).

The linear state feedback control is used as

$$u = Kx \tag{2.4-1}$$

Performance criteria remain the same as defined in Table 1-1.

2.4.2 LMI Formulation

The derivation of the LMI formulation is similar with the process from (2.2-3) to (2.2-14) for the noisy case and from (2.2-19) to (2.2-26) for the non-noisy case. Because there are no perturbations on the gain, (i.e. no Δ_K terms), by replacing $\tilde{Y}$ with Y in (2.2-14), we obtain the LMI result for noisy case. A similar derivation can be done for the non-noisy case.

So, the LMI results for the noisy and non-noisy case are given as follows,

$$\left[\begin{array}{c|c|c|c|c|c|c}
\begin{matrix}-AQ-BY\\ -QA-Y^TB\\ -\alpha I-\Psi_{11}\end{matrix} & \begin{matrix}\frac{\beta}{2}(QC_z^T+Y^TD_z^T)\\ -F\end{matrix} & \begin{matrix}QC_f^T\\ +Y^TD_f^T\\ +\Psi_{12}\end{matrix} & \begin{matrix}\sqrt{\delta}(QC_z^T\\ +Y^TD_z^T)\end{matrix} & Q & Y^T & 0 \\ \hline
* & \begin{matrix}\frac{\beta}{2}(E_z^T+E_z)\\ -\varepsilon I\end{matrix} & E_f & \sqrt{\delta}E_z & 0 & 0 & I \\ \hline
* & * & \alpha I-\Psi_{22} & 0 & 0 & 0 & 0 \\ \hline
* & * & * & I & 0 & 0 & 0 \\ \hline
* & * & * & * & \Phi_{11} & \Phi_{12} & \Phi_{13} \\ \hline
* & * & * & * & * & \Phi_{22} & \Phi_{23} \\ \hline
* & * & * & * & * & * & \Phi_{33}
\end{array}\right] > 0 \tag{2.4-2}$$

$$\left[\begin{array}{c:c:c:c:c} -AQ-BY-QA^T-Y^TB^T & QC_f^{\ T}+Y^TD_f^{\ T} & \sqrt{\delta}(QC_z^{\ T}+Y^TD_z^{\ T}) & Q & Y^T \\ -\alpha I-\Psi_{11} & +\Psi_{12} & & & \\ \hdashline * & \alpha I-\Psi_{22} & 0 & 0 & 0 \\ \hdashline * & * & I & 0 & 0 \\ \hdashline * & * & * & \Phi_{11} & \Phi_{12} \\ \hdashline * & * & * & * & \Phi_{22} \end{array}\right]>0 \quad (2.4\text{-}3)$$

2.5 Resilient Controller design, Special Case II

In this section, we discuss a special case of the resilient controller design with only perturbations in the feedback gain and no perturbation in the system parameters.

2.5.1 System Model and Performance Criteria

System model is described as (2.1-1) and state feedback control (2.1-2) and its perturbation (2.1-3). The linear and nonlinear components of the system as shown in (2.1-5) to (2.1-8) no longer have parameter perturbations.

Performance criteria remain the same as defined in Table 1-1.

2.5.2 LMI Formulation

For non-noisy cases, following the similar derivation process from (2.2-3) to (2.2-9), we have

$$\begin{bmatrix} -AQ-B\tilde{Y} \\ -QA^T-\tilde{Y}^TB^T-\alpha I & \frac{\beta}{2}(QC_z{}^T+\tilde{Y}^TD_z{}^T)-F & QC_f{}^T+\tilde{Y}^TD_f{}^T & \sqrt{\delta}(QC_z{}^T+\tilde{Y}^TD_z{}^T) \\ * & -\varepsilon I+\frac{\beta}{2}(E_z{}^T+E_z) & E_f & \sqrt{\delta}E_z \\ * & * & \alpha I & 0 \\ * & * & * & I \end{bmatrix} > 0$$

(2.5-1)

Then follow a similar process from (2.2-14) to (2.2-18), we have

$$\left[\begin{array}{c|c|c|c|c} \begin{matrix} -AQ-BY \\ -QA^T-Y^TB^T \\ -\alpha I-BNB^T \end{matrix} & \begin{matrix} \frac{\beta}{2}(QC_z{}^T+Y^TD_z{}^T) \\ +\frac{\beta}{2}BND_z{}^T-F \end{matrix} & \begin{matrix} QC_f{}^T+Y^TD_f{}^T \\ +BND_f{}^T \end{matrix} & \begin{matrix} \sqrt{\delta}(QC_z{}^T+Y^TD_z{}^T \\ +BND_z{}^T) \end{matrix} & Q \\ \hline * & \begin{matrix} \frac{\beta}{2}(E_z{}^T+E_z)-\varepsilon I \\ -\frac{\beta^2}{4}D_zND_z{}^T \end{matrix} & E_f-\frac{\beta}{2}D_zND_f{}^T & \sqrt{\delta}(E_z-\frac{\beta}{2}D_zND_z{}^T) & 0 \\ \hline * & * & \alpha I-D_fND_f{}^T & -\sqrt{\delta}D_fND_z{}^T & 0 \\ \hline * & * & * & I-\delta D_zND_z{}^T & 0 \\ \hline * & * & * & * & M \end{array}\right] > 0$$

(2.5-2)

For non-noisy cases, following the similar derivation process from (2.2-19) to (2.2-22), we have

$$\begin{bmatrix} -AQ-B\tilde{Y}-QA^T-\tilde{Y}^TB^T-\alpha I & QC_f{}^T+\tilde{Y}^TD_f{}^T & \sqrt{\delta}(QC_z{}^T+\tilde{Y}^TD_z{}^T) \\ * & \alpha I & 0 \\ * & * & I \end{bmatrix} > 0 \quad (2.5\text{-}3)$$

Then follow a similar process from (2.2-27) to (2.2-30), we have

$$\left[\begin{array}{c|c|c|c} \begin{matrix} -AQ-B\tilde{Y}-QA^T-\tilde{Y}^TB^T \\ -\alpha I-BNB^T \end{matrix} & \begin{matrix} QC_f{}^T+\tilde{Y}^TD_f{}^T \\ +BND_f{}^T \end{matrix} & \begin{matrix} \sqrt{\delta}(QC_z{}^T+\tilde{Y}^TD_z{}^T \\ +BND_z{}^T) \end{matrix} & Q \\ \hline * & \alpha I-D_fND_f{}^T & -\sqrt{\delta}D_fND_z{}^T & 0 \\ \hline * & * & I-\delta D_zND_z{}^T & 0 \\ \hline * & * & * & M \end{array}\right] > 0 \quad (2.5\text{-}4)$$

The same system (2.3-5) in example 2-2 is simulated to compare the maximum perturbation results of Section 2.2 and Section 2.5, giving in the following table.

Table 2-5 Comparison of maximum perturbation bound

	$\sigma_{\max}$ of Section 2.2	$\sigma_{\max}$ of Section 2.5
Asy. Stb.	0.56	0.98
***H*₂ Ctrl.**	0.36	0.82
H_∞ Ctrl.	0.23	0.66
Input S. P.	0.15	0.53
Output S. P.	0.18	0.39
Very S. P.	0.12	0.24

Table 2-5 shows that in the proposed method in this chapter, without the systems parameters perturbation, maximum perturbations allowed in the feedback gain can be larger.

2.6 Conclusion

In this chapter, a robust and resilient state feedback controller design has been presented for a class of uncertain nonlinearities for general performance criteria. Uncertainties are allowed in both the center and the radius of the cone in which the nonlinearity resides as well as the feedback gain. With this method, control systems can be more robust and allow less accurate system models to be controlled. We have shown that a common framework for various performance criteria using linear matrix inequality techniques can be developed to solve the proposed controller design problem. Simulation results illustrate the developed theory.

CHAPTER 3

DISCRETE-TIME ROBUST AND RESILIENT CONTROLLER DESIGN WITH GENERAL CRITERIA FOR UNCERTAIN CONIC NONLINEAR SYSTEMS WITH DISTURBANCES

3.0 Introduction

In this chapter, a discrete-time robust and resilient state feedback scheme is proposed to control a large class of uncertain nonlinear systems with locally conic type nonlinearities and driven by finite energy disturbances using linear matrix inequalities. In order to allow the robust control of systems whose models contain a higher degree of uncertainty, perturbations regarding the center and the boundaries of the cone in which the nonlinearity resides are considered in this chapter. The resilience property is achieved in the presence of bounded perturbations in the feedback gain. Results are presented for various performance criteria in a unified design framework. Illustrative examples are included to demonstrate the effectiveness of the proposed methodology.

In Section 3.1, the system model and the uncertain nonlinearities are introduced and in Section 3.2, LMI formulations are derived for several cases and the main theorem is given. Section 3.3 contains two simulations studies of two different types of system. Two special cases of the design method proposed in this chapter are discussed in Section 2.4 and 2.5.

3.1 Problem Formulation

Let us consider a discrete-time nonlinear system,

$$x_{k+1} = f(x_k, u_k, w_k) \tag{3.1-1}$$

where $x_k \in R^n$ is the state, $u_k \in R^m$ is the input, and $w_k \in R^w$ is an l_2 disturbance input.

A linear state feedback control is used in this system

$$u_k = Kx_k \tag{3.1-2}$$

where the feedback gain K is perturbed as $\tilde{K} = K + \Delta_K$, with the perturbation bounded as,

$$\Delta_K{}^T M \Delta_K \le N \tag{3.1-3}$$

A resilient control design is used to accommodate the perturbations on the feedback gain.

The performance output is given as

$$z_k = C_z x_k + D_z u_k + E_z w_k \tag{3.1-4}$$

It is assumed that the nonlinear function is analytic and can be expanded into a linear component,

$$x_{k+1,lin} = \tilde{A} x_k + \tilde{B} u_k + \tilde{F} w_k \tag{3.1-5}$$

And a nonlinear component $\mathfrak{F}$

$$\mathfrak{F} = f(x_k, u_k, w_k) - (\tilde{A} x_k + \tilde{B} u_k + \tilde{F} w_k) \tag{3.1-6}$$

It is assumed that there is uncertainty in the linear part, so that the system parameters are perturbed where

$$\tilde{A} = A + \Delta_A, \tilde{B} = B + \Delta_B, \tilde{F} = F + \Delta_F \tag{3.1-7}$$

It is also assumed that the nonlinear part of the system satisfies

$$\begin{aligned}\mathfrak{F}^T\mathfrak{F} &= \left\| f(x_k, u_k, w_k) - (\tilde{A}x_k + \tilde{B}u_k + \tilde{F}w_k) \right\|^2 \\ &\le \alpha(\tilde{C}_f x_k + \tilde{D}_f u_k + \tilde{E}_f w_k)^T (\tilde{C}_f x_k + \tilde{D}_f u_k + \tilde{E}_f w_k)\end{aligned} \tag{3.1-8}$$

There is also uncertainty regarding the maximum deviation from the linear part, so that the boundary parameters are perturbed where

$$\tilde{C}_f = C_f + \Delta_{C_f}, \tilde{D}_f = D_f + \Delta_{D_f}, \tilde{E}_f = E_f + \Delta_{E_f} \tag{3.1-9}$$

Similarly as stated in Section 2.1, by having perturbations on both system parameters and radius parameters as given in (3.1-7) and (3.1-9), we will have robustness on both the center line and the radius of the cone, i.e., we can have uncertainties in both the linear and nonlinear parts of the system.

Figure 2.1-1 also relates to the discrete-time case for the scalar case with no noise. The cone in which the nonlinearity resides is shown as the shaded region.

The perturbations $\Delta_A, \Delta_B, \Delta_F, \Delta_{C_f}, \Delta_{D_f}, \Delta_{E_f}$ are bounded as follows,

$$\begin{bmatrix} \Delta_A & \Delta_B & \Delta_F \\ \Delta_{C_f} & \Delta_{D_f} & \Delta_{E_f} \end{bmatrix} \Phi \begin{bmatrix} \Delta_A{}^T & \Delta_{C_f}{}^T \\ \Delta_B{}^T & \Delta_{D_f}{}^T \\ \Delta_F{}^T & \Delta_{E_f}{}^T \end{bmatrix} \le \Psi \tag{3.1-10}$$

where $\Phi = \begin{bmatrix} \Phi_{11} & \Phi_{12} & \Phi_{13} \\ & \Phi_{22} & \Phi_{23} \\ * & & \Phi_{33} \end{bmatrix}, \Psi = \begin{bmatrix} \Psi_{11} & \Psi_{12} \\ * & \Psi_{22} \end{bmatrix}$ are positive definite symmetric matrices.

Let us consider the discrete-time inequality

$$V_k - V_{k+1} - \delta \|z_k\|^2 - \varepsilon \|w_k\|^2 + \beta z_k{}^T w_k > 0 \tag{3.1-11}$$

as introduced in Section 1.5. The continuous time performance criteria given in Table 1-2 are used in this design.

3.2 LMI Formulations and Main Result

In this section, the main theorem of the controller is given and the proof of the theorem for various cases is derived.

3.2.1 Main Theorem

Theorem 3-1. There exists a resilient and robust state feedback controller (3.1-2) for systems with conic-type nonlinearity (3.1-8) and performance output (3.1-4), if the LMI (3.2-1) is feasible for some Y, and the positive definite matrices Q, M, N, Φ, Ψ and α. The control gain is found by $K = YQ^{-1}$. In addition, for design parameters $\delta > 0$, $\beta = 1, \varepsilon > 0$, the very strict passivity criterion is also satisfied.

$$S_1 = \begin{bmatrix} s_{11} & s_{12} & s_{13} & s_{14} & s_{15} & s_{16} & s_{17} & s_{18} & s_{19} \\ & s_{22} & s_{23} & s_{24} & s_{25} & s_{26} & s_{27} & s_{28} & s_{29} \\ & & s_{33} & s_{34} & s_{35} & s_{36} & s_{37} & s_{38} & s_{39} \\ & & & s_{44} & s_{45} & s_{46} & s_{47} & s_{48} & s_{49} \\ & & & & s_{55} & s_{56} & s_{57} & s_{58} & s_{59} \\ & & & & & s_{66} & s_{67} & s_{68} & s_{69} \\ & & * & & & & s_{77} & s_{78} & s_{79} \\ & & & & & & & s_{88} & s_{89} \\ & & & & & & & & s_{99} \end{bmatrix} > 0 \qquad (3.2\text{-}1)$$

where the matrices elements, S_{ij}, are given as,

$$s_{11} = Q,$$
$$s_{12} = \frac{\beta}{2}(QC_z^{\ T} + Y^T D_z^{\ T}),$$
$$s_{13} = QA^T + Y^T B^T,$$
$$s_{14} = QC_f^{\ T} + Y^T D_f^{\ T},$$
$$s_{15} = \sqrt{\delta}(QC_z^{\ T} + Y^T D_z^{\ T}),$$
$$s_{16} = Q,$$
$$s_{17} = Y^T,$$
$$s_{18} = 0,$$
$$s_{19} = Q,$$
$$s_{22} = \frac{\beta}{2}(E_z + E_z^{\ T}) - \varepsilon I - \frac{\beta^2}{4} D_z D_z^{\ T}$$
$$s_{23} = F^T - \frac{\beta}{2} D_z N B^T,$$
$$s_{24} = E_f^{\ T} - \frac{\beta}{2} D_z N D_f^{\ T},$$
$$s_{25} = \sqrt{\delta}(E_z^{\ T} - \frac{\beta}{2} D_z N D_z^{\ T}),$$
$$s_{26} = 0,$$
$$s_{27} = -\frac{\beta}{2} D_z N,$$
$$s_{28} = I,$$
$$s_{29} = 0,$$
$$s_{33} = Q - \alpha I - \Psi_{11} - BNB^T,$$
$$s_{34} = -\Psi_{12} - BND_f^{\ T},$$
$$s_{35} = -\sqrt{\delta} BND_z^{\ T},$$
$$s_{36} = 0,$$
$$s_{37} = -BN,$$
$$s_{38} = s_{39} = 0,$$
$$s_{44} = -\Psi_{22} - D_f N D_f^{\ T},$$
$$s_{45} = -\sqrt{\delta} D_f N D_z^{\ T},$$
$$s_{46} = s_{48} = s_{49} = 0,$$
$$s_{47} = -BN,$$
$$s_{55} = I - \delta D_z N D_z^{\ T},$$
$$s_{56} = s_{58} = s_{59} = 0,$$
$$s_{57} = -\sqrt{\delta} D_z N,$$
$$s_{66} = \Phi_{11},$$
$$s_{67} = \Phi_{12},$$
$$s_{68} = \Phi_{13},$$

$s_{69} = 0,$
$s_{77} = \Phi_{22} - N,$
$s_{78} = \Phi_{23},$
$s_{79} = 0,$
$s_{88} = \Phi_{33},$
$s_{89} = 0,$
$s_{99} = M$

Comments: In the above LMI, system parameters *A, B,* C_z , D_z , E_z, nonlinear bound parameters C_f , D_f , E_f and performance parameters *δ, β, ε* are all known. The unknowns are *Q, Y*, intermediate (slack) variable *α*, and the perturbation bound parameters *M, N,* Φ and Ψ. All unknowns are in linear form in the above LMI.

Corollary 3-1. For design parameters $\delta > 0, \beta = 1, \varepsilon = 0$, Theorem 3-1 holds for the output strict passivity criterion.

Corollary 3-2. For design parameters $\delta = 1, \beta = 0, \varepsilon < 0$, Theorem 3-1 holds for the H_∞ controller criterion.

Corollary 3-3. For design parameters $\delta = 0, \beta = 1, \varepsilon > 0$, Theorem 3-1 holds for the input strict passivity criterion.

Corollary 3-4. For design parameters $\delta > 0, \beta = 0, \varepsilon = 0$, and replacing LMI (3.2-1) with LMI (3.2-2), then Theorem 3-1 holds for the H_2 controller criterion.

$$S_2 = \begin{bmatrix} s_{11} & s_{13} & s_{14} & s_{15} & s_{16} & s_{17} & s_{19} \\ & s_{33} & s_{34} & s_{35} & s_{36} & s_{37} & s_{39} \\ & & s_{44} & s_{45} & s_{46} & s_{47} & s_{49} \\ & & & s_{55} & s_{56} & s_{57} & s_{59} \\ & & & & s_{66} & s_{67} & s_{69} \\ & & * & & & s_{77} & s_{79} \\ & & & & & & s_{99} \end{bmatrix} > 0 \qquad (3.2\text{-}2)$$

Corollary 3-5. For design parameters $\delta = 0, \beta = 0, \varepsilon = 0$, and replacing LMI (3.2-1) with LMI (3.2-2), then Theorem 3-1 holds for Asymptotic stability.

The proof of the theorem is given for several cases in the next a few sections.

3.2.2 General Form

The development leading to an LMI framework is given below.

Substituting V_k and V_{k+1} into (3.1-11), we have

$$x_k^T P x_k - \delta \|z_k\|^2 - \varepsilon \|w_k\|^2 + \beta z_k^T w_k - (x_{k+1,lin} + \mathfrak{F})^T P (x_{k+1,lin} + \mathfrak{F}) \geq 0 \qquad (3.2\text{-}3)$$

Applying Lemma 1 and moving all terms containing $\mathfrak{F}$ to the right hand side of the inequality, we have

$$\begin{bmatrix} x_k^T P x_k - \delta \|z_k\|^2 - \varepsilon \|w_k\|^2 + \beta z_k^T w_k & x_{k+1,lin}{}^T P \\ P x_{k+1,lin} & P \end{bmatrix} \geq \begin{bmatrix} 0 & -\mathfrak{F}^T P \\ -P\mathfrak{F} & 0 \end{bmatrix} \qquad (3.2\text{-}4)$$

From the non-negative definite matrix with $\alpha > 0$

$$\begin{bmatrix} \alpha^{-0.5}\mathfrak{F}^T \\ \alpha^{0.5} P \end{bmatrix} \begin{bmatrix} \alpha^{-0.5}\mathfrak{F} & \alpha^{0.5} P \end{bmatrix} = \begin{bmatrix} \alpha^{-1}\mathfrak{F}^T\mathfrak{F} & \mathfrak{F}^T P \\ P\mathfrak{F} & \alpha P^2 \end{bmatrix} \geq 0 \qquad (3.2\text{-}5)$$

we obtain,

$$\begin{bmatrix} \alpha^{-1}\mathfrak{F}^T\mathfrak{F} & 0 \\ 0 & \alpha P^2 \end{bmatrix} \geq \begin{bmatrix} 0 & \mathfrak{F}^T P \\ P\mathfrak{F} & 0 \end{bmatrix} \qquad (3.2\text{-}6)$$

Then the following inequality

$$\begin{bmatrix} x_k^T P x_k - \delta \|z_k\|^2 - \varepsilon \|w_k\|^2 + \beta z_k^T w_k & x_{k+1,lin}{}^T P \\ P x_{k+1,lin} & P \end{bmatrix} \geq \begin{bmatrix} \alpha^{-1}\mathfrak{F}^T\mathfrak{F} & 0 \\ 0 & \alpha P^2 \end{bmatrix} \qquad (3.2\text{-}7)$$

is a sufficient condition for (3.2-4).

Moving all the terms in (3.2-7) to the left side and using Lemma 1, we have,

$$x_k^T P x_k - \delta \|z_k\|^2 - \varepsilon \|w_k\|^2 + \beta z_k^T w_k - \alpha^{-1} \mathfrak{F}^T \mathfrak{F} \\ - x_{k+1,lin}^T P(P - \alpha P^2)^{-1} P x_{k+1,lin} > 0 \tag{3.2-8}$$

Using the nonlinear part bound (3.1-8), we obtain a sufficient condition for (3.2-8)

$$x_k^T P x_k - \delta \|z_k\|^2 - \varepsilon \|w_k\|^2 + \beta z_k^T w_k \\ - x_{k+1,lin}^T P(P - \alpha P^2)^{-1} P x_{k+1,lin} \\ - (\tilde{C}_f x_k + \tilde{D}_f u_k + \tilde{E}_f w_k)^T (\tilde{C}_f x_k + \tilde{D}_f u_k + \tilde{E}_f w_k) > 0 \tag{3.2-9}$$

Substituting z_k, w_k and $x_{k+1,lin}$ into (3.2-9), the inequality can be rewritten in quadratic form as

$$\begin{bmatrix} x^T & w^T \end{bmatrix} H \begin{bmatrix} x \\ w \end{bmatrix} \geq 0 \tag{3.2-10}$$

where

$$H = \begin{bmatrix} h_{11} & h_{12} \\ h_{12}^T & h_{22} \end{bmatrix} > 0$$

with

$$h_{11} = P - \delta(C_z + D_z\tilde{K})^T (C_z + D_z\tilde{K}) - (\tilde{C}_f + \tilde{D}_f\tilde{K})^T (\tilde{C}_f + \tilde{D}_f\tilde{K}) \\ -(\tilde{A} + \tilde{B}\tilde{K})^T P(P - \alpha P^2)^{-1} P(\tilde{A} + \tilde{B}\tilde{K})$$

$$h_{12} = -\delta(C_z + D_z\tilde{K})^T E_z + \frac{\beta}{2}(C_z + D_z\tilde{K})^T - (\tilde{C}_f + \tilde{D}_f\tilde{K})^T \tilde{E}_f \\ -(\tilde{A} + \tilde{B}\tilde{K})^T P(P - \alpha P^2)^{-1} P\tilde{F}$$

$$h_{22} = -\delta E_z^T E_z - \varepsilon I + \frac{\beta}{2}(E_z + E_z^T) - \tilde{E}_f^T \tilde{E}_f \\ -\tilde{F}^T P(P - \alpha P^2)^{-1} P\tilde{F}$$

Separating the terms with $P(P - \alpha P^2)^{-1}$, (3.2-10) can be rewritten as

$$\begin{bmatrix} h'_{11} & h'_{12} \\ h'^T_{12} & h'_{22} \end{bmatrix} - \begin{bmatrix} (\tilde{A} + \tilde{B}\tilde{K})^T P \\ \tilde{F}^T P \end{bmatrix} (P - \alpha P^2)^{-1} \begin{bmatrix} P(\tilde{A} + \tilde{B}\tilde{K}) & P\tilde{F} \end{bmatrix} > 0 \tag{3.2-11}$$

Applying Lemma 1 to (3.2-11) twice, we have

$$\begin{bmatrix} h'_{11} & h'_{12} & (\tilde{A}+\tilde{B}\tilde{K})^T P \\ h'^{T}_{12} & h'_{22} & \tilde{F}^T P \\ P(\tilde{A}+\tilde{B}\tilde{K}) & P\tilde{F} & P-\alpha P^2 \end{bmatrix} > 0 \tag{3.2-12}$$

where

$$h'_{11} = P - \delta(C_z + D_z\tilde{K})^T(C_z + D_z\tilde{K}) - (\tilde{C}_f + \tilde{D}_f\tilde{K})^T(\tilde{C}_f + \tilde{D}_f\tilde{K})$$

$$h'_{12} = -\delta(C_z + D_z\tilde{K})^T E_z + \frac{\beta}{2}(C_z + D_z\tilde{K})^T - (\tilde{C}_f + \tilde{D}_f\tilde{K})^T \tilde{E}_f$$

$$h'_{22} = -\delta E_z^{\ T} E_z - \varepsilon I + \frac{\beta}{2}(E_z + E_z^{\ T}) - \tilde{E}_f^{\ T}\tilde{E}_f$$

3.2.3 Case When Noise Is Present

Pre- and post-multiplying (3.2-12) by $\begin{bmatrix} Q & 0 & 0 \\ 0 & I & 0 \\ 0 & 0 & Q \end{bmatrix}$ where $Q = P^{-1}$, writing $\tilde{Y}$ as $\tilde{K}Q$ and using Lemma 1, we obtain,

$$\left[\begin{array}{c:c:c:c} \begin{matrix} Q \\ -\delta(QC_z^{\ T} + \tilde{Y}^T D_z)(C_z Q + D_z\tilde{Y}) \end{matrix} & \begin{matrix} \frac{\beta}{2}(QC_z^{\ T} + \tilde{Y}^T D_z^{\ T}) \\ -\delta(QC_z^{\ T} + \tilde{Y}^T D_z)E_z \end{matrix} & Q\tilde{A}^T + \tilde{Y}^T\tilde{B}^T & Q\tilde{C}_f^{\ T} + \tilde{Y}^T\tilde{D}_f^{\ T} \\ \hdashline * & \begin{matrix} -\delta E_z^{\ T} E_z - \varepsilon I \\ +\frac{\beta}{2}(E_z + E_z^{\ T}) \end{matrix} & \tilde{F}^T & \tilde{E}_f^{\ T} \\ \hdashline * & * & Q - \alpha I & 0 \\ \hdashline * & * & * & I \end{array}\right] > 0$$

(3.2-13)

Rearranging all the terms with $\Delta_A, \Delta_B, \Delta_F, \Delta_{C_f}, \Delta_{D_f}, \Delta_{E_f}$ in (3.2-13), we obtain,

$$\left[\begin{array}{c|c|c|c} Q - \delta(QC_z^T + \tilde{Y}^T D_z)(C_z Q + D_z \tilde{Y}) & \frac{\beta}{2}(QC_z^T + \tilde{Y}^T D_z^T) - \delta(QC_z^T + \tilde{Y}^T D_z)E_z & QA^T + \tilde{Y}^T B^T & QC_f^T + \tilde{Y}^T D_f^T \\ \hline * & -\delta E_z^T E_z - \varepsilon I + \frac{\beta}{2}(E_z + E_z^T) & F^T & E_f^T \\ \hline * & * & Q - \alpha I & 0 \\ \hline * & * & * & I \end{array}\right]$$

$$> \left[\begin{array}{c|c|c|c} 0 & 0 & -Q\Delta_A^T - \tilde{Y}^T \Delta_B^T & -Q\Delta_{C_f}^T - \tilde{Y}^T \Delta_{D_f}^T \\ \hline * & 0 & -\Delta_F^T & -\Delta_{E_f}^T \\ \hline * & * & 0 & 0 \\ \hline * & * & * & 0 \end{array}\right] \tag{3.2-14}$$

The right side of (3.2-14) can be rewritten and an upper bound on it can be established by using Lemma 2 as follows

$$\left[\begin{array}{c|c|c|c} 0 & 0 & -Q\Delta_A^T - \tilde{Y}^T \Delta_B^T & -Q\Delta_{C_f}^T - \tilde{Y}^T \Delta_{D_f}^T \\ \hline * & 0 & -\Delta_F^T & -\Delta_{E_f}^T \\ \hline * & * & 0 & 0 \\ \hline * & * & * & 0 \end{array}\right]$$

$$= \begin{bmatrix} 0 & 0 & 0 \\ 0 & 0 & 0 \\ \Delta_A & \Delta_B & \Delta_F \\ \Delta_{C_f} & \Delta_{D_f} & \Delta_{E_f} \end{bmatrix} \begin{bmatrix} -Q & 0 & 0 & 0 \\ -\tilde{Y} & 0 & 0 & 0 \\ 0 & -I & 0 & 0 \end{bmatrix} + \begin{bmatrix} -Q & -\tilde{Y}^T & 0 \\ 0 & 0 & -I \\ 0 & 0 & 0 \\ 0 & 0 & 0 \end{bmatrix} \begin{bmatrix} 0 & 0 & \Delta_A^T & \Delta_{C_f}^T \\ 0 & 0 & \Delta_B^T & \Delta_{D_f}^T \\ 0 & 0 & \Delta_F^T & \Delta_{E_f}^T \end{bmatrix} \tag{3.2-15}$$

$$< \begin{bmatrix} 0 & 0 & 0 \\ 0 & 0 & 0 \\ \Delta_A & \Delta_B & \Delta_F \\ \Delta_{C_f} & \Delta_{D_f} & \Delta_{E_f} \end{bmatrix} \Phi \begin{bmatrix} 0 & 0 & \Delta_A^T & \Delta_{C_f}^T \\ 0 & 0 & \Delta_B^T & \Delta_{D_f}^T \\ 0 & 0 & \Delta_F^T & \Delta_{E_f}^T \end{bmatrix} + \begin{bmatrix} -Q & -\tilde{Y}^T & 0 \\ 0 & 0 & -I \\ 0 & 0 & 0 \\ 0 & 0 & 0 \end{bmatrix} \Phi^{-1} \begin{bmatrix} -Q & 0 & 0 & 0 \\ -\tilde{Y} & 0 & 0 & 0 \\ 0 & -I & 0 & 0 \end{bmatrix}$$

The left term in third line of (3.2-15) can be rewritten and by using bound condition (3.1-10):

$$\begin{bmatrix} 0 & 0 & 0 \\ 0 & 0 & 0 \\ \Delta_A & \Delta_B & \Delta_F \\ \Delta_{C_f} & \Delta_{D_f} & \Delta_{E_f} \end{bmatrix} \Phi \begin{bmatrix} 0 & 0 & \Delta_A{}^T & \Delta_{C_f}{}^T \\ 0 & 0 & \Delta_B{}^T & \Delta_{D_f}{}^T \\ 0 & 0 & \Delta_F{}^T & \Delta_{E_f}{}^T \end{bmatrix}$$

$$= \begin{bmatrix} 0 & 0 \\ 0 & 0 \\ I & 0 \\ 0 & I \end{bmatrix} \begin{bmatrix} \Delta_A & \Delta_B & \Delta_F \\ \Delta_{C_f} & \Delta_{D_f} & \Delta_{E_f} \end{bmatrix} \Phi \begin{bmatrix} \Delta_A{}^T & \Delta_{C_f}{}^T \\ \Delta_B{}^T & \Delta_{D_f}{}^T \\ \Delta_F{}^T & \Delta_{E_f}{}^T \end{bmatrix} \begin{bmatrix} 0 & 0 & I & 0 \\ 0 & 0 & 0 & I \end{bmatrix} \tag{3.2-16}$$

$$= \begin{bmatrix} 0 & 0 \\ 0 & 0 \\ I & 0 \\ 0 & I \end{bmatrix} \Psi \begin{bmatrix} 0 & 0 & I & 0 \\ 0 & 0 & 0 & I \end{bmatrix} = \begin{bmatrix} 0 & 0 & 0 & 0 \\ & 0 & 0 & 0 \\ & & \Psi_{11} & \Psi_{12} \\ * & & & \Psi_{22} \end{bmatrix}$$

Substituting (3.2-15) and (3.2-16) into (3.2-14), (3.2-17) is a sufficient condition for (3.2-14) to hold.

$$\left[\begin{array}{c:c:c:c} \begin{matrix} Q \\ -\delta(QC_z{}^T + \tilde{Y}^T D_z)(C_z Q + D_z \tilde{Y}) \end{matrix} & \begin{matrix} \frac{\beta}{2}(QC_z{}^T + \tilde{Y}^T D_z{}^T) \\ -\delta(QC_z{}^T + \tilde{Y}^T D_z)E_z \end{matrix} & QA^T + \tilde{Y}^T B^T & QC_f{}^T + \tilde{Y}^T D_f{}^T \\ \hdashline * & \begin{matrix} -\delta E_z{}^T E_z - \varepsilon I \\ +\frac{\beta}{2}(E_z + E_z{}^T) \end{matrix} & F^T & E_f{}^T \\ \hdashline * & * & Q - \alpha I - \Psi_{11} & -\Psi_{12} \\ \hdashline * & * & * & -\Psi_{22} \end{array}\right]$$

$$- \begin{bmatrix} Q & \tilde{Y}^T & 0 \\ 0 & 0 & I \\ 0 & 0 & 0 \\ 0 & 0 & 0 \end{bmatrix} \Phi^{-1} \begin{bmatrix} Q & 0 & 0 & 0 \\ \tilde{Y} & 0 & 0 & 0 \\ 0 & I & 0 & 0 \end{bmatrix} > 0 \tag{3.2-17}$$

Applying Lemma 1 twice to (3.2-17), we have

$$\begin{bmatrix} Q & \frac{\beta}{2}(QC_z{}^T+\tilde{Y}^T D_z{}^T) & QA^T+\tilde{Y}^T B^T & QC_f{}^T+\tilde{Y}^T D_f{}^T & \begin{matrix}\sqrt{\delta}(QC_z{}^T\\ +\tilde{Y}^T D_z{}^T)\end{matrix} & Q & Y^T & 0 \\ * & \frac{\beta}{2}(E_z+E_z{}^T)-\varepsilon I & F^T & E_f{}^T & \sqrt{\delta}E_z{}^T & 0 & 0 & I \\ * & * & Q-\alpha I-\Psi_{11} & -\Psi_{12} & 0 & 0 & 0 & 0 \\ * & * & * & -\Psi_{22} & 0 & 0 & 0 & 0 \\ * & * & * & * & I & 0 & 0 & 0 \\ * & * & * & * & * & \Phi_{11} & \Phi_{12} & \Phi_{13} \\ * & * & * & * & * & * & \Phi_{22} & \Phi_{23} \\ * & * & * & * & * & * & * & \Phi_{33} \end{bmatrix} > 0$$

(3.2-18)

Rearranging all the terms with $\Delta_K\ (\tilde{Y})$ to the right side of the inequality, we have,

$$\begin{bmatrix} Q & \frac{\beta}{2}(QC_z{}^T+\tilde{Y}^T D_z{}^T) & QA^T+\tilde{Y}^T B^T & QC_f{}^T+\tilde{Y}^T D_f{}^T & \begin{matrix}\sqrt{\delta}(QC_z{}^T\\ +\tilde{Y}^T D_z{}^T)\end{matrix} & Q & Y^T & 0 \\ * & \frac{\beta}{2}(E_z+E_z{}^T)-\varepsilon I & F^T & E_f{}^T & \sqrt{\delta}E_z{}^T & 0 & 0 & I \\ * & * & Q-\alpha I-\Psi_{11} & -\Psi_{12} & 0 & 0 & 0 & 0 \\ * & * & * & -\Psi_{22} & 0 & 0 & 0 & 0 \\ * & * & * & * & I & 0 & 0 & 0 \\ * & * & * & * & * & \Phi_{11} & \Phi_{12} & \Phi_{13} \\ * & * & * & * & * & * & \Phi_{22} & \Phi_{23} \\ * & * & * & * & * & * & * & \Phi_{33} \end{bmatrix} \geq$$

$$\begin{bmatrix} 0 & -\frac{\beta}{2}Q\Delta_K{}^T D_z{}^T & -Q\Delta_K{}^T B^T & -Q\Delta_K{}^T D_f{}^T & -\sqrt{\delta}Q\Delta_K{}^T D_z{}^T & 0 & -Q\Delta_K{}^T & 0 \\ * & 0 & 0 & 0 & 0 & 0 & 0 & 0 \\ * & * & 0 & 0 & 0 & 0 & 0 & 0 \\ * & * & * & 0 & 0 & 0 & 0 & 0 \\ * & * & * & * & 0 & 0 & 0 & 0 \\ * & * & * & * & * & 0 & 0 & 0 \\ * & * & * & * & * & * & 0 & 0 \\ * & * & * & * & * & * & * & 0 \end{bmatrix}$$

(3.2-19)

A bound for the right side of (3.2-19) is found by applying Lemma 2 as

$$
\begin{bmatrix} 0 \\ -\frac{\beta}{2}D_z \\ -B \\ -D_f \\ -\sqrt{\delta}D_z \\ 0 \\ -I \\ 0 \end{bmatrix} \Delta_k \begin{bmatrix} Q \\ 0 \\ 0 \\ 0 \\ 0 \\ 0 \\ 0 \\ 0 \end{bmatrix}^T + \begin{bmatrix} Q \\ 0 \\ 0 \\ 0 \\ 0 \\ 0 \\ 0 \\ 0 \end{bmatrix} \Delta_k^{\ T} \begin{bmatrix} 0 \\ -\frac{\beta}{2}D_z \\ -B \\ -D_f \\ -\sqrt{\delta}D_z \\ 0 \\ -I \\ 0 \end{bmatrix}^T \le \begin{bmatrix} 0 \\ -\frac{\beta}{2}D_z \\ -B \\ -D_f \\ -\sqrt{\delta}D_z \\ 0 \\ -I \\ 0 \end{bmatrix} \Delta_k M \Delta_k^{\ T} \begin{bmatrix} 0 \\ -\frac{\beta}{2}D_z \\ -B \\ -D_f \\ -\sqrt{\delta}D_z \\ 0 \\ -I \\ 0 \end{bmatrix}^T + \begin{bmatrix} Q \\ 0 \\ 0 \\ 0 \\ 0 \\ 0 \\ 0 \\ 0 \end{bmatrix} M^{-1} \begin{bmatrix} Q \\ 0 \\ 0 \\ 0 \\ 0 \\ 0 \\ 0 \\ 0 \end{bmatrix}^T
$$

(3.2-20)

Then, using the bound (3.1-3), the right side of (3.2-20) can be rewritten as

$$
\begin{bmatrix}
0 & 0 & 0 & 0 & 0 & 0 & 0 & 0 \\
* & \frac{\beta^2}{4}D_zND_z^{\ T} & \frac{\beta}{2}D_zNB^T & \frac{\beta}{2}D_zND_f^{\ T} & \frac{\beta}{2}\sqrt{\delta}D_zND_z^{\ T} & 0 & \frac{\beta}{2}D_zN & 0 \\
* & * & BNB^T & BND_f^{\ T} & \sqrt{\delta}BND_z^{\ T} & 0 & BN & 0 \\
* & * & * & D_fND_f^{\ T} & \sqrt{\delta}D_fND_z^{\ T} & 0 & D_fN & 0 \\
* & * & * & * & \delta D_zND_z^{\ T} & 0 & \sqrt{\delta}D_zN & 0 \\
* & * & * & * & * & 0 & 0 & 0 \\
* & * & * & * & * & * & N & 0 \\
* & * & * & * & * & * & * & 0
\end{bmatrix} + \begin{bmatrix} Q \\ 0 \\ 0 \\ 0 \\ 0 \\ 0 \\ 0 \\ 0 \end{bmatrix} M^{-1} \begin{bmatrix} Q \\ 0 \\ 0 \\ 0 \\ 0 \\ 0 \\ 0 \\ 0 \end{bmatrix}^T
$$

(3.2-21)

Substituting (3.2-21) into (3.2-19) and using Lemma 1, we obtain,

$$\left[\begin{array}{c:c:c:c:c:c:c:c:c} Q & \frac{\beta}{2}(QC_z^{\ T}+\tilde{Y}^TD_z^{\ T}) & QA^T+\tilde{Y}^TB^T & QC_f^{\ T}+\tilde{Y}^TD_f^{\ T} & \begin{array}{c}\sqrt{\delta}(QC_z^{\ T}\\ +\tilde{Y}^TD_z^{\ T})\end{array} & Q & Y^T & 0 & Q \\ \hdashline * & \begin{array}{c}\frac{\beta}{2}(E_z+E_z^{\ T})-\varepsilon I\\ -\frac{\beta^2}{4}D_zND_z^{\ T}\end{array} & \begin{array}{c}F^T\\ -\frac{\beta}{2}D_zNB^T\end{array} & \begin{array}{c}E_f^{\ T}\\ -\frac{\beta}{2}D_zND_f^{\ T}\end{array} & \begin{array}{c}\sqrt{\delta}(E_z^{\ T}\\ -\frac{\beta}{2}D_zND_z^{\ T})\end{array} & 0 & -\frac{\beta}{2}D_zN & I & 0 \\ \hdashline * & * & \begin{array}{c}Q-\alpha I-\Psi_{11}\\ -BNB^T\end{array} & -\Psi_{12}-BND_f^{\ T} & -\sqrt{\delta}BND_z^{\ T} & 0 & -BN & 0 & 0 \\ \hdashline * & * & * & -\Psi_{22}-D_fND_f^{\ T} & -\sqrt{\delta}D_fND_z^{\ T} & 0 & -D_fN & 0 & 0 \\ \hdashline * & * & * & * & I-\delta D_zND_z^{\ T} & 0 & -\sqrt{\delta}D_zN & 0 & 0 \\ \hdashline * & * & * & * & * & \Phi_{11} & \Phi_{12} & \Phi_{13} & 0 \\ \hdashline * & * & * & * & * & * & \Phi_{22}-N & \Phi_{23} & 0 \\ \hdashline * & * & * & * & * & * & * & \Phi_{33} & 0 \\ \hdashline * & * & * & * & * & * & * & * & M \end{array}\right] \geq 0$$

(3.2-22)

3.2.4 Case When Noise Is Not Present

This is a special case. When $w_k = 0$, from (3.2-10) we only have

$$x^T h_{11} x > 0 \tag{3.2-23}$$

We want $h_{11} > 0$, which is

$$\begin{aligned} P-\delta(C_z+D_z\tilde{K})^T(C_z+D_z\tilde{K})-(\tilde{C}_f+\tilde{D}_f\tilde{K})^T(\tilde{C}_f+\tilde{D}_f\tilde{K}) \\ -(\tilde{A}+\tilde{B}\tilde{K})^T P(P-\alpha P^2)^{-1}P(\tilde{A}+\tilde{B}\tilde{K})>0 \end{aligned} \tag{3.2-24}$$

Applying Lemma 1 to (3.2-24), we have

$$\begin{bmatrix} h_{11}^{'} & (\tilde{A}+\tilde{B}\tilde{K})^T P \\ P(\tilde{A}+\tilde{B}\tilde{K}) & P-\alpha P^2 \end{bmatrix} > 0 \tag{3.2-25}$$

where $h_{11}^{'} = P-\delta(C_z+D_z\tilde{K})^T(C_z+D_z\tilde{K})-(\tilde{C}_f+\tilde{D}_f\tilde{K})^T(\tilde{C}_f+\tilde{D}_f\tilde{K})$

By pre- and post-multiplying (3.2-25) by $\begin{bmatrix} Q & 0 \\ 0 & Q \end{bmatrix}$ where $Q = P^{-1}$ and using $\tilde{Y} = \tilde{K}Q = (K + \Delta_K)Q$, we obtain,

$$\begin{bmatrix} Q - \delta(QC_z{}^T + \tilde{Y}^T D_z{}^T)(C_z Q + D_z \tilde{Y}) \\ -(Q\tilde{C}_f{}^T + \tilde{Y}^T \tilde{D}_f{}^T)(\tilde{C}_f Q + \tilde{D}_f \tilde{Y}) & Q\tilde{A}^T + \tilde{Y}^T \tilde{B}^T \\ * & Q - \alpha I \end{bmatrix} > 0 \tag{3.2-26}$$

Applying Lemma 1 to (3.2-26), we obtain,

$$\begin{bmatrix} Q - \delta(QC_z{}^T + \tilde{Y}^T D_z{}^T)(C_z Q + D_z \tilde{Y}) & Q\tilde{A}^T + \tilde{Y}^T \tilde{B}^T & Q\tilde{C}_f{}^T + \tilde{Y}^T \tilde{D}_f{}^T \\ * & Q - \alpha I & 0 \\ * & * & I \end{bmatrix} > 0 \tag{3.2-27}$$

Rearranging all the terms with $\Delta_A, \Delta_B, \Delta_F, \Delta_{C_f}, \Delta_{D_f}$, we have

$$\begin{bmatrix} Q - \delta(QC_z{}^T + \tilde{Y}^T D_z{}^T)(C_z Q + D_z \tilde{Y}) & QA^T + \tilde{Y}^T B^T & QC_f{}^T + \tilde{Y}^T D_f{}^T \\ * & Q - \alpha I & 0 \\ * & * & I \end{bmatrix}$$
$$> \begin{bmatrix} 0 & -Q\Delta_A{}^T - \tilde{Y}^T \Delta_B{}^T & -Q\Delta_{C_f}{}^T - \tilde{Y}^T \Delta_{D_f}{}^T \\ * & 0 & 0 \\ * & * & 0 \end{bmatrix} \tag{3.2-28}$$

The right side of (3.2-28) can be rewritten and an upper bound on it can be established by using Lemma 2 as follows

$$\begin{bmatrix} 0 & -Q\Delta_A{}^T - \tilde{Y}^T\Delta_B{}^T & -Q\Delta_{C_f}{}^T - \tilde{Y}^T\Delta_{D_f}{}^T \\ * & 0 & 0 \\ * & * & 0 \end{bmatrix}$$

$$= \begin{bmatrix} 0 & 0 \\ \Delta_A & \Delta_B \\ \Delta_{C_f} & \Delta_{D_f} \end{bmatrix} \begin{bmatrix} -Q & 0 & 0 \\ -\tilde{Y} & 0 & 0 \end{bmatrix} + \begin{bmatrix} -Q & -\tilde{Y}^T \\ 0 & 0 \\ 0 & 0 \end{bmatrix} \begin{bmatrix} 0 & \Delta_A{}^T & \Delta_B{}^T \\ 0 & \Delta_{C_f}{}^T & \Delta_{D_f}{}^T \end{bmatrix} \tag{3.2-29}$$

$$\le \begin{bmatrix} 0 & 0 \\ \Delta_A & \Delta_B \\ \Delta_{C_f} & \Delta_{D_f} \end{bmatrix} \Phi \begin{bmatrix} 0 & \Delta_A{}^T & \Delta_B{}^T \\ 0 & \Delta_{C_f}{}^T & \Delta_{D_f}{}^T \end{bmatrix} + \begin{bmatrix} Q & \tilde{Y}^T \\ 0 & 0 \\ 0 & 0 \end{bmatrix} \Phi^{-1} \begin{bmatrix} Q & 0 & 0 \\ \tilde{Y} & 0 & 0 \end{bmatrix}$$

The left term in third line of (3.2-28) can be rewritten and by using bound condition (3.1-10):

$$\begin{bmatrix} 0 & 0 \\ \Delta_A & \Delta_B \\ \Delta_{C_f} & \Delta_{D_f} \end{bmatrix} \Phi \begin{bmatrix} 0 & \Delta_A{}^T & \Delta_B{}^T \\ 0 & \Delta_{C_f}{}^T & \Delta_{D_f}{}^T \end{bmatrix}$$

$$= \begin{bmatrix} 0 & 0 \\ I & 0 \\ 0 & I \end{bmatrix} \begin{bmatrix} \Delta_A & \Delta_B \\ \Delta_{C_f} & \Delta_{D_f} \end{bmatrix} \Phi \begin{bmatrix} \Delta_A{}^T & \Delta_{C_f}{}^T \\ \Delta_B{}^T & \Delta_{D_f}{}^T \end{bmatrix} \begin{bmatrix} 0 & I & 0 \\ 0 & 0 & I \end{bmatrix} \tag{3.2-30}$$

$$= \begin{bmatrix} 0 & 0 \\ I & 0 \\ 0 & I \end{bmatrix} \Psi \begin{bmatrix} 0 & I & 0 \\ 0 & 0 & I \end{bmatrix} = \begin{bmatrix} 0 & 0 & 0 \\ * & \Psi_{11} & \Psi_{12} \\ * & * & \Psi_{22} \end{bmatrix}$$

Substituting (3.2-29) and (3.2-30) into (3.2-28), (3.2-31) is a sufficient condition for (3.2-28) to hold.

$$\begin{bmatrix} Q - \delta(QC_z{}^T + \tilde{Y}^T D_z{}^T)(C_z Q + D_z \tilde{Y}) & QA^T + \tilde{Y}^T B^T & QC_f{}^T + \tilde{Y}^T D_f{}^T \\ * & Q - \alpha I - \Psi_{11} & -\Psi_{12} \\ * & * & -\Psi_{22} \end{bmatrix} - \begin{bmatrix} Q & \tilde{Y}^T \\ 0 & 0 \\ 0 & 0 \end{bmatrix} \Phi^{-1} \begin{bmatrix} Q & 0 & 0 \\ \tilde{Y} & 0 & 0 \end{bmatrix} > 0 \tag{3.2-31}$$

Applying Lemma 1 twice to (3.2-31), we have

$$\begin{bmatrix} Q & Q\tilde{A}^T+\tilde{Y}^T\tilde{B}^T & QC_f^{\,T}+\tilde{Y}^T D_f^{\,T} & \sqrt{\delta}(QC_z^{\,T}+\tilde{Y}^T D_z^{\,T}) & Q & \tilde{Y} \\ * & Q-\alpha I-\Psi_{11} & -\Psi_{12} & 0 & 0 & 0 \\ * & * & -\Psi_{22} & 0 & 0 & 0 \\ * & * & * & I & 0 & 0 \\ * & * & * & * & \Phi_{11} & \Phi_{12} \\ * & * & * & * & * & \Phi_{22} \end{bmatrix} > 0 \quad (3.2\text{-}32)$$

Rearranging all the terms with $\Delta_K\,(\tilde{Y})$ to the right side of the inequality, we have,

$$\begin{aligned} &\begin{bmatrix} Q & QA^T+Y^T B^T & QC_f^{\,T}+Y^T D_f^{\,T} & \sqrt{\delta}(QC_z^{\,T}+Y^T D_z^{\,T}) & Q & Y \\ * & Q-\alpha I-\Psi_{11} & -\Psi_{12} & 0 & 0 & 0 \\ * & * & -\Psi_{22} & 0 & 0 & 0 \\ * & * & * & I & 0 & 0 \\ * & * & * & * & \Phi_{11} & \Phi_{12} \\ * & * & * & * & * & \Phi_{22} \end{bmatrix} \\ &> \left[\begin{array}{c|c|c|c|c|c} 0 & -Q\Delta_K^{\,T}B^T & -Q\Delta_K^{\,T}D_f^{\,T} & -\sqrt{\delta}Q\Delta_K^{\,T}D_z^{\,T} & 0 & -Q\Delta_K^{\,T} \\ \hline * & 0 & 0 & 0 & 0 & 0 \\ \hline * & * & 0 & 0 & 0 & 0 \\ \hline * & * & * & 0 & 0 & 0 \\ \hline * & * & * & * & 0 & 0 \\ \hline * & * & * & * & * & 0 \end{array}\right] \end{aligned} \quad (3.2\text{-}33)$$

A bound for the right side of (3.2-33) is found by applying Lemma 2 as

$$\begin{bmatrix} 0 \\ -B \\ -D_f \\ -\sqrt{\delta}D_z \\ 0 \\ -I \end{bmatrix} \Delta_k \begin{bmatrix} Q \\ 0 \\ 0 \\ 0 \\ 0 \\ 0 \end{bmatrix}^T + \begin{bmatrix} Q \\ 0 \\ 0 \\ 0 \\ 0 \\ 0 \end{bmatrix} \Delta_k^{\,T} \begin{bmatrix} 0 \\ -B \\ -D_f \\ -\sqrt{\delta}D_z \\ 0 \\ -I \end{bmatrix}^T \le \frac{1}{\sigma} \begin{bmatrix} 0 \\ -B \\ -D_f \\ -\sqrt{\delta}D_z \\ 0 \\ -I \end{bmatrix} \Delta_k M \Delta_k^{\,T} \begin{bmatrix} 0 \\ -B \\ -D_f \\ -\sqrt{\delta}D_z \\ 0 \\ -I \end{bmatrix}^T + \begin{bmatrix} Q \\ 0 \\ 0 \\ 0 \\ 0 \\ 0 \end{bmatrix} M^{-1} \begin{bmatrix} Q \\ 0 \\ 0 \\ 0 \\ 0 \\ 0 \end{bmatrix}^T$$

(3.2-34)

Then, using the bound (3.1-3), the right side of (3.2-20) can be rewritten as

$$\begin{bmatrix} 0 & 0 & 0 & 0 & 0 & 0 \\ * & BNB^T & BND_f^{\ T} & \sqrt{\delta}BND_z^{\ T} & 0 & BN \\ * & * & D_fND_f^{\ T} & \sqrt{\delta}D_fND_z^{\ T} & 0 & D_fN \\ * & * & * & \delta D_zND_z^{\ T} & 0 & \sqrt{\delta}D_zN \\ * & * & * & * & 0 & 0 \\ * & * & * & * & * & N \end{bmatrix} + \begin{bmatrix} Q \\ 0 \\ 0 \\ 0 \\ 0 \\ 0 \end{bmatrix} M^{-1} \begin{bmatrix} Q \\ 0 \\ 0 \\ 0 \\ 0 \\ 0 \end{bmatrix}^T \tag{3.2-35}$$

Substituting (3.2-35) into (3.2-33) and using Lemma 1, we obtain,

$$\left[\begin{array}{c:c:c:c:c:c:c} Q & QA^T + Y^TB^T & QC_f^{\ T} + Y^TD_f^{\ T} & \sqrt{\delta}(QC_z^{\ T} + Y^TD_z^{\ T}) & Q & Y & Q \\ \hdashline * & Q-\alpha I - \Psi_{11} - BNB^T & -\Psi_{12} - BND_f^{\ T} & -\sqrt{\delta}BND_z^{\ T} & 0 & -BN & 0 \\ \hdashline * & * & -\Psi_{22} - D_fND_f^{\ T} & -\sqrt{\delta}D_fND_z^{\ T} & 0 & -D_fN & 0 \\ \hdashline * & * & * & I - \delta D_zND_z^{\ T} & 0 & -\sqrt{\delta}D_zN & 0 \\ \hdashline * & * & * & * & \Phi_{11} & \Phi_{12} & 0 \\ \hdashline * & * & * & * & * & \Phi_{22} & 0 \\ \hdashline * & * & * & * & * & * & M \end{array}\right] \tag{3.2-36}$$

3.3 Simulation Studies

Example 3-1. Chua's circuit with chaotic behavior is used in this example. The state space model is given by

$$\begin{bmatrix} x_1 \\ x_2 \\ x_3 \end{bmatrix}_{k+1} = \begin{bmatrix} -\alpha_c & \alpha_c & 0 \\ 1 & -1 & 1 \\ 0 & -\beta_c & -\mu \end{bmatrix} \begin{bmatrix} x_1 \\ x_2 \\ x_3 \end{bmatrix}_k - \begin{bmatrix} \alpha_c f(x_1) \\ 0 \\ 0 \end{bmatrix} + \begin{bmatrix} 1 \\ 1 \\ 1 \end{bmatrix} u_k + \begin{bmatrix} 1 \\ 1 \\ 1 \end{bmatrix} w_k \tag{3.3-1}$$

where

$$f(x_1) = bx_1 + 0.5(a-b)(|x_1+1| - |x_1-1|), w_k = e^{-k}$$

with the parameters

$$\alpha_c = 9.1,\ \beta_c = 16.5811,\ \mu = 0.138083,\ a = -1.3659, b = -0.7408$$

The discretized Chua's circuit system with the sampling period of T=0.01s is given as

$$\begin{bmatrix} x_1 \\ x_2 \\ x_3 \end{bmatrix}_{k+1} = \begin{bmatrix} 0.909 & 0.091 & 0 \\ 0.01 & 0.99 & 0.01 \\ 0 & -0.1658 & 0.9986 \end{bmatrix} \begin{bmatrix} x_1 \\ x_2 \\ x_3 \end{bmatrix}_k - \begin{bmatrix} 0.091 f(x_{1,k}) \\ 0 \\ 0 \end{bmatrix} + \begin{bmatrix} 0.01 \\ 0.01 \\ 0.01 \end{bmatrix} u_k + \begin{bmatrix} 0.01 \\ 0.01 \\ 0.01 \end{bmatrix} w_k \tag{3.3-2}$$

The design parameters for the performance output are given in Table 3-1.

Table 3-1 Design parameters of Example 3-1

	Asy. Stb.	H_2 Ctrl.	H_∞ Ctrl.	Input S. P.	Output S. P.	Very S. P.
δ	0	1	1	0	1	1
β	0	0	0	1	1	1
ε	0	0	-1	0.05	0	0.05

In all cases, C_f, C_z are chosen to be 0.1*I_3 and D_f, D_z are chosen to be [0.1; 0.1; 0.1]. E_f, E_z are chosen to be 0.1*I_3 for the noisy cases and zero matrix for non-noisy cases.

The time evolution of the state variables of the open loop chaotic Chua's circuit is shown in Figure 3.3-1. The initial values of the state variables are chosen to be [1;1;1].

To verify the robustness and resilience property of the controller, the system matrix and coefficients of the nonlinearity are perturbed as follows

$\alpha_c = 8.9,\ \beta_c = 17\ \mu = 0.15,\ a = -1.4, b = -0.76$

And the feedback gain K are perturbed as shown in Table 3-2. The value of σ_P is also shown in Table 3-2, which results for this SISO system using $\Delta_K = K - K_p$.

After the proposed control is applied, we see the controlled perturbed system in Figure 3.3-2 for non-noisy cases and in Figure 3.3-3 for noisy cases. The feedback gains are perturbed within the bound of σ as given in the third and fourth column of Table 3-2 for each case, the systems can still be controlled and desired performance criterion is still achieved.

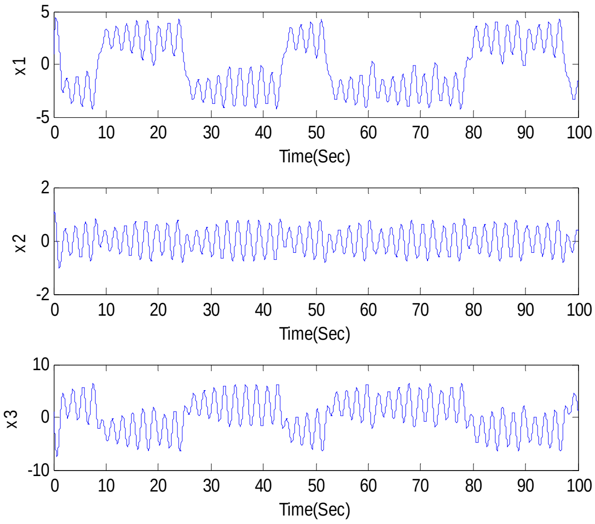

Figure 3.3-1 The state variables of the controlled system with perturbed gain

Table 3-2 Feedback gain K, perturbed gain K_p and their corresponding $\sigma_{\max}, \sigma_P$

	Feedback Gain K	Perturbed Gain K_p	$\sigma_{\max}$	σ_P
Asy. Stb.	[-0.86 -9.15 1.2]	[-0.9 -9 1.1]	0.25	0.18
H_2 Ctrl.	[-2.1 -13.28 0.9]	[-2 -13.2 1]	0.168	0.162
H_∞ Ctrl.	[-2.32 -10.38 0.85]	[-2.3 -10.3 0.9]	0.124	0.096
Input S. P.	[-1.22 -7.03 0.36]	[-1.2 -7 0.3]	0.093	0.07
Output S. P.	[-0.8 -5.85 0.15]	[-0.78 -5.8 0.14]	0.083	0.055
Very S. P.	[-0.89 -6.24 -0.8]	[-0.87 -6.22 -0.85]	0.052	0.05

Criteria are verified to be achieved in Table 3-3. The numerical values of the terms that can be calculated prior to the design process are given in the second column of Table 3-3, while values of the other terms are shown in the third column. From the calculation, all the performance criteria are verified as shown in the table. Notice that the case of asymptotic stability is verified from Figure 3.3-2.

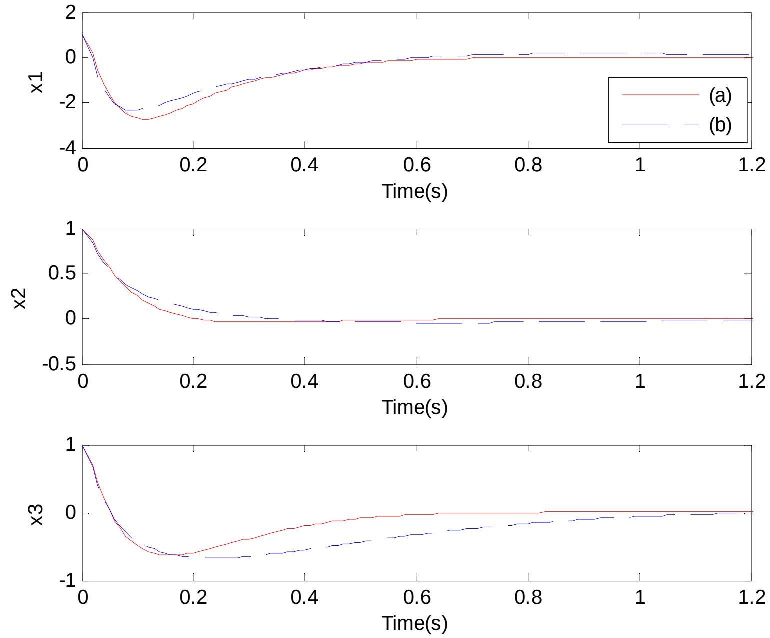

Figure 3.3-2 The state variables of Chua's circuit with the controller having perturbed control gain for non-noisy cases. (a) Asymptotic stability, (b) H_2 control.

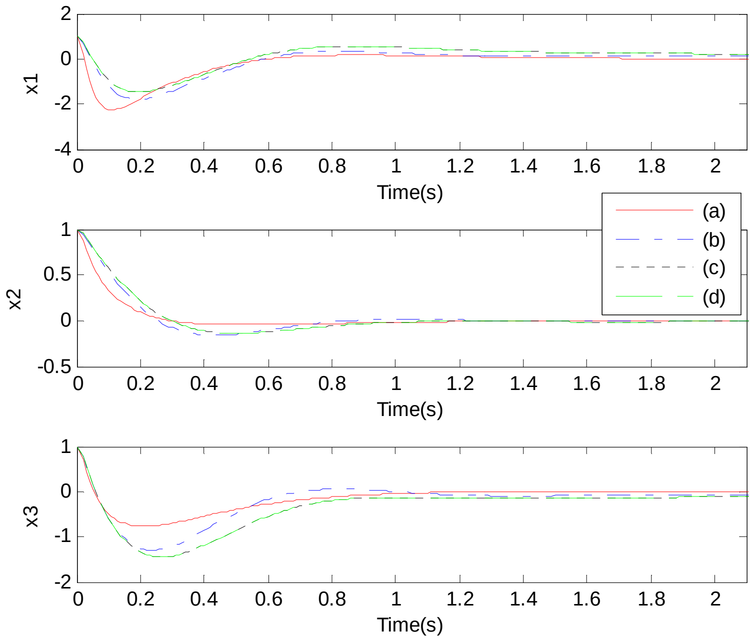

Figure 3.3-3 The state variables of Chua's circuit with the controller having perturbed control gain for noisy cases. (a) H_∞ controller (b) Output strict Passivity (c) Very strict Passivity (d) Input strict Passivity

Table 3-3 Validation of the performance criteria

Criteria	Pre-calculated Values		Simulation Results
Input S. P.	$\varepsilon \sum_i \lVert w_i \rVert^2$		$\sum_i z_i^T w_i$
	2.475	<	8.35
H_2 Ctrl.	$\delta^{-1} \lVert x_0 \rVert^2$		$\sum_i \lVert z_i \rVert^2 / \lambda_{\max}(P)$
	3	>	2.756

H$_\infty$ Ctrl.	$-\varepsilon\sum_i \lVert w_i \rVert^2$		$\sum_i \lVert z_i \rVert^2$
	49.5	>	6.26
Output S. P.	0		$\sum_i z_i^T w_i - \delta \sum_i \lVert z_i \rVert^2$
	0	<	4.56
Very S. P.	$\varepsilon\sum_i \lVert w_i \rVert^2$		$\sum_i z_i^T w_i - \delta \sum_i \lVert z_i \rVert^2$
	2.475	<	4.97

3.4 Conclusion

In this chapter, a robust and resilient state feedback controller design has been presented for a class of uncertain discrete-time nonlinear systems for general performance criteria. Uncertainties are allowed in both the center and the radius of the cone in which the nonlinearity resides as well as the feedback gain. With this method, control systems can be more robust and allow less accurate system models to be controlled. We have shown that a common framework for various performance criteria using linear matrix inequality techniques can be developed to solve the proposed controller design problem.

CHAPTER 4

ANALYSIS OF PERFORMANCE RESILIENCE OF STATE FEEDBACK CONTROLLERS FOR CONTINUOUS-TIME SYSTEMS

4.0 Introduction

In this chapter, a procedure is presented for performance analysis of the resilience property of continuous time linear systems with state feedback controllers. The resilience property is defined in terms of both multiplicative and additive perturbations on the controller gain that will maintain eigenvalues of the closed loop system in a specified region in the complex plane. In this chapter, this region is chosen as a vertical strip. Maximum gain perturbation bounds are obtained based on the designer's choices of the controller eigenvalue region. Linear matrix inequality techniques are used throughout the analysis process. Illustrative examples are included to demonstrate the effectiveness of the proposed methodology.

After designing the controller, the designers are able to determine upper bounds on the allowable deviations from nominal that the controller gains can have while still maintaining the desired performance specifications, specified by eigenvalue locations.

In Section 4.1, the system model and problem formulation are introduced. The solution of the analysis problem is derived in Section 4.2. Further analysis is given in Section 4.3. Some illustrative simulation studies and example discussion are presented in Section 4.4. Conclusions are given in Section 4.5.

4.1 Problem Formulation

Let us consider a continuous time linear system,

$$\dot{x} = Ax + Bu \tag{4.1-1}$$

where $x \in R^n$ is the state, $u \in R^m$ is the input.

A linear state feedback controller is used in this system,

$$u = \tilde{K}x \tag{4.1-2}$$

where the feedback gain K may in general be perturbed both additively and multiplicatively as,

$$\tilde{K} = \Delta_c K \Delta_b + \Delta_a \tag{4.1-3}$$

where $\Delta_a \in R^{m\times n}$, $\Delta_b \in R^{n\times n}$, $\Delta_c \in R^{m\times m}$.

However, in the following analysis, the perturbation

$$\tilde{K} = K\Delta_b + \Delta_a \tag{4.1-4}$$

will be used without losing generality. The validation of the use of this alternative form is given in the last part of this section.

The perturbation, $(\tilde{K} - K)$, is assumed to be bounded by

$$(K\Delta_b + \Delta_a - K)^T M_0 (K\Delta_b + \Delta_a - K) \le M_1 \tag{4.1-5}$$

where $M_0 \in R^{m\times m}$, $M_1 \in R^{n\times n}$ are symmetric positive definite matrices.

As stated in the introduction, our goal is to analyze the state feedback design to determine how large the perturbation bound can be so that the performance of the system with perturbed controller gains remains acceptable. In addition to achieving stability, we will also identify acceptable state feedback controller performance in terms of regions in the complex plane within which the eigenvalues of the perturbed controller must remain. Eigenvalue positions result in different system performances such as settling time, percentage overshoot and rise time [2]. As shown in Figure 4.1-1, for this work the eigenvalues of the closed loop system $\dot{x} = [A + B(K\Delta_b + \Delta_a)]x$ are chosen to lie within the vertical strip between $-\sigma_a$ and $-\sigma_b$ to guarantee upper and lower bounds on the settling (or response) time.

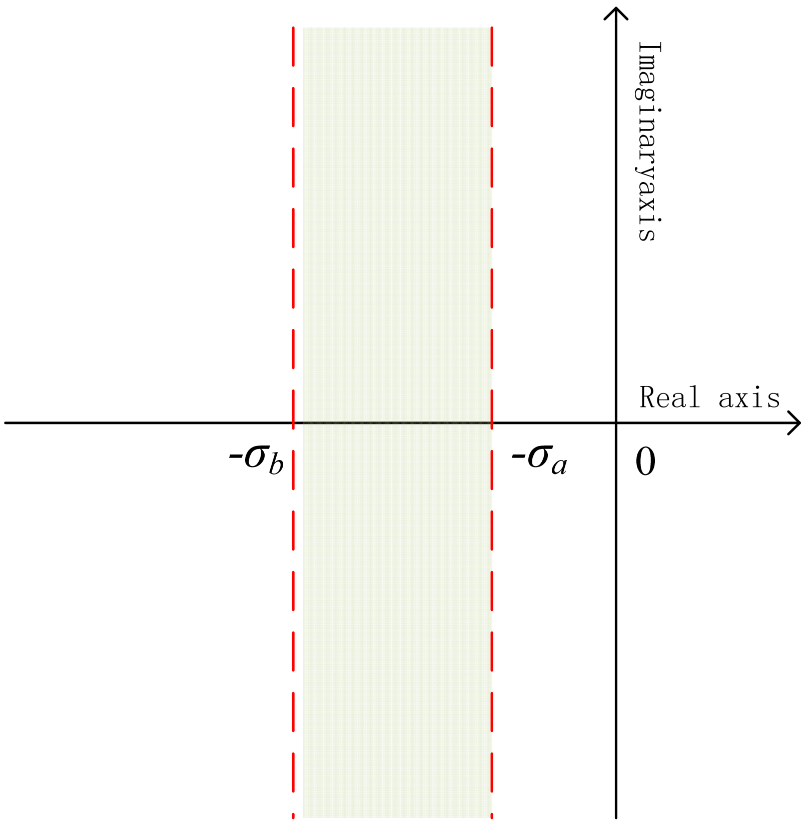

Figure 4.1-1 Desired controller eigenvalues region

The resilience analysis is based on satisfying the following Lyapunov inequalities [34], for $P > 0$, $P \in R^{n\times n}$.

$$(A + B\tilde{K} + \sigma_a I)^T P + P(A + B\tilde{K} + \sigma_a I) < 0 \tag{4.1-6}$$

and

$$(A + B\tilde{K} + \sigma_b I)^T P + P(A + B\tilde{K} + \sigma_b I) > 0 \tag{4.1-7}$$

Validation of the alternate perturbation form (4.1-4):

Let K be of full rank, then, the perturbed gain (4.1-3) can be expressed as $\tilde{K} = K\Delta_b + \Delta_a$ with Δ_b providing the independent multiplicative perturbations and Δ_a providing the independent additive perturbations.

Case 1. Single input systems.

K is a $1\times n$ row vector, where n is the system order. Since Δ_c is a scalar, having a diagonal matrix Δ_b will give each element in K an independent multiplier. For example

$$\begin{bmatrix} k_1 & \cdots & k_n \end{bmatrix} \begin{bmatrix} \Delta_{b1} & 0 & 0 \\ 0 & \ddots & 0 \\ 0 & 0 & \Delta_{bn} \end{bmatrix} = \begin{bmatrix} \Delta_{b1}k_1 & \cdots & \Delta_{bn}k_n \end{bmatrix} \tag{4.1-8}$$

Therefore, Δ_c can be absorbed by Δ_b.

Case 2. Multiple input systems.

K is an $m\times n$ matrix ($m \leq n$), where m is the input order and Δ_b is an $n\times n$ matrix as

$$\begin{bmatrix} k_{11} & \cdots & \cdots & k_{1n} \\ \vdots & \ddots & \ddots & \vdots \\ k_{m1} & \ddots & \ddots & k_{mn} \end{bmatrix} \begin{bmatrix} \Delta_{b11} & \cdots & \cdots & \Delta_{b1n} \\ \vdots & \ddots & \ddots & \vdots \\ \vdots & \ddots & \ddots & \vdots \\ \Delta_{bn1} & \cdots & \ddots & \Delta_{bnn} \end{bmatrix} = K\Delta_b + \Delta_a \tag{4.1-9}$$

So the problem reduces to finding an $n\times n$ matrix Δ_b to have independent multipliers on each element in K. Notice that (4.1-9) is in a "$AX = B$" form. If K is of full rank m (which physically implies that there are no redundant actuators), because $m \leq n$, the number of unknowns is greater than or equal to the number of equations (n^2 compared to $m\times n$), so there is at least one solution.

To get the solution of Δ_b, we use the full rank property of *K*, such that $KK^T(KK^T)^{-1} = I_m$. So, $K\Delta_b = \tilde{K}$, for a given perturbed gain, becomes $K\Delta_b = KK^T(KK^T)^{-1}\tilde{K}$, then we have

$$\Delta_b = K^T(KK^T)^{-1}\tilde{K} \tag{4.1-10}$$

Equation (4.1-10) is one possible set of solution of (4.1-9). A general solution can be expressed as follows

$$\Delta_b = K^T(KK^T)^{-1}\tilde{K} + Z \tag{4.1-11}$$

where *Z* is any square matrix with dimension n such that *KZ=0* (zero matrix with dimension $m \times n$). This completes the proof. Therefore, from this point on, it will be assumed that $\tilde{K} = K\Delta_b + \Delta_a$.

4.2 Main LMI Results

Theorem 4-1. The system (4.1-1) with controller (4.1-2) is performance resilient in the sense of maintaining the controlled system eigenvalues within a desired region, if the following LMIs are feasible for some $P, M_0, M_1 > 0$. The bound parameters M_0 and M_1 to maximize the perturbation bound defined in (4.1-5) are found by these LMIs.

$$\begin{bmatrix} -(A+BK)^T P - P(A+BK) - 2\sigma_a P - M_1 & PB \\ B^T P & M_0 \end{bmatrix} > 0 \tag{4.2-1}$$

$$\begin{bmatrix} (A+BK)^T P + P(A+BK) + 2\sigma_b P - M_1 & PB \\ B^T P & M_0 \end{bmatrix} > 0 \tag{4.2-2}$$

Comment: In LMIs (4.2-1) and (4.2-2), *A, B, K,* σ_a and σ_b are all known. The unknowns are *P*, M_0 and M_1. All unknowns are in linear form in the above LMIs.

Proof:

It is desired to have the controller eigenvalues between the vertical lines at $-\sigma_a$ and $-\sigma_b$ in Figure 4.1-1 in the presence of the perturbations on the controller gain *K*.

4.2.1 Controller Eigenvalue Right Bound Condition

From (4.1-6), the following inequality describes a strip region with a right bound:

$$\begin{aligned} &-(A+B(K\Delta_b+\Delta_a)+\sigma_a I+BK-BK)^T P \\ &\qquad -P(A+B(K\Delta_b+\Delta_a)+\sigma_a I+BK-BK)>0 \end{aligned} \tag{4.2-3}$$

Rearranging and moving the terms with "Δ" to the right hand side of the inequality, we have

$$\begin{aligned} &-(A+BK)^T P-P(A+BK)-2\sigma_a P \\ &\qquad >(K\Delta_b+\Delta_a-K)^T B^T P+PB(K\Delta_b+\Delta_a-K) \end{aligned} \tag{4.2-4}$$

Applying Lemma 2 to the right hand side of (4.2-4), we have

$$\begin{aligned} &(K\Delta_b+\Delta_a-K)^T B^T P+PB(K\Delta_b+\Delta_a-K) \\ &\qquad \le (K\Delta_b+\Delta_a-K)^T M_0(K\Delta_b+\Delta_a-K)+PBM_0^{-1}B^T P \end{aligned} \tag{4.2-5}$$

Substituting (4.2-5) into (4.2-4) and using (4.1-5) we have

$$-(A+BK)^T P-P(A+BK)-2\sigma_a P-M_1-PBM_0^{-1}B^T P>0 \tag{4.2-6}$$

which is a sufficient condition for (4.2-3) or (4.2-4) to hold.

Applying lemma 1 (4.2-6) we obtain (4.2-1).

4.2.2 Controller Eigenvalue Left Bound Condition

Similar to (4.2-3), using extra term $\sigma_b I$, we have the inequality which describes a strip region with a left bound as

$$\begin{aligned} &-(A+B(K\Delta_b+\Delta_a)+\sigma_b I+BK-BK)^T P \\ &\qquad -P(A+B(K\Delta_b+\Delta_a)+\sigma_b I+BK-BK)<0 \end{aligned} \tag{4.2-7}$$

Rearranging (4.2-7), we have

$$\begin{aligned} &(A+BK)^T P+P(A+BK)+2\sigma_b P \\ &\qquad +(K\Delta_b+\Delta_a-K)^T B^T P+PB(K\Delta_b+\Delta_a-K)>0 \end{aligned} \tag{4.2-8}$$

Applying Lemma 2 for the second line of (4.2-8), we have

$$\begin{aligned} &(K\Delta_b+\Delta_a-K)^T B^T P+PB(K\Delta_b+\Delta_a-K) \\ &\qquad \geq -(K\Delta_b+\Delta_a-K)^T M_0(K\Delta_b+\Delta_a-K)-PBM_0^{-1}B^T P \end{aligned} \tag{4.2-9}$$

Substituting (4.2-9) into (4.2-8) and applying bound (4.1-5), we obtain

$$(A+BK)^T P+P(A+BK)+2\sigma_b P-M_1-PBM_0^{-1}B^T P>0 \tag{4.2-10}$$

which is a sufficient condition for (4.2-7) or (4.2-8) to hold.

Applying lemma 1 to (4.2-10), we obtain LMI (4.2-2). This completes the proof of Theorem 4-1.

4.3 Further Analysis

In the following analysis and simulation examples, we consider a special case and let $M_0=I$, $M_1=\delta_K I$ and analyze how Δ_a and Δ_b are related to δ_K, based on a maximum δ_K value obtained from the LMIs.

For multiple input systems, using Lemma 3 and Theorem 4-1 with M_0 and M_1 defined above, (4.1-5) can be rewritten in a matrix form as

$$\begin{bmatrix} K & I \end{bmatrix} \begin{bmatrix} \Delta_b - I \\ \Delta_a \end{bmatrix} \begin{bmatrix} \Delta_b - I & \Delta_a \end{bmatrix}^T \begin{bmatrix} K \\ I \end{bmatrix}^T \leq \delta_K I \tag{4.3-1}$$

After we obtain δ_K from the LMIs, we can substitute K, Δ_a and Δ_b into (4.3-1) . If the inequality is satisfied, the closed loop system will be guaranteed to have desired performance.

To visualize (4.3-1), we study a special case of single input systems, where the perturbed gain can be written as

$$\begin{aligned} & K\Delta_b + \Delta_a - K \\ & = \begin{bmatrix} k_1 & \cdots & k_n \end{bmatrix} (\begin{bmatrix} \Delta_{b1} & 0 & 0 \\ 0 & \ddots & 0 \\ 0 & 0 & \Delta_{bn} \end{bmatrix} - I_n) + \begin{bmatrix} \Delta_{a1} & \cdots & \Delta_{an} \end{bmatrix} \end{aligned} \tag{4.3-2}$$

Substituting (4.3-2) into (4.1-5), we have

$$\begin{bmatrix} (\Delta_{b1} - 1)k_1 + \Delta_{a1} & \cdots & (\Delta_{bn} - 1)k_n + \Delta_{an} \end{bmatrix} \begin{bmatrix} k_1(\Delta_{b1} - 1) + \Delta_{a1} \\ \vdots \\ k_n(\Delta_{bn} - 1) + \Delta_{an} \end{bmatrix} \leq \delta_K \tag{4.3-3}$$

which is in the form of

$$\sum_{i=1}^{n} [(\Delta_{bi} - 1)k_i + \Delta_{ai}]^2 \leq \delta_K \tag{4.3-4}$$

For example, for a second order system, (4.3-4) will become

$$[(\Delta_{b1} - 1)k_1 + \Delta_{a1}]^2 + [(\Delta_{b2} - 1)k_2 + \Delta_{a2}]^2 \leq \delta_K \tag{4.3-5}$$

which can be rewritten as

$$\left(\frac{\Delta_{b1} - (1 - \Delta_{a1}/k_1)}{\sqrt{\delta_K}/k_1} \right)^2 + \left(\frac{\Delta_{b2} - (1 - \Delta_{a2}/k_2)}{\sqrt{\delta_K}/k_2} \right)^2 \leq 1 \tag{4.3-6}$$

When $\Delta_a = 0$, which means there are only multiplicative perturbations and no additive perturbations, (4.3-6) becomes

$$\left(\frac{\Delta_{b1}-1}{\sqrt{\delta_K}/k_1}\right)^2 + \left(\frac{\Delta_{b2}-1}{\sqrt{\delta_K}/k_2}\right)^2 \le 1 \qquad (4.3\text{-}7)$$

Inequality (4.3-7) is in the form of an ellipse whose semi-major and semi-minor axes are $\sqrt{\delta_K}/k_1$ and $\sqrt{\delta_K}/k_2$, with center at (1,1). Based on the maximum δ_K and the original k_1, k_2 values, if Δ_{b1} and Δ_{b2} are inside the ellipse, the desired system performance introduced previously will be guaranteed.

Similarly, (4.3-6) is a function of a set of ellipses with the same semi-major and semi-minor axes as (4.3-7), but with different centers based on the values of Δ_{a1} and Δ_{a2}. Comparing to (4.3-7), the size of the ellipses does not change. Values of Δ_{a1} and Δ_{a2} shift the center position of the ellipses.

When $\Delta_b = 0$, which means there are only additive perturbations and no multiplicative perturbations, then (4.3-6) and (4.3-7) become a circle function instead of an ellipse.

The recommended procedure of analysis is as follows:

Given system (4.1-1) and the nominal (unperturbed) feedback gain *K*,

1. Choose the desired closed loop system eigenvalue region (σ_a and σ_b values) corresponding to the desired system performance shown in Figure 4.1-1.
2. Solve LMIs (4.2-1) and (4.2-2) for maximum δ_K.

3. Use maximum δ_K in (4.3-1), and based on the known gain K and its perturbation Δ_a and Δ_b, determine whether the system performance is in the desired region.

4.4 Simulation Studies and Analysis

This section contains simulation results of the controller performance analysis proposed in this chapter. An unstable second order system is chosen to demonstrate possible application of the proposed analysis procedure.

$$\begin{bmatrix} \dot{x}_1 \\ \dot{x}_2 \end{bmatrix} = \begin{bmatrix} -0.2 & 2 \\ -1 & 0.5 \end{bmatrix} \begin{bmatrix} x_1 \\ x_2 \end{bmatrix} + \begin{bmatrix} 0.5 \\ 0.5 \end{bmatrix} u \tag{4.4-1}$$

The eigenvalues of the open loop system at $0.15 \pm 1.37i$ are in the right complex plane, so the state variables of the open loop system diverge quickly.

We follow the process described previously for this example. Controller gain $K = \begin{bmatrix} -2.38 & -4.22 \end{bmatrix}$ is used to place the controller eigenvalues on the real axis at -1 and -2.

Step 1: We choose the desired controller eigenvalue region to be a strip between -3 and -0.5.

Step 2: Solving LMI (4.2-1), the maximized δ_K form the LMI for right bound condition is 0.833. Solving LMI (4.2-2) the maximized δ_K for left bound condition is 0.936. The perturbation bound δ_K overall, is found as the smaller value of the maximum δ_K values found with LMIs (4.2-1) and (4.2-2) resulting for the right and left boundaries of the controller region. So the maximum allowed value for both bounds is **0.833**.

Step 3: For illustrative purposes, in this example, we study a case with only multiplicative perturbations, i.e. $\tilde{K} = K\Delta_b$. Substituting the parameters into (4.3-7), we have

$$\left(\frac{\Delta_{b1}-1}{0.385}\right)^2 + \left(\frac{\Delta_{b2}-1}{0.216}\right)^2 \leq 1 \tag{4.4-2}$$

Inequality (4.4-2) describes an ellipse with semi-major axis of length 0.385 and semi-minor axis of 0.216, centered at (1,1), showing in red in Figure 4.4-2.

In the analysis problem, when we have the values of Δ_b, using (4.4-2), we will know if the desired controller performance is satisfied. The degree of sharpness the analysis will be discussed in the following via the example above.

For the system, the largest actual controller gain perturbations can be determined by finding maximum δ_K for which the eigenvalues of $A + B\tilde{K}$ remain within the specified region as compared with the theoretical value. By defining $\tilde{K}$ as the original gain plus the extra perturbed part

$$\tilde{K} = \begin{bmatrix} K_1 & K_2 \end{bmatrix} + \begin{bmatrix} \delta_c \cos\theta & \delta_c \sin\theta \end{bmatrix} \tag{4.4-3}$$

where $\delta_c = \sqrt{\Delta_K \Delta_K{}^T} = \sqrt{\delta_K}$.

By sweeping θ through 360 degrees, and for each degree increment, finding the maximum value for δ_c by incrementing δ_c until the eigenvalues of $A + B\tilde{K}$ exit the specified region, we obtain maximum value of δ_c for each angle which is the maximum perturbation tolerance for that particular angle.

The results for δ_c^2 values for each angle are shown in Figure 4.4-1 for the controller gain tolerances. This figure shows that using unperturbed *K* (-2.38, -4.22) as center, for each angle 0º through 360º, how much perturbation it can have on each direction. The figure shows that the maximum perturbation is highly direction dependent.

As shown in Figure 4.4-1, the minimum among these maximum allowable values is 0.90 at 305º, determined from closed loop system simulation. This minimum value 0.9 from simulation is very close to the bound 0.833 which is obtained from the LMIs.

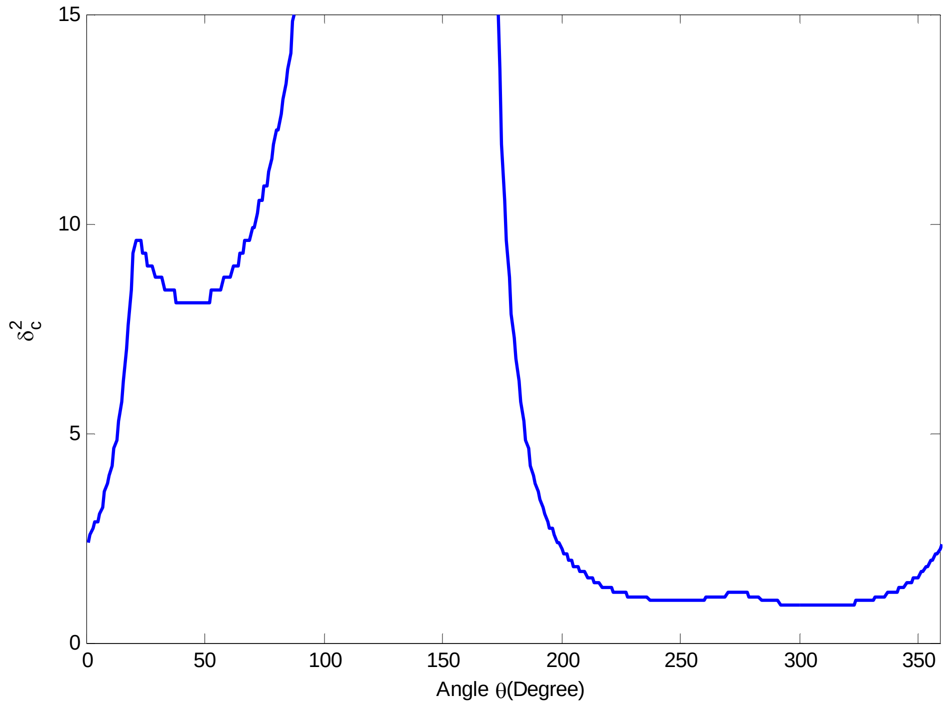

Figure 4.4-1 Perturbations allowed in each direction for *K*

Notice that the perturbation tolerance in some of the directions can be very large and is not shown in Figure 4.4-1. in For instance, large perturbation can be added in the directions from about 90º to 170º for *K* and the desired system performance is still maintained.

Figure 4.4-1 is an intuitive way to study perturbations in different directions in terms of *K*. However, in order to discuss the degree of sharpness of the proposed LMI result, we need to transfer all these δ_c values to Δ_{b1} and Δ_{b2} coordinates so that comparison can be made with (4.4-2), which is derived from LMI results.

Rearranging definition (4.4-3), we have

$$\left[K_1(\Delta_{b1}-1) \quad K_2(\Delta_{b2}-1)\right] = \left[\delta_c \cos\theta \quad \delta_c \sin\theta\right] \tag{4.4-4}$$

which means

$$\left[\Delta_{b1} \quad \Delta_{b2}\right] = \left[\delta_c \frac{\cos\theta}{K_1}+1 \quad \delta_c \frac{\sin\theta}{K_2}+1\right] \tag{4.4-5}$$

After substituting all θ and δ_c values, we obtain 360 pairs of Δ_{b1} and Δ_{b2} values, which are plotted in blue in Figure 4.4-2. LMI result (4.4-2) is plotted in red.

We can see from the blue colored bounds in Figure 4.4-2 that the minimum deviation distance from (1,1) for all 360 degrees is very close to the red ellipse, which is from the LMI result. This shows that the proposed bound is very sharp for this system. While large perturbations may be allowed in certain directions, LMI result provides a safe and guaranteed bound for all directions.

The minimum value in Figure 4.4-1, 0.902 at 305°, will transfer to the point C(0.783, 1.175) in Figure 4.4-2, if we use (4.4-5). From simulation results in blue, that point is the closest point to the center (1, 1) and to the ellipse. If we draw a straight line using point (0.783, 1.175) and center (1, 1), we will get the intersection point on the ellipse (0.81, 1.15). Besides the unperturbed case, we use these two data points in Figure 4.4-2 as two different sets of perturbed gains to obtain a state variable co-plot comparison in Figure 4.4-3. Moreover, for comparison purposes, we choose another point (0.58, 1.35) on that straight line. This point exceeds the bound of the simulation result of δ_c in the corresponding direction.

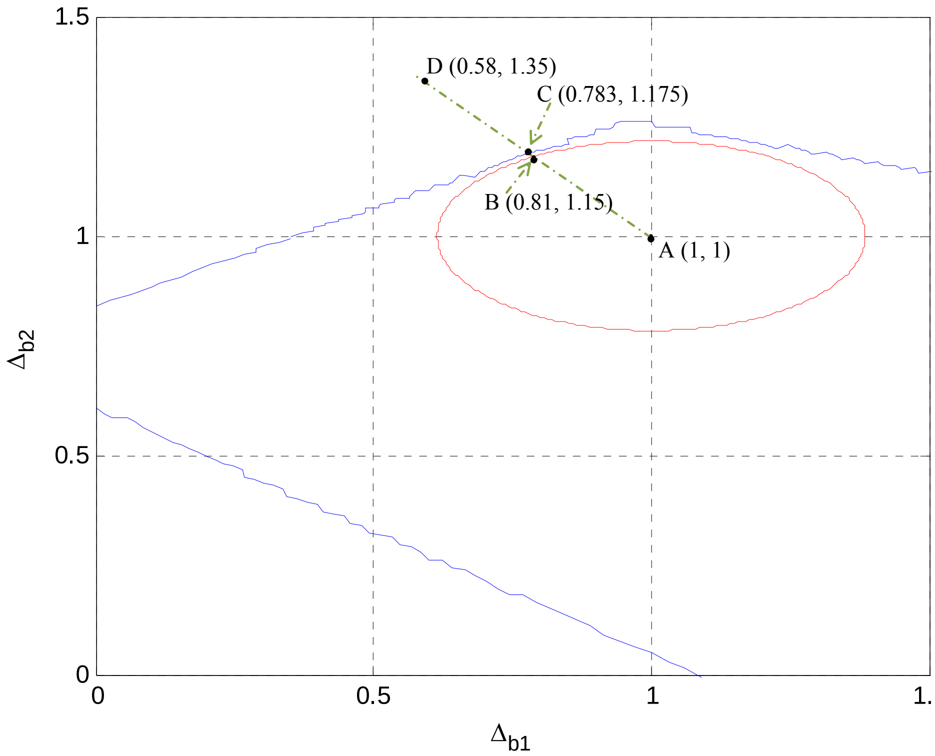

Figure 4.4-2 Comparison of Δ_{b1} and Δ_{b2} behavior of LMI result and simulation result

The co-plot of the state variables with x_0=[-1; 1] for all cases is given in Figure 4.4-3. And closed loop controller eigenvalues for all cases are given in Figure 4.4-4. We can tell that the responses are different in terms of settling time. By observing the eigenvalue location we can also see in Figure 4.4-4 that although the system response is stable for all cases, the desired performance is not achieved for case (d), represented by the black “x”.

As we stated in the introduction, the LMI result gives a safe and guaranteed bound on gain perturbation for all directions, which provides us a quick and convenient way of performing this analysis without conducting extensive simulations.

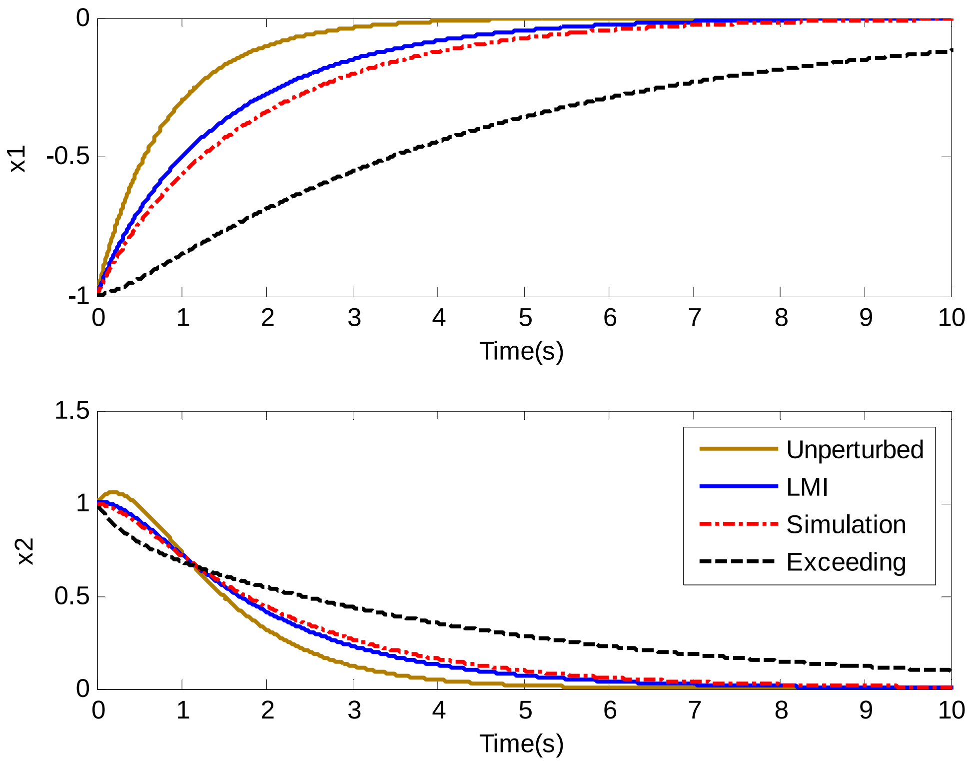

Figure 4.4-3 Co-plots of the state variables in four cases, (a) No perturbation, (b) LMI result, (c) Simulation result (d) Exceeding limit

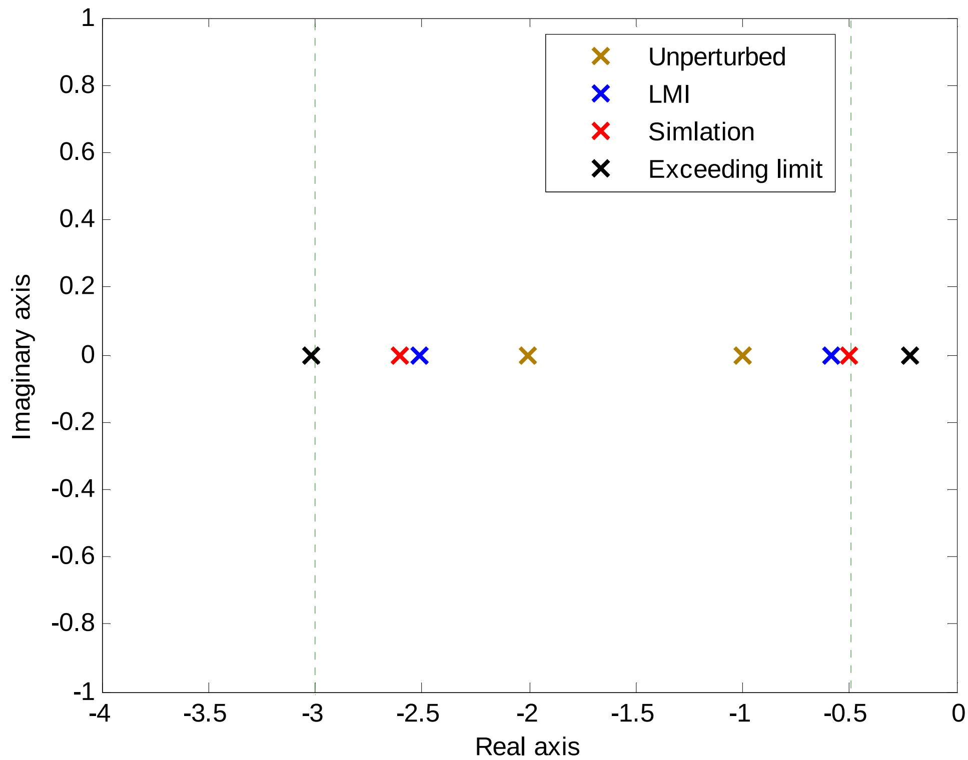

Figure 4.4-4 Eigenvalue positions of all four cases

4.5 Conclusion

In this chapter, a performance analysis procedure for a resilient state feedback controller has been presented for continuous-time linear systems. By defining controller eigenvalue regions, multiplicative and additive perturbation bounds allowed in controller gains are found. With this method, designers can evaluate the resilience degree of their controllers based on the design parameters chosen and adjust design parameters to fit appropriate design requirements. LMI techniques are used throughout the process.

CHAPTER 5

ANALYSIS OF PERFORMANCE RESILIENCE OF STATE FEEDBACK CONTROLLERS FOR CONTINUOUS-TIME SYSTEMS

5.0 Introduction

In this chapter, a procedure is presented for performance analysis of the resilience property of discrete-time systems with perturbed controller and observer gains. The resilience property is defined in terms of both multiplicative and additive perturbations on the gains so that the closed loop eigenvalues do not leave a specified region in the complex plane. In this work, this region is chosen as a disk in the unit circle. Maximum gain perturbation bounds can be obtained based on the designer's choice of the controller eigenvalue region. Linear matrix inequality techniques are used throughout the analysis process. Illustrative examples are included to demonstrate the effectiveness of the proposed methodology.

This chapter is the discrete-time counterpart of Chapter 4. In Section 5.1, the system model and problem formulation are introduced. The solution of the analysis problem is derived in Section 5.2. Further analysis is given in Section 5.3. Some illustrative simulation studies and example discussion are presented in Section 5.4. Conclusions are given in Section 5.5.

5.1 Problem Formulation

Let us consider a discrete-time linear system,

$$x_{k+1} = Ax_k + Bu_k \tag{5.1-1}$$

where $x_k \in R^n$ is the state, $u_k \in R^m$ is the input.

A linear state feedback controller is used in this system,

$$u_k = \tilde{K}x_k \tag{5.1-2}$$

where the feedback gain K may in general be perturbed as,

$$\tilde{K} = \Delta_c K \Delta_b + \Delta_a \tag{5.1-3}$$

both additively and multiplicatively. Similar to (4.1-4), the following form will be used in this chapter without loss of generality

$$\tilde{K} = K\Delta_b + \Delta_a \tag{5.1-4}$$

where $\Delta_a \in R^{m\times n}, \Delta_b \in R^{n\times n}$.

The perturbation is assumed to be bounded by

$$(K\Delta_b + \Delta_a - K)^T M_0 (K\Delta_b + \Delta_a - K) \le M_1 \tag{5.1-5}$$

where $M_0 \in R^{m\times m}, M_1 \in R^{n\times n}$ are symmetric positive definite matrices.

As stated in the introduction, our goal is to analyze the state feedback design to determine how large the perturbations can be so that the performance of the system with perturbed controller gains remains acceptable. In addition to achieving stability, we will also identify acceptable state feedback controller performance in terms of regions in the complex plane within which the eigenvalues of the perturbed controller must remain. Eigenvalue positions result in different system performances such as settling time, percentage overshoot and rise time. As shown in Figure 5.1-1, for this work the eigenvalues of the closed loop system $x_{k+1} = [A + B(K\Delta_b + \Delta_a)]x_k$ are chosen to lie within the disk of center $(\sigma, 0)$, radius r to guarantee a multiple of response criteria including settling and rise time together with a bound on the overshoot [2].

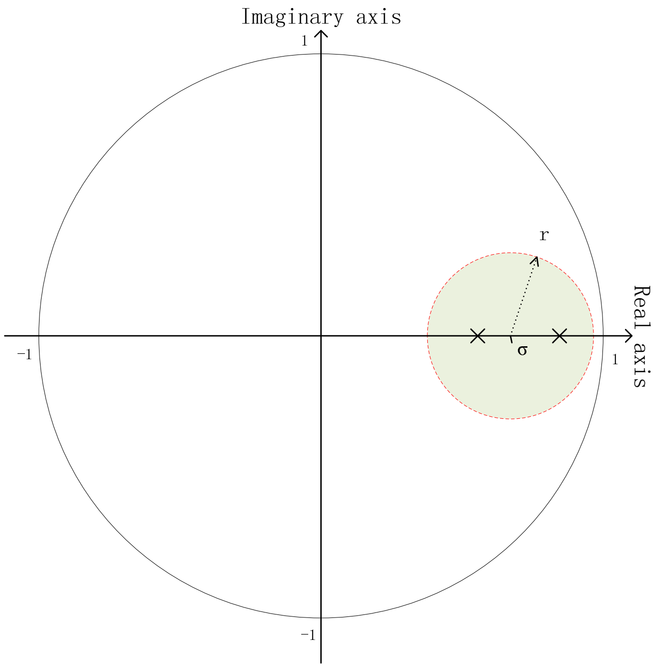

Figure 5.1-1 Desired controller eigenvalues region

The resilience analysis is based on satisfying the following Lyapunov inequality [34], for $P > 0$, $P \in R^{n\times n}$.

$$r^2 P - (A + B\tilde{K} - \sigma I)^T P(A + B\tilde{K} - \sigma I) > 0 \qquad (5.1\text{-}6)$$

5.2 Main Result

Theorem 5-1. The system (5.1-1) with controller (5.1-2) is performance resilient in the sense of maintaining the controlled system eigenvalues within the desired region, if the following LMI is feasible for some $P, M_0, M_1 > 0$. The bound parameters, M_0 and M_1, defined by (5.1-5) are found by this LMI.

$$\begin{bmatrix} r^2P - M_1 I & (A+BK-\sigma I)^T P & 0 \\ P(A+BK-\sigma I) & P & PB \\ 0 & B^T P & M_0 \end{bmatrix} > 0 \tag{5.2-1}$$

Comment: In LMI (5.2-1), *A, B, K,* σ and *r* are all known. The unknowns are *M_0, M_1* and *P*. Note that all unknowns are in linear form in the above LMI.

Proof:

It is desired to have the controller eigenvalues within the disk region of center $(\sigma, 0)$, radius r in Figure 5.1-1, in the presence of the perturbations on the controller gain K.

Applying Lemma 1 to (5.1-6), the disk region condition, and substituting $\tilde{K}$, we have

$$\begin{bmatrix} r^2P & (A+B(K\Delta_b+\Delta_a)-\sigma I)^T P \\ P(A+B(K\Delta_b+\Delta_a)-\sigma I) & P \end{bmatrix} > 0 \tag{5.2-2}$$

Rearranging and moving the terms with "Δ" to the right hand side of the inequality (5.2-2) and adding $\begin{bmatrix} 0 & (BK)^T P \\ PBK & 0 \end{bmatrix}$ to both sides, we have

$$\begin{aligned} &\begin{bmatrix} r^2P & (A+BK-\sigma I)^T P \\ P(A+BK-\sigma I) & P \end{bmatrix} \\ &> \begin{bmatrix} 0 & [BK-B(K\Delta_b+\Delta_a)]^T P \\ P[BK-B(K\Delta_b+\Delta_a)] & 0 \end{bmatrix} \end{aligned} \tag{5.2-3}$$

The right hand side of (5.2-3) can be rewritten and by using Lemma 2, an upper bound of it will be obtained.

$$\begin{bmatrix} 0 & [BK - B(K\Delta_b + \Delta_a)]^T P \\ P[BK - B(K\Delta_b + \Delta_a)] & 0 \end{bmatrix}$$
$$= \begin{bmatrix} (K - K\Delta_b - \Delta_a)^T \\ 0 \end{bmatrix} \begin{bmatrix} 0 & B^T P \end{bmatrix} + \begin{bmatrix} 0 \\ PB \end{bmatrix} \begin{bmatrix} K - K\Delta_b - \Delta_a & 0 \end{bmatrix} \tag{5.2-4}$$
$$\leq \begin{bmatrix} (K - K\Delta_b - \Delta_a)^T M_0 (K - K\Delta_b - \Delta_a) & 0 \\ 0 & 0 \end{bmatrix} + \begin{bmatrix} 0 \\ PB \end{bmatrix} M_0^{-1} \begin{bmatrix} 0 & B^T P \end{bmatrix}$$

Substituting (5.2-4) into (5.2-3) and applying (5.1-5), we have

$$\begin{bmatrix} r^2 P - M_1 & (A + BK - \sigma I)^T P \\ P(A + BK - \sigma I) & P \end{bmatrix} - \begin{bmatrix} 0 \\ PB \end{bmatrix} M_0^{-1} \begin{bmatrix} 0 & B^T P \end{bmatrix} > 0 \tag{5.2-5}$$

which is a sufficient condition for (5.2-2) or (5.2-3) to hold.

Applying Lemma 1 to (5.2-5), we obtain LMI (5.2-1). This completes the proof of Theorem 5-1.

5.3 Further Analysis

Analysis process from (4.3-1) to (4.3-7) can also be used in the discrete-time case of this chapter when we let $M_0 = I,\ M_1 = \delta_K I$ and analyze how Δ_a and Δ_b are related to δ_K, based on a maximum δ_K value obtained from the LMI. Therefore in the simulation example in next section, the following result will be used again.

$$\left(\frac{\Delta_{b1} - 1}{\sqrt{\delta_K / k_1}} \right)^2 + \left(\frac{\Delta_{b2} - 1}{\sqrt{\delta_K / k_2}} \right)^2 \leq 1 \tag{5.3-1}$$

Inequality (5.3-1) is in the form of an ellipse whose semi-major and semi-minor axes are $\sqrt{\delta_K / k_1}$ and $\sqrt{\delta_K / k_2}$, with center at (1,1). Based on the maximum δ_K and the original k_1, k_2 values, if Δ_{b1} and Δ_{b2} are inside the ellipse, the desired system performance introduced previously will be guaranteed.

The recommended procedure of analysis is as follows:

Given system (5.1-1) and the nominal (unperturbed) feedback gain *K*,

1. Choose the desired closed loop system eigenvalue region (σ and *r* values) corresponding to the desired system performance shown in Figure 5.1-1.

2. Solve LMI (5.2-1) for maximum δ_K.

3. Use maximum δ_K, and based on the known gain *K* and its perturbation Δ_a and Δ_b, determine whether the system performance is in the desired region.

5.4 Simulation Study

This section contains simulation results of the controller performance analysis proposed in this work. An unstable second order system is chosen to demonstrate possible application of the proposed methodology.

$$\begin{bmatrix} x_1 \\ x_2 \end{bmatrix}_{k+1} = \begin{bmatrix} 0.998 & 0.02 \\ -0.01 & 1.005 \end{bmatrix} \begin{bmatrix} x_1 \\ x_2 \end{bmatrix}_k + \begin{bmatrix} 0.1 \\ 0.1 \end{bmatrix} u_k \tag{5.4-1}$$

The eigenvalues of the open loop system are $1.0015 \pm 0.0137i$ (outside of the unit circle) and the state variables of the open loop system diverge quickly.

We follow the process described previously for this example. Controller gain $K = \begin{bmatrix} -7.79 & 5.16 \end{bmatrix}$ is used to place the controller eigenvalues on the real axis at 0.84 and 0.9.

Step 1: We choose the desired controller eigenvalue region to be a disk with center (0.87, 0) and radius 0.1.

Step 2: Solving LMI (5.2-1), the maximized δ_K for the disk condition is **0.077.**

Step 3: For illustrative purposes, in this example, we study a case with only multiplicative perturbations, i.e. $\tilde{K} = K\Delta_b$. Substituting the parameters into (5.3-1), we have

$$\left(\frac{\Delta_{b1}-1}{0.0356}\right)^2 + \left(\frac{\Delta_{b2}-1}{0.0538}\right)^2 \le 1 \tag{5.4-2}$$

Inequality (5.4-2) describes an ellipse with semi-major axis of length 0.0356 and semi-minor axis of 0.0538, centered at (1,1).

In the analysis, when we have the values of Δ_b, using (5.4-2), we will know if the desired controller performance is satisfied.

The degree of sharpness of the analysis will be discussed in the following via the example above.

For the system, the largest actual controller gain perturbations can be determined by finding the maximum δ_K for which the eigenvalues of $A+B\tilde{K}$ remain within the specified region as compared with the theoretical value. By defining $\tilde{K}$ as the original gain plus the extra perturbed part

$$\tilde{K} = \begin{bmatrix} K_1 & K_2 \end{bmatrix} + \begin{bmatrix} \delta_c \cos\theta & \delta_c \sin\theta \end{bmatrix} \tag{5.4-3}$$

where $\delta_c = \sqrt{\Delta_K \Delta_K{}^T} = \sqrt{\delta_K}$.

By sweeping θ through 360 degrees, and for each degree increment, finding the maximum value for δ_c by incrementing δ_c until the eigenvalues of $A+B\tilde{K}$ exit the specified region, we obtain maximum value of δ_c for each angle which is the maximum perturbation tolerance for that particular angle.

The results for δ_c^2 values for each angle are shown in Figure 5.4-1 for the controller gain tolerances. This figure shows that using unperturbed K (-7.79, 5.16) as center, for each angle 0º through 360º, how much perturbation it can have on each direction. The figure shows that the maximum perturbation is highly direction dependent.

As shown in Figure 5.4-1, the minimum among these maximum allowable values is 0.0805 at 230º, determined from closed loop system simulation. This minimum value 0.0805 from simulation is very close to the bound 0.077 which is obtained from the LMI.

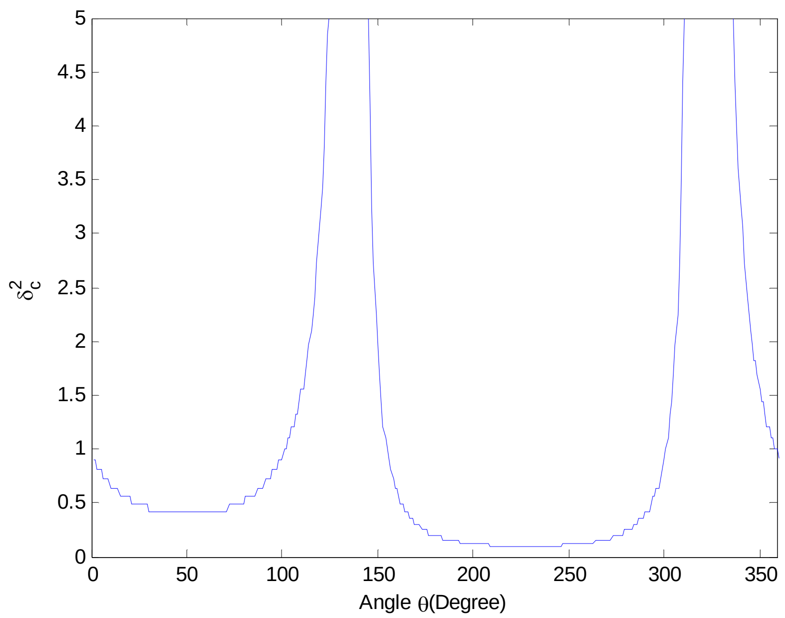

Figure 5.4-1 Perturbations allowed in each direction for K

Notice that the perturbation tolerance in some of the directions can be very large. For instance, large perturbation can be added in the directions from about 110º to 150º for K and the desired system performance is still maintained.

Figure 5.4-1 is an intuitive way to study perturbations in different directions in terms of *K*. However, in order to discuss the degree of sharpness of the proposed LMI result, we need to transfer all these δ_c values to Δ_{b1} and Δ_{b2} coordinates so that comparison can be made with (5.4-2), which is derived from LMI results.

Rearranging definition (5.4-3), we have

$$\left[K_1(\Delta_{b1}-1) \quad K_2(\Delta_{b2}-1)\right]=\left[\delta_c\cos\theta \quad \delta_c\sin\theta\right] \tag{5.4-4}$$

which means,

$$\left[\Delta_{b1} \quad \Delta_{b2}\right]=\left[\delta_c\cos\theta/K_1+1 \quad \delta_c\sin\theta/K_2+1\right] \tag{5.4-5}$$

After substituting all θ and δ_c values, we obtain 360 pairs of Δ_{b1} and Δ_{b2} values, which are plotted in blue in Figure 5.4-2 and a key portion zoomed in Figure 5.4-3. LMI result (5.4-2) is plotted in red.

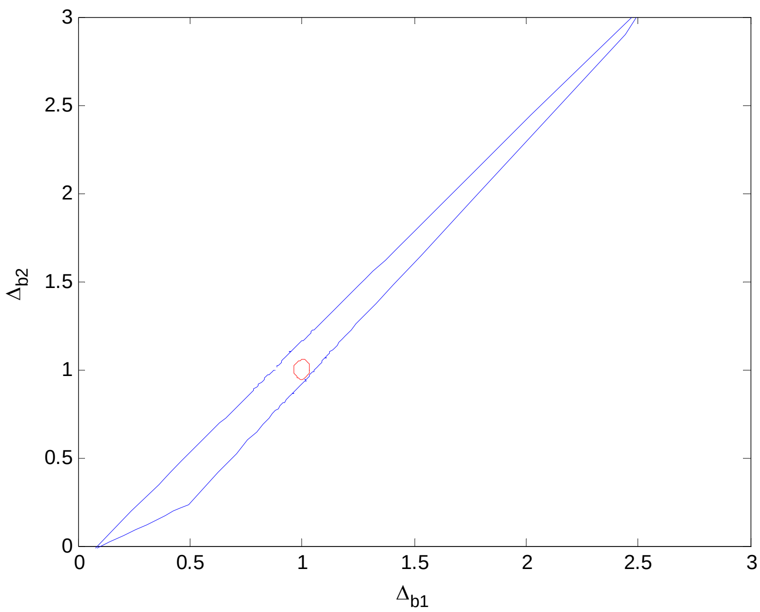

Figure 5.4-2 Comparison of Δb_1 and Δb_2 behavior of LMI result and simulation result

We can see from the blue colored bounds in Figure 5.4-3 that the minimum deviation distance from (1,1) for all 360 degrees is very close to the red ellipse, which is from the LMI result. This shows that the proposed bound is very sharp for this system. While large perturbations may be allowed in certain directions, LMI result provides a safe and guaranteed bound for all directions.

The minimum value in Figure 5.4-1, 0.0805 at 230º, will transfer to the point C, coordinate (1.0234, 0.958) in Figure 5.4-3, if we use (5.4-5). In all the data from simulation results in blue, that point is the closest point to the center point A (1,1) and to the ellipse. If we draw a straight line using point C and center A, we will get the intersection point B on the ellipse (1.0228, 0.959). Besides the unperturbed case, we use these two data points in Figure 5.4-3 as two different sets of perturbed gains to obtain a state variable co-plot comparison in Figure 5.4-4. Moreover, for comparison purposes, we choose another point D (1.045, 0.919) on that straight line. This point exceeds the bound of the simulation result of δ_c in the corresponding direction.

The co-plot of the state variables with x_0=[-1; 1] for all cases is given in Figure 5.4-4. And closed loop controller eigenvalues for all cases are given in Figure 5.4-5. We can tell that the responses are different in terms of settling time. By observing the eigenvalue location we can also see in Figure 5.4-5 that although the system response is stable for all cases, desired performance is not achieved for case (d), presented by the black “x”.

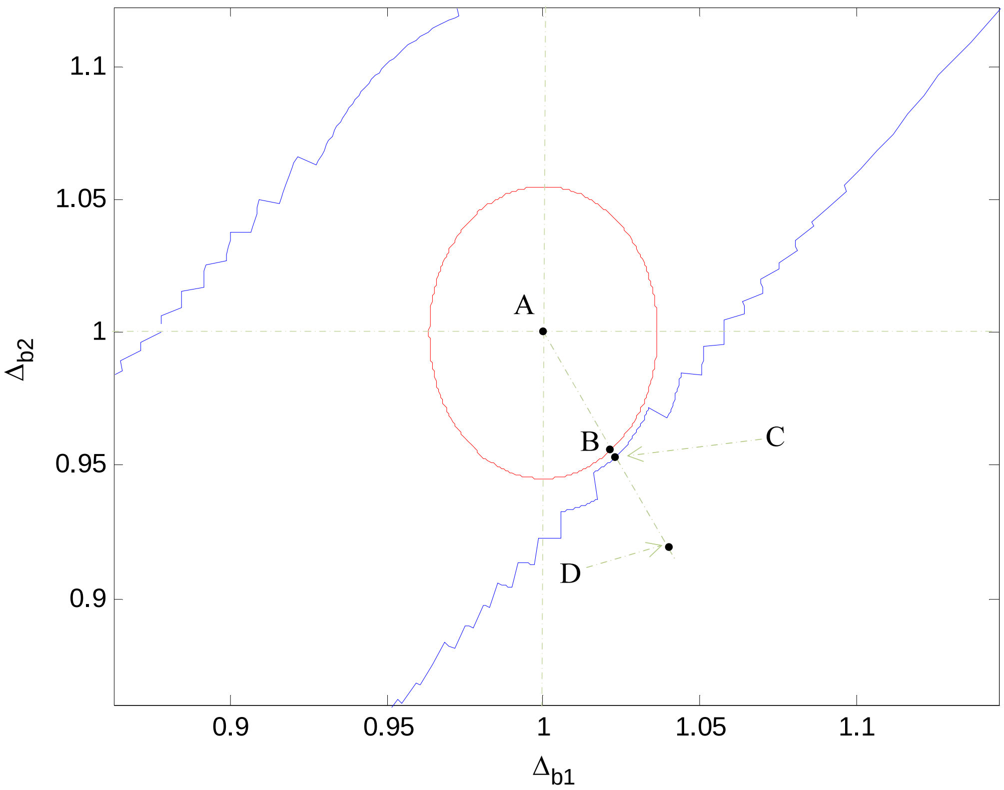

Figure 5.4-3 Comparison of Δ_{b1} and Δ_{b2} behavior of LMI result and simulation result (zoomed-in)

As we stated in the introduction, the LMI result gives a safe and guaranteed bound on gain perturbations for all directions, which provides us a quick and convenient way of performing this analysis without conducting extensive simulations.

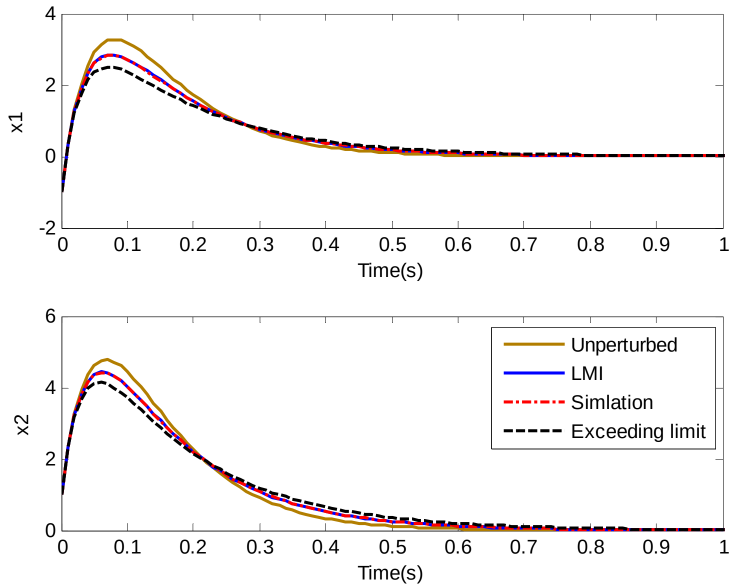

Figure 5.4-4 Co-plots of the state variables in four cases, (a) No perturbation, (b) LMI result, (c) Simulation result (d) Exceeding limit

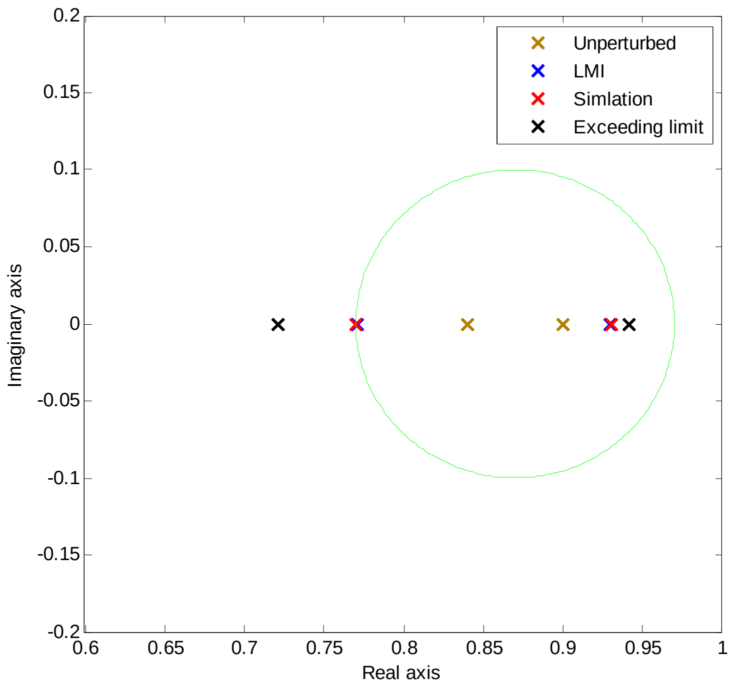

Figure 5.4-5 Eigenvalue positions of all four cases

5.5 Conclusion

In this chapter, performance analysis procedure for a resilient state feedback controller has been presented for discrete-time linear systems. By defining controller eigenvalue regions, multiplicative and additive perturbation bounds allowed in controller gains are found. With this method, designers can evaluate the resilience degree of their controllers based on the design parameters chosen and adjust design parameters to fit appropriate design requirements. LMI techniques are used throughout the process.

CHAPTER 6

ANALYSIS OF PERFORMANCE RESILIENCE OF DYNAMIC FEEDBACK CONTROLLERS FOR CONTINUOUS-TIME SYSTEMS

6.0 Introduction

In this chapter, a procedure is presented for performance analysis of the resilience of continuous-time systems controlled by full-order dynamic feedback compensators. The resilience property is defined in terms of perturbations on both the controller and observer gains that will maintain controller and observer eigenvalues in disjoint vertical strips in the complex plane. Maximum gain perturbation bounds can be obtained based on the designer's choices of controller and observer eigenvalue. The linear matrix inequality technique is used throughout the analysis process. Illustrative examples are included to demonstrate the effectiveness of the proposed methodology.

The work of this chapter is an extension of chapter 4, where the performance resilience analysis is extended to a dynamic (state estimate) feedback controller. Perturbations can be allowed in both controller and observer gains. In Section 6.1, the system model and problem formulation are introduced. The solution of the analysis problem is derived in Section 6.2. Some illustrative simulation studies and example discussion are presented in Section 6.3. Conclusions are given in Section 6.4.

6.1 Problem Formulation

Let us consider a continuous time linear system,

$$\dot{x} = Ax + Bu \tag{6.1-1}$$

$$y = Cx + Du \tag{6.1-2}$$

where $x \in R^n$ is the state, $u \in R^m$ is the input and y is the measure output.

A linear state estimate feedback control is used in this system.

$$u = \tilde{K}\hat{x} \tag{6.1-3}$$

where the feedback gain K may be perturbed due to the reasons cited in the introduction, where $\tilde{K} = K + \Delta_K$, and $\hat{x}$ is the state estimate.

We use a Luenberger (identity) observer

$$\dot{\hat{x}} = A\hat{x} + Bu + \tilde{L}(y - C\hat{x} - Du) \tag{6.1-4}$$

where the observer gain L is also perturbed as $\tilde{L} = L + \Delta_L$.

We assume that the perturbations on both the feedback and observer gains are bounded as,

$$\Delta_K M_0 \Delta_K{}^T < M_1, \quad \Delta_L{}^T N_0 \Delta_L < N_1 \tag{6.1-5}$$

For error of the state estimation defined as,

$$e = x - \hat{x} \tag{6.1-6}$$

we obtain the error update equation by subtracting (6.1-4) from (6.1-1) as

$$\dot{e} = [A - (L + \Delta_L)C]e \tag{6.1-7}$$

As stated in the introduction, our goal is to analyze the dynamic feedback design to determine how large the perturbation bounds can be so that the performance of the system with perturbed controller and observer gains remains acceptable. We will identify acceptable dynamic feedback controller performance in terms of regions in the complex plane within which the eigenvalues of the perturbed controller and observer must remain. As shown in Figure 6.1-1, the eigenvalues of the closed loop system $\dot{x} = [A + B(K + \Delta_K)]x$ will lie in the vertical strip between -*a* and -*b* and similarly, the eigenvalues of $\dot{e} = [A - (L + \Delta_L)C]e$ will remain in the region between -*c* and -*d*. Moreover, in a state estimate feedback control scheme, for the observer to be efficient, we will require $c \geq 5b$ for faster observer dynamics to guarantee good closed loop performance.

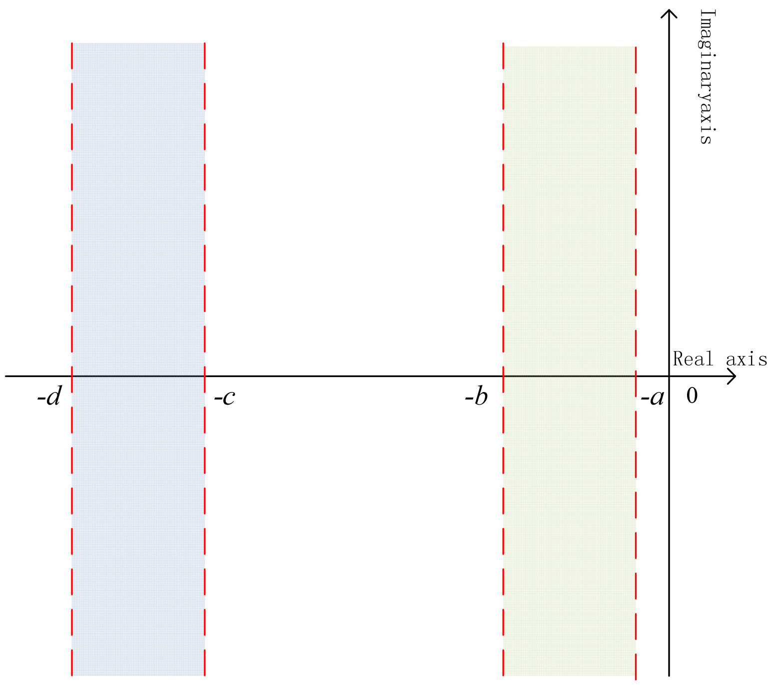

Figure 6.1-1 Desired controller and observer eigenvalues region

By introducing an augmented state variable $X = \begin{bmatrix} x \\ e \end{bmatrix}$, the dynamics of the closed loop system will be

$$
\begin{aligned}
\dot{X} = \begin{bmatrix} \dot{x} \\ \dot{e} \end{bmatrix} &= \begin{bmatrix} A + B(K + \Delta_K) & -B(K + \Delta_K) \\ 0 & A - (L + \Delta_L)C \end{bmatrix} \begin{bmatrix} x \\ e \end{bmatrix} \\
&= \begin{bmatrix} A + BK & -BK \\ 0 & A - LC \end{bmatrix} \begin{bmatrix} x \\ e \end{bmatrix} + \begin{bmatrix} B\Delta_K & -B\Delta_K \\ 0 & -\Delta_L C \end{bmatrix} \begin{bmatrix} x \\ e \end{bmatrix} \\
&= (\mathbb{A} + \Delta)X
\end{aligned}
\tag{6.1-8}
$$

The resilience analysis is based on a Lyapunov energy approach using functions $V_x = x^T P_c x$ and $V_e = e^T P_o e$ such that $\dot{V}_x < 0$ and $\dot{V}_e < 0$ based on the decoupled nature of the state and observer dynamics in (6.1-8).

6.2 Main Results

Theorem 6-1. Dynamic feedback controller design will have resilient properties in the sense of maintaining their eigenvalues within the regions shown in Figure 6.1-1 for perturbed feedback gain (6.1-3) and perturbed observer gain (6.1-4) for the system described by (6.1-8), if the following LMIs are feasible for some positive definite matrices P_c, P_o, M_0 and M_1.

$$
\begin{bmatrix} -(A + BK)^T P_c - P_c(A + BK) - 2aP_c - M_1 & P_c B \\ B^T P_c & M_0 \end{bmatrix} > 0 \tag{6.2-1}
$$

$$
\begin{bmatrix} (A + BK)^T P_c + P_c(A + BK) + 2bP_c - M_1 & P_c B \\ B^T P_c & M_0 \end{bmatrix} > 0 \tag{6.2-2}
$$

$$
\begin{bmatrix} -(A - LC)P_o - P_o(A - LC)^T - 2cP_o - N_1 & P_o C^T \\ CP_o & N_0 \end{bmatrix} > 0 \tag{6.2-3}
$$

$$
\begin{bmatrix} (A - LC)P_o + P_o(A - LC)^T + 2dP_o - N_1 & P_o C^T \\ CP_o & N_0 \end{bmatrix} > 0 \tag{6.2-4}
$$

Comment: In LMIs (6.2-1) to (6.2-4), system parameters *A, B, K*, and bound parameters *a, b, c, d* are all known. The unknowns are P_c, P_o, M_0, M_1, N_0 and N_1. All unknowns are in linear form in the above LMIs.

The proof of Theorem 6-1 is given in the following sections.

6.2.1 Controller Eigenvalue Conditions

It is desired to have the controller eigenvalues between the vertical lines at -*a* and -*b* in Figure 6.1-1 in the presence of the perturbations on the control gain *K*.

Controller eigenvalue right bound condition:

From (6.1-8) and (6.2-3), we have

$$(A+B\tilde{K}+aI)P_c+P_c(A+B\tilde{K}+aI)^T<0 \tag{6.2-5}$$

Rearranging (6.2-5), we have

$$-(A+BK)^T P_c-P_c(A+BK)-2aP_c>\Delta_K{}^T B^T P_c+P_cB\Delta_K \tag{6.2-6}$$

Applying Lemma 2 to the right hand side of (6.2-6), we have

$$\Delta_K{}^T B^T P_c+P_cB\Delta_K\le\Delta_K M_0\Delta_K{}^T+P_cBM_0{}^{-1}B^T P_c \tag{6.2-7}$$

Substituting (6.2-7) into (6.2-6) and using (6.1-5) we have

$$-(A+BK)^T P_c-P_c(A+BK)-2aP_c-M_1-P_cBM_0{}^{-1}B^T P_c>0 \tag{6.2-8}$$

which is a sufficient condition for (6.2-6) to hold.

Applying lemma 1 to (6.2-8) we obtain LMI (6.2-1).

Controller eigenvalue left bound condition:

Similarly to (6.2-5), we have

$$(A+B\tilde{K}+bI)^T P_c+P_c(A+B\tilde{K}+bI)>0 \tag{6.2-9}$$

Rearranging (6.2-9), we have

$$(A+BK)^T P_c + P_c(A+BK) + 2bP_c + \Delta_K{}^T B^T P_c + P_c B\Delta_K > 0 \qquad (6.2\text{-}10)$$

Applying Lemma 2 to the last two terms of (6.2-10), a bound can be found as

$$\Delta_K{}^T B^T P_c + P_c B\Delta_K \le -\Delta_K M_0 \Delta_K{}^T - P_c B M_0{}^{-1} B^T P_c \qquad (6.2\text{-}11)$$

Substituting (6.2-11) into (6.2-10) and using (6.1-5) we have

$$(A+BK)^T P_c + P_c(A+BK) + 2bP_c - M_1 - P_c B M_0{}^{-1} B^T P_c > 0 \qquad (6.2\text{-}12)$$

which is a sufficient condition for (6.2-10) to hold.

Applying lemma 1 to (6.2-12) we obtain (6.2-2).

6.2.2 Observer Eigenvalue Conditions

It is desired to have the observer eigenvalues between the vertical lines at -c and -d in Figure 6.1-1 in the presence of the perturbations on observer gain *L*.

For the observer right and left bounds, we start from the following inequalities, respectively

$$(A - \tilde{L}C + cI)P_o + P_o(A - \tilde{L}C + cI)^T < 0 \qquad (6.2\text{-}13)$$

$$(A - \tilde{L}C + dI)P_o + P_o(A - \tilde{L}C + dI)^T > 0 \qquad (6.2\text{-}14)$$

The process to derive LMIs (6.2-3) and (6.2-4) which result for the observer boundary follows the same sequence of steps used to derive LMIs (6.2-1) and (6.2-2) and is therefore omitted.

The recommended procedure of analysis is as follows:

Given the system (6.1-1), and the nominal (unperturbed) feedback gains *K* and *L*,

1. Choose the desired controller and observer eigenvalue regions (*a, b, c, d* values) shown in Figure 6.1-1.

2. Solve LMIs (6.2-1)-(6.2-4) for M_0, M_1, N_0 and N_1 for maximum bound condition.

3. Use maximum bound M_0, M_1, N_0 and N_1, and based on the known gain K, L and their perturbation, determine whether the system performance is in the desired region.

6.3 Simulation Studies

This section contains simulation results of the controller designs proposed in this work. An unstable second order system is chosen to demonstrate possible application of the proposed methodology.

$$\begin{aligned}\begin{bmatrix}\dot{x}_1\\ \dot{x}_2\end{bmatrix}&=\begin{bmatrix}-0.2 & 2\\ -1 & 0.5\end{bmatrix}\begin{bmatrix}x_1\\ x_2\end{bmatrix}+\begin{bmatrix}0.5\\ 0.5\end{bmatrix}u\\ y&=\begin{bmatrix}0.5 & 0.5\end{bmatrix}\begin{bmatrix}x_1\\ x_2\end{bmatrix}\end{aligned}\tag{6.3-1}$$

The eigenvalues of the open loop system are $0.15 \pm 1.37i$, the state variables of the open loop system diverge fast.

We consider a special case and let $M_0 = I,\ M_1 = \delta_K I$ and $N_0 = I,\ N_1 = \delta_L I$ to obtain maximum δ_K and δ_L values from the LMIs.

We follow the process described previously for this example. Controller and observer gains $K = \begin{bmatrix}-1.13 & -3.87\end{bmatrix}$ and $L = \begin{bmatrix}-77.64\\ 136.24\end{bmatrix}$ are used to place the controller poles on the x-axis at -1, -1.2 and observer poles at -14, -15.

The closed loop system parameter matrices are

$$A_c = A + BK = \begin{bmatrix}-0.76 & 0.065\\ -1.56 & -1.43\end{bmatrix},\quad A_o = A - LC = \begin{bmatrix}38.62 & 40.82\\ -69.12 & -67.62\end{bmatrix}\tag{6.3-2}$$

For this example, in the case of perturbations, we want the controller eigenvalues to stay in the strip region between -2 and -0.2 and the observer eigenvalues to stay in the strip region between -12 and -17.

For the controller region described in step 3, LMIs (6.2-1) and (6.2-2) are solved for the maximum δ_K .

The perturbation bound, δ_K , is found as the smaller value of the maximum δ_K values found with LMIs (6.2-1) and (6.2-2) resulting for the right and left boundaries of the controller region. For controller eigenvalues located in the strip between -0.2 and -1.2, the maximum δ_K from the LMI analysis is found to be **0.29**.

A similar process is used to solve for the maximum value of δ_L that results from the solution of LMIs (6.2-3) and (6.2-4) for the observer eigenvalue region. For the observer eigenvalues are in the region between -12 and -17, $\boldsymbol{\delta_L = 0.23}$.

For system (6.3-1), the maximum controller and observer gain perturbations can be determined by finding maximum δ_K and δ_L for which the eigenvalues of $A+B\tilde{K}$ and $A-\tilde{L}C$ remain within the specified region to compare with the theoretical value. By defining $\tilde{K} = K + [\delta_c \cos\theta \quad \delta_c \sin\theta]$ where $\delta_c = \sqrt{\Delta_K \Delta_K{}^T} = \sqrt{\delta_K}$ and similarly for L, and sweeping θ through 360°, the maximum values for δ_K and δ_L can be found by incrementing δ_K and δ_L until the eigenvalues of $A+B\tilde{K}$ and $A-\tilde{L}C$ exit the specified regions.

The results for $\delta_c{}^2$ and $\delta_o{}^2$ (δ_K and δ_L) values are shown in Figure 6.3-1 (a) and (b) for the controller and observer gain tolerances, respectively. Both figures show that the maximum perturbation is highly direction dependent.

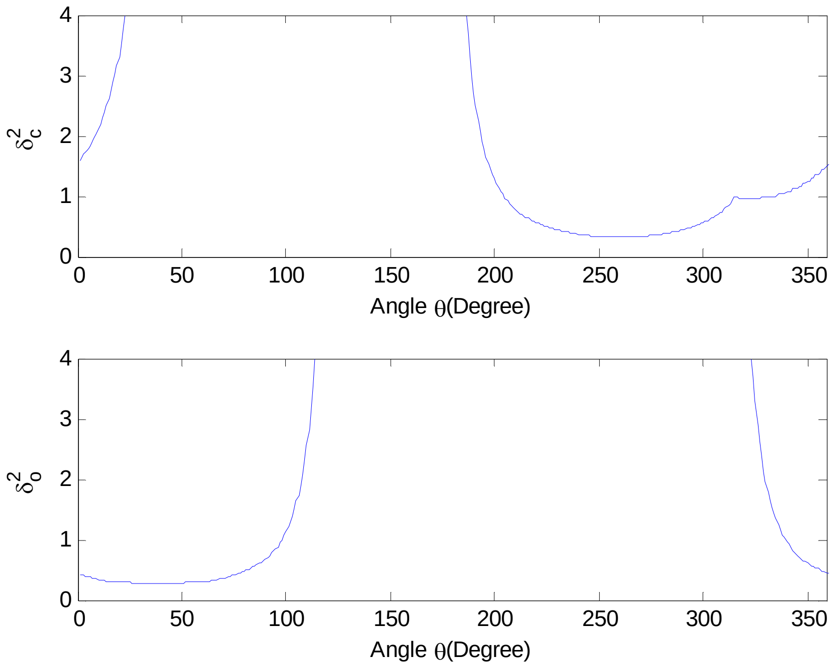

Figure 6.3-1 Perturbation allowed on each direction for (a) K and (b) L

As shown in Figure 6.3-1, the minimum of the maximum allowable values for $\delta_K = 0.315@260^\circ$ and $\delta_L = 0.255@45^\circ$ as determined from closed loop system simulation. These bounds from simulation are very close the bounds found using the LMIs, where $\delta_K = 0.29, \quad \delta_L = 0.23$.

Notice that the perturbation tolerance in some of the directions can be very large. For instance, in Figure 6.3-1(a), large perturbation can be added in the directions from about 50º to 180º for K and the systems performance is still achieved. Similarly, in Figure 6.3-1 (b), for the case of L, large perturbation can be added in the directions from about 110º to 330º.

To test the resilience property of the controlled system, we perturb K and L in their minimum perturbation tolerance directions, 260º and 45º, respectively. We apply the perturbed gains to control the system to validate the effectiveness of the resilient dynamic feedback controller, and moreover, to test if the controller and observer eigenvalues remain in the desired regions.

The minimum of the maximum allowable perturbed controller and observer gains are obtained by adding $\Delta K_{pLMI} = 0.29\angle 260^o$ and $\Delta L_{pLMI} = 0.23\angle 45^o$ to the unperturbed K and L gains used to originally place the eigenvalues of the closed loop system. Another set of perturbed gains $\Delta K_{psim} = 0.315\angle 260^o$ and $\Delta L_{psim} = 0.255\angle 45^o$ based on simulation result bounds in Figure 6.3-1 are also plotted. A third set of perturbed gains $\Delta K_{pe} = 0.8\angle 260^o$ and $\Delta L_{pe} = 0.6\angle 45^o$ are chosen, where ΔK_{pe} and ΔL_{pe} exceeds the allowable perturbation bounds.

In addition to the unperturbed gain case, the co-plots of the states of the controlled system using three sets of perturb gains are shown in Figure 6.3-2. The state variables converge to zero for all four controllers. The general shape of the response is the same for both sets of perturbed gains, however, the settling time are different for different cases, as expected.

The controller eigenvalue positions for all cases are shown in Figure 6.3-3 and the observer eigenvalue positions are shown in Figure 6.3-4. And Figure 6.3-5 gives a whole picture of all eigenvalue positions. We can tell that eigenvalues stay in the desire regions for all cases except for case (d).

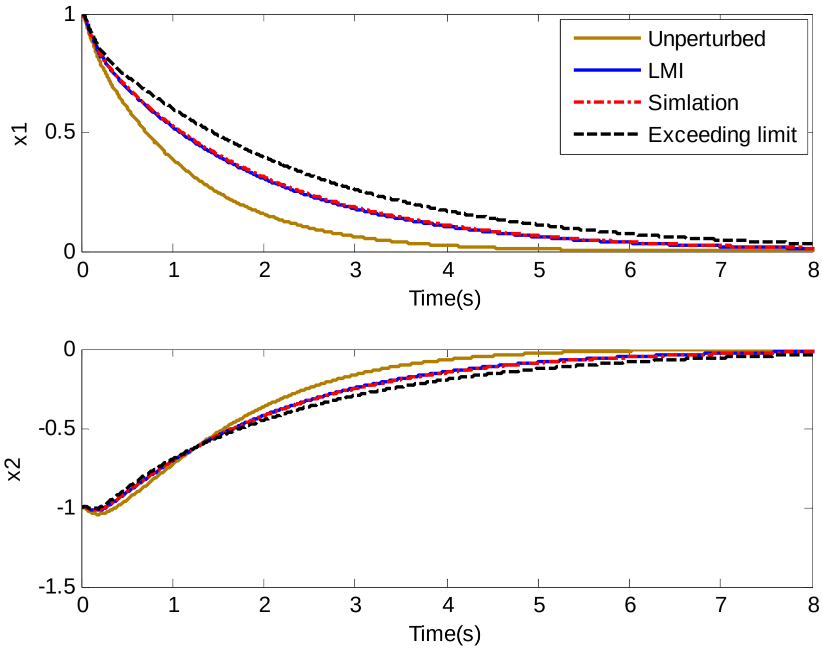

Figure 6.3-2 Co-plots of the state variables in four cases, (a) No perturbation, (b) LMI result, (c) Simulation result (d) Exceeding limit

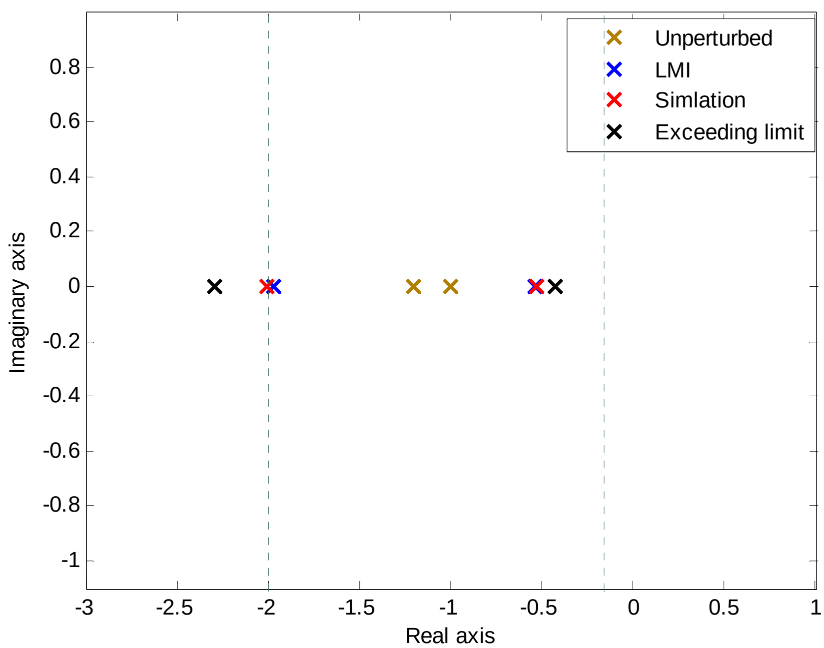

Figure 6.3-3 Controller eigenvalue positions of all four cases

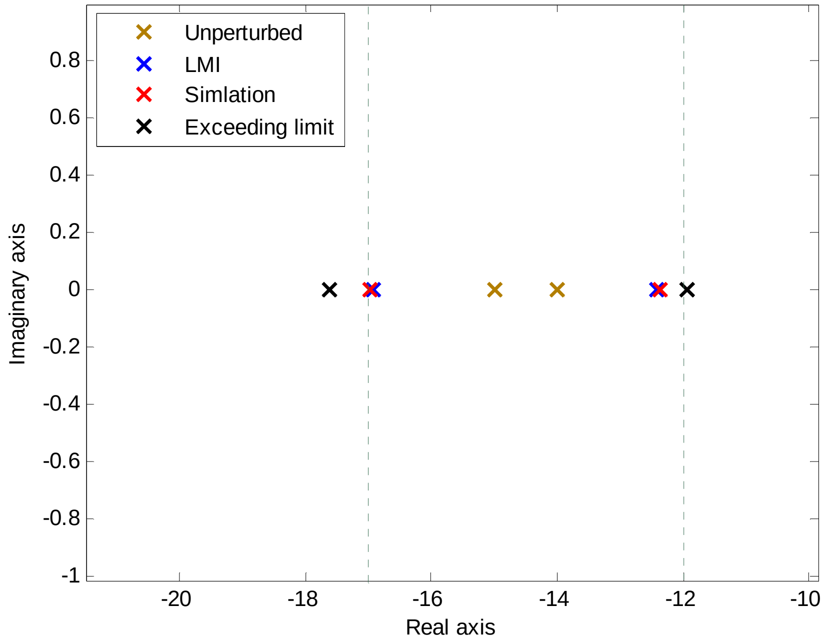

Figure 6.3-4 Observer eigenvalue positions of all four cases

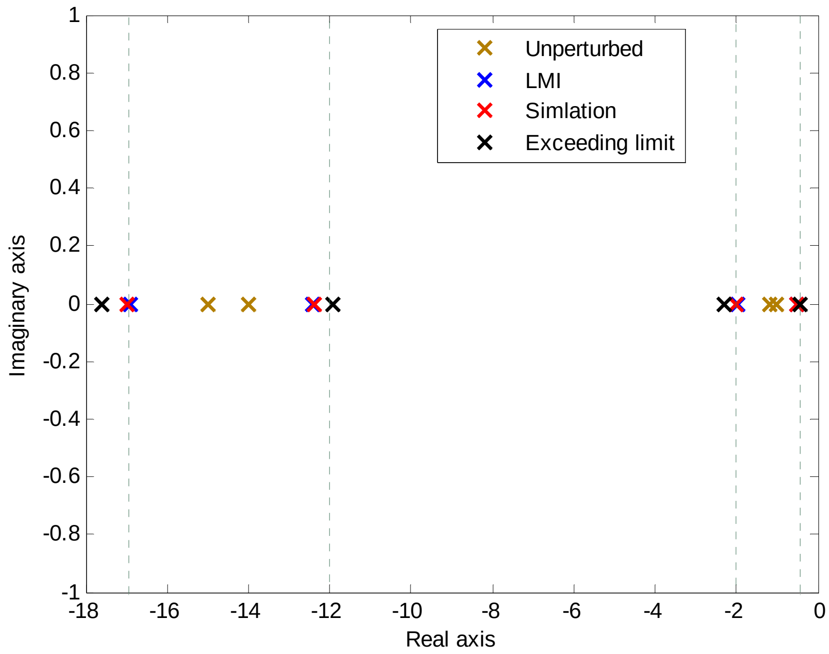

Figure 6.3-5 Controller and observer eigenvalue positions of all four cases

6.4 Conclusion

In this chapter, performance analysis procedures for a resilient full-order dynamic feedback controller have been presented for continuous-time linear systems. By defining controller and observer gain regions, perturbation bounds allowed in both controller and observer gains are found. With this method, designers can evaluate the resilience degree of their dynamic controllers based on the design parameters chosen and adjust design parameters to fit appropriate design requirements. LMI techniques are used throughout the process.

CHAPTER 7

ANALYSIS OF PERFORMANCE RESILIENCE OF DYNAMIC FEEDBACK CONTROLLERS FOR DISCRETE-TIME SYSTEMS

7.0 Introduction

In this chapter, a procedure is presented for performance analysis intended to evaluate the resilience of discrete-time systems controlled by full-order dynamic feedback compensators. Acceptable performance is specified by disks in the complex plane within which the eigenvalues of the controller and the observer remain in the presence of perturbations in the controller and observer gains. Maximum gain perturbation bounds can be obtained based on the designer's choices of controller and observer eigenvalue regions. The linear matrix inequality technique is used throughout the analysis process. Illustrative examples are included to demonstrate the effectiveness of the proposed methodology.

The work of this chapter is an extension of Chapter 5, where the performance resilient analysis is extended to a dynamic (state estimate) feedback controller with perturbations can be allowed in both controller and observer gains. And it is the discrete-time counterpart of Chapter 6. In section 7.1, the system model and problem formulation are introduced. The solution of the analysis problem is derived in Section 7.2. Some illustrative simulation studies and example discussion are presented in Section 7.3. Conclusions are given in Section 7.4.

7.1 Problem Formulation

Let us consider a discrete-time linear system,

$$x_{k+1} = Ax_k + Bu_k \tag{7.1-1}$$

$$y_k = Cx_k + Du_k \tag{7.1-2}$$

where $x_k \in R^n$ is the state, $u_k \in R^m$ is the input and $y_k \in R^p$ is the measured output.

A linear state estimate feedback control is used in this system

$$u_k = \tilde{K}\hat{x}_k \tag{7.1-3}$$

where the feedback gain is perturbed as $\tilde{K} = K + \Delta_K$, and $\hat{x}_k$ is the state estimate.

We use a Luenberger (identity) observer

$$\hat{x}_{k+1} = A\hat{x}_k + Bu_k + \tilde{L}(y_k - C\hat{x}_k - Du_k) \tag{7.1-4}$$

where the observer gain is also perturbed as $\tilde{L} = L + \Delta_L$.

For error of the state estimation defined as,

$$e_k = x_k - \hat{x}_k \tag{7.1-5}$$

we obtain the error update equation by subtracting (7.1-4) from (7.1-1) as

$$e_{k+1} = [A - (L + \Delta_L)C]e_k \tag{7.1-6}$$

We assume that the perturbations on both the feedback and observer gains are bounded as,

$$\Delta_K M_0 \Delta_K{}^T < M_1, \quad \Delta_L{}^T N_0 \Delta_L < N_1 \tag{7.1-7}$$

By introducing an augmented state variable $X_k = \begin{bmatrix} x_k \\ e_k \end{bmatrix}$, the dynamics of the closed loop system are

$$
\begin{aligned}
X_{k+1} &= \begin{bmatrix} x_{k+1} \\ e_{k+1} \end{bmatrix} = \begin{bmatrix} A+B(K+\Delta_K) & -B(K+\Delta_K) \\ 0 & A-(L+\Delta_L)C \end{bmatrix} \begin{bmatrix} x_k \\ e_k \end{bmatrix} \\
&= \begin{bmatrix} A+BK & -BK \\ 0 & A-LC \end{bmatrix} \begin{bmatrix} x_k \\ e_k \end{bmatrix} + \begin{bmatrix} B\Delta_K & -B\Delta_K \\ 0 & -\Delta_L C \end{bmatrix} \begin{bmatrix} x_k \\ e_k \end{bmatrix} \\
&= (\mathbb{A}+\Delta) X_k
\end{aligned}
\tag{7.1-8}
$$

As stated in the introduction, our goal is to analyze the dynamic feedback design to determine how large the perturbation bounds can be so that the performance of the system with perturbed controller and observer gains remains acceptable. We will identify acceptable dynamic feedback controller performance in terms of regions in the complex plane within which the eigenvalues of the perturbed controller and observer must remain. As shown in Figure 7.1-1, the eigenvalues of the closed loop system $x_{k+1} = [A + B(K + \Delta_K)]x_k$ will lie in the circular region of radius r_c centered on the real axis at a_c. Similarly, the eigenvalues of $e_{k+1} = [A - (L + \Delta_L)C]e_k$ will remain within the region of radius r_o centered on the real axis at a_o.

The resilience analysis is based on a Lyapunov energy approach using functions $V_{x_k} = x_k^T P_c x_k$ and $V_{e_k} = e_k^T P_o e_k$ such that

$$
V_{x_k} - V_{x_{k+1}} > 0, \quad V_{e_k} - V_{e_{k+1}} > 0 \tag{7.1-9}
$$

based on the decoupled nature of the state and observer dynamics in (7.1-8).

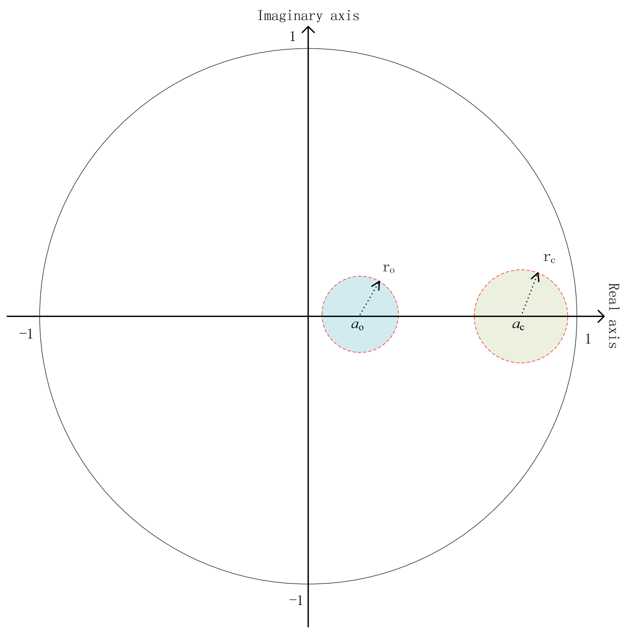

Figure 7.1-1 Desired controller and observer eigenvalues region

7.2 Main Results

Theorem 7-1. Discrete-time dynamic feedback controller design will have resilient properties in the sense of maintaining the controller and observer eigenvalues within the regions shown in Figure 7.1-1 for perturbed feedback gain (7.1-3) and perturbed observer gain (7.1-4) for the system described by (7.1-8), if the following LMIs are feasible for some positive definite matrices M_0, M_1 N_0, N_1, P_c and P_o.

$$\begin{bmatrix} r_c^2 P_c - M_1 & (A+BK-a_c I)^T P_c & 0 \\ P_c(A+BK-a_c I) & P_c & P_c B \\ 0 & B^T P_c & M_0 \end{bmatrix} > 0 \tag{7.2-1}$$

$$\begin{bmatrix} r_o^2 P_o - N_1 & (A+BK-a_o I)^T P_o & 0 \\ P_o(A+BK-a_o I) & P_o & P_o C^T \\ 0 & CP_o & N_0 \end{bmatrix} > 0 \tag{7.2-2}$$

Comment: In LMI (7.2-1) and (7.2-2) system parameters A, B, K, and bound parameters a_c, r_c, a_o, r_o are all known. The unknowns are M_0, M_1 N_0, N_1, P_c and P_o. Note that all unknowns are in linear form in the above LMI.

Proof of Theorem 7-1 is given in the following sections.

7.2.1 Controller Eigenvalue Conditions

It is desired to have the controller eigenvalues inside a disk region with center a_c and radius r_c in Figure 7.1-1 in the presence of perturbations on the control gain K. In the following, the covariance form of the Lyapunov equation will be used.

From (7.1-8) and (7.1-9), and considering a circular region description, we have

$$r_c^2 P_c - (A + B\tilde{K} - a_c I)^T P_c (A + B\tilde{K} - a_c I) > 0 \tag{7.2-3}$$

Inequality (7.2-3) defines a circle centered at coordinate (a_c, 0) with a radius less than r_c.

Applying Lemma 1 to (7.2-3) and moving terms with Δ_K to the right hand side of the inequality we have

$$\begin{bmatrix} r_c^2 P_c & (A + BK - a_c I)^T P_c \\ P_c (A + BK - a_c I) & P_c \end{bmatrix} > \begin{bmatrix} 0 & -\Delta_K{}^T B^T P_c \\ -P_c B \Delta_K & 0 \end{bmatrix} \tag{7.2-4}$$

An upper bound for the right hand side of (7.2-4) is found using lemma 2 as follows:

$$\begin{bmatrix} 0 & -\Delta_K{}^T B^T P_c \\ -P_c B \Delta_K & 0 \end{bmatrix}$$
$$= \begin{bmatrix} -\Delta_K{}^T \\ 0 \end{bmatrix} \begin{bmatrix} 0 & B^T P_c \end{bmatrix} + \begin{bmatrix} 0 \\ P_c B \end{bmatrix} \begin{bmatrix} -\Delta_K & 0 \end{bmatrix} \tag{7.2-5}$$
$$\leq \begin{bmatrix} \Delta_K M_0 \Delta_K{}^T & 0 \\ 0 & 0 \end{bmatrix} + \begin{bmatrix} 0 \\ P_c B \end{bmatrix} M_0{}^{-1} \begin{bmatrix} 0 & B^T P_c \end{bmatrix}$$

By requiring the left hand side of (7.2-4) to be greater than the right hand side of (7.2-5), then (7.2-4) will be satisfied. Making this requirement and using condition (7.1-7), we obtain

$$\begin{bmatrix} r_c{}^2 P_c - M_1 & (A + BK - a_c I)^T P_c \\ P_c (A + BK - a_c I) & P_c \end{bmatrix} - \begin{bmatrix} 0 \\ P_c B \end{bmatrix} M_0{}^{-1} \begin{bmatrix} 0 & B^T P_c \end{bmatrix} > 0 \tag{7.2-6}$$

Applying Lemma 1 to (7.2-6), we have (7.2-1).

7.2.2 Observer Eigenvalue Conditions

It is desired that the eigenvalues of the observer remain within the disk with center at (a_o,0) and radius r_o, even in the presence of perturbations on the observer gain, L.

For the observer bound, we start from

$$r_o{}^2 P_o - (A - \tilde{L}C - a_o I) P_o (A - \tilde{L}C - a_o I)^T > 0 \tag{7.2-7}$$

The process to derive LMI (7.2-2) which results for the observer boundary follows the same sequence of steps used to derive LMI (7.2-1) and is therefore omitted.

7.3 Simulation Studies

This section contains simulation results of the controller design proposed in this work. An unstable second order system with a sampling period T=0.01s is chosen to demonstrate the application of the proposed methodology and is given below as,

$$\begin{bmatrix} x_1 \\ x_2 \end{bmatrix}_{k+1} = \begin{bmatrix} 0.998 & 0.02 \\ -0.01 & 1.005 \end{bmatrix} \begin{bmatrix} x_1 \\ x_2 \end{bmatrix}_k + \begin{bmatrix} 0.01 \\ 0.005 \end{bmatrix} u_k$$
$$y_k = \begin{bmatrix} 0.1 & 0.1 \end{bmatrix} \begin{bmatrix} x_1 \\ x_2 \end{bmatrix}_k \tag{7.3-1}$$

A plot of the state variables for the open loop system is given in Figure 7.3-1, showing the strong divergence of the open loop system. The initial conditions of the states are chosen to be [1; -1].

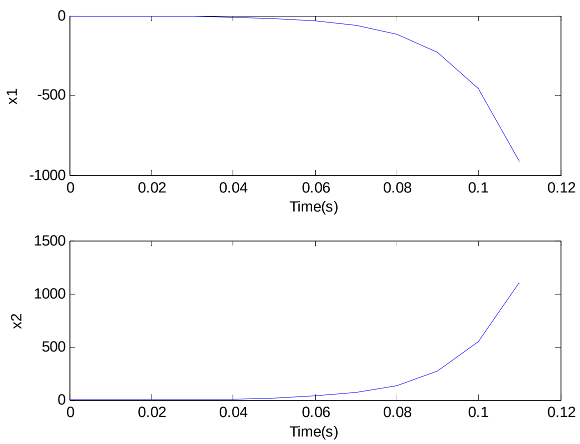

Figure 7.3-1 State variables of the open loop system

We follow the process described previously for this example. Controller and observer gains $K = \begin{bmatrix} -4.03 & 2.2 \end{bmatrix}$ and $L = \begin{bmatrix} -178.38 \\ 195.11 \end{bmatrix}$ are used to place the controller poles on the *x*-axis at 0.9 and 0.92 and the observer poles at 0.18 and 0.15.

For this example, in the case of perturbations, we want the controller eigenvalues to stay in the disk region with center at a_c=0.85 and radius r_c=0.12, and the observer eigenvalues to stay in the disk region with center at a_o=0.16 and radius r_o=0.1.

For the controller region described, LMI (7.2-1) is solved for the maximum δ_K. The controller eigenvalues will remain in the disk region centered at a_c=0.85 and radius r_c=0.12, if the controller gain perturbation is bounded by $\delta_K = 0.25$.

A similar process is used to solve for the maximum value of δ_L that results from the solution of LMI (7.2-2) for the observer eigenvalue region. For the observer disk region centered at center at a_o=0.16 and radius r_o=0.1, the maximum $\delta_L = 0.006$.

For the system (7.3-1), the maximum controller and observer gain perturbations can be determined by finding max δ_K and δ_L for which the eigenvalues of $A + B\tilde{K}$ and $A - \tilde{L}C$ remain within the specified region to compare with the theoretical value. By defining $\tilde{K} = K + [\delta_c \cos\theta \quad \delta_c \sin\theta]$ where $\delta_c = \sqrt{\Delta_K \Delta_K{}^T} = \sqrt{\delta_K}$ and similarly for L, and sweeping θ through 360°, the maximum values for δ_K and δ_L can be found by incrementing δ_K and δ_L until the eigenvalues of $A + B\tilde{K}$ and $A - \tilde{L}C$ exit the specified regions.

The values for δ_c^2 and δ_o^2 (δ_K and δ_L) are calculated based on the requirements above and shown in Figure 7.3-2 (a) and (b). These figures also show that the maximum perturbation is highly direction dependent.

As shown in Figure 7.3-2, the minimum of the maximum allowable values for $\delta_K = 0.267@50^\circ$ and $\delta_L = 0.0066@45^\circ$ as determined from closed loop system simulation with various gain perturbations can be compared to $\delta_K = 0.25$ and $\delta_L = 0.006$ from our analysis LMIs.

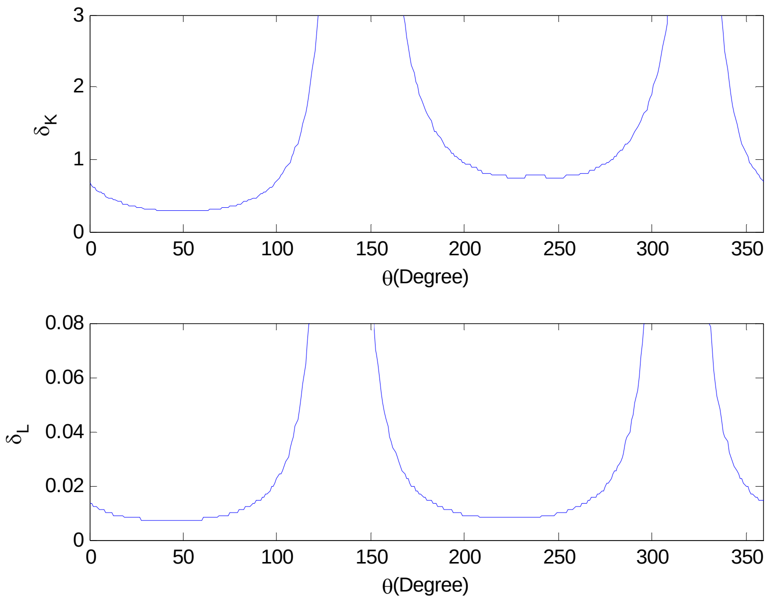

Figure 7.3-2 Perturbation allowed in each direction for (a) K and (b) L

Notice that the perturbation tolerance in some of the directions can be very large. For instance, in Figure 7.3-2 (a), large perturbation can be added to K in the directions from about 130º to 170º and 305º to 335º and the system performance is still achieved. And in Figure 7.3-2 (b), for the case of L, large perturbation can be added to L at around 120º -150º and 300º -330º.

To test the resilience property of the controlled system, we perturb K and L in their minimum perturbation tolerance directions, 50º and 45º, respectively. We apply the perturbed gains to control the system to validate the effectiveness of the resilient dynamic feedback controller, and moreover, to test if the controller and observer eigenvalues remain in the desired regions.

The minimum of the maximum allowable perturbed controller and observer gains are obtained by adding $\Delta K_{pLMI} = 0.25\angle 50^o$ and $\Delta L_{pLMI} = 0.006\angle 45^o$ to the unperturbed K and L gains used to originally place the eigenvalues of the closed loop system. Another set of perturbed gains $\Delta K_{psim} = 0.267\angle 50^o$ and $\Delta L_{psim} = 0.0066\angle 45^o$ based on simulation result bounds in Figure 7.3-2 are also plotted. A third set of perturbed gains $\Delta K_{pe} = 0.8\angle 50^o$ and $\Delta L_{pe} = 0.6\angle 45^o$ are chosen, where ΔK_{pe} and ΔL_{pe} exceeds the allowable perturbation bounds.

In addition to the unperturbed gain case, the co-plots of the states of the controlled system using three sets of perturb gains are shown in Figure 7.3-3. The state variables converge to zero for all four controllers. The general shape of the response is the same for both sets of perturbed gains, however, the settling time are different for different cases, as expected.

The controller eigenvalue positions for all cases are shown in Figure 7.3-4 and the observer eigenvalue positions are shown in Figure 7.3-5. And Figure 7.3-6 gives a whole picture of all eigenvalue positions. We can tell that eigenvalues stay in the desire regions for all cases except for case (d).

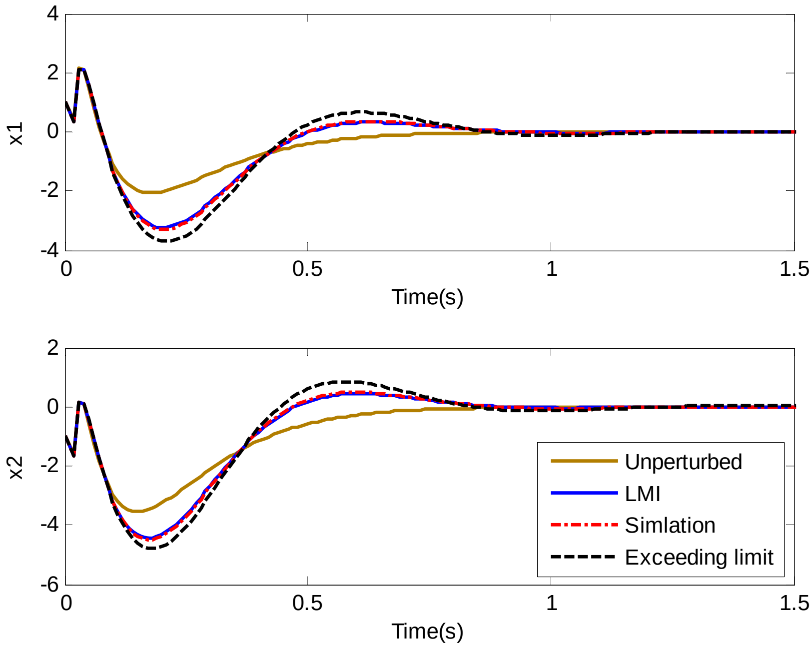

Figure 7.3-3 Co-plots of the state variables in four cases, (a) No perturbation, (b) LMI result, (c) Simulation result (d) Exceeding limit

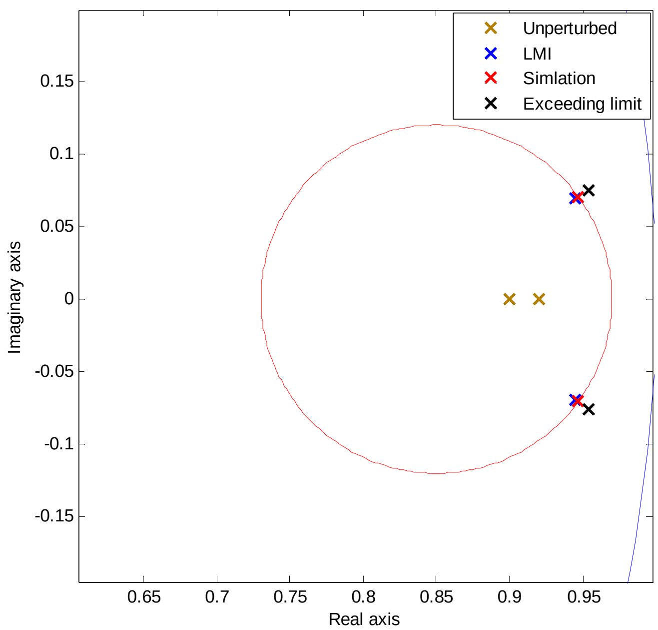

Figure 7.3-4 Controller eigenvalue positions of all four cases

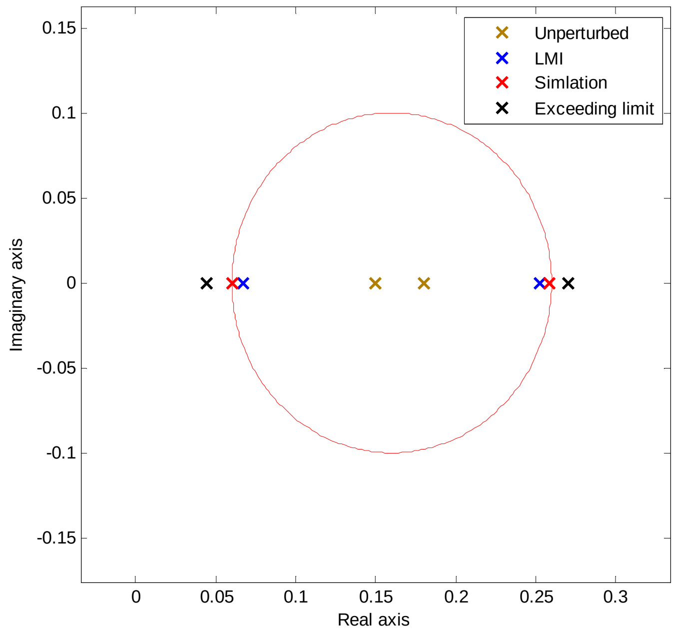

Figure 7.3-5 Observer eigenvalue positions of all four cases

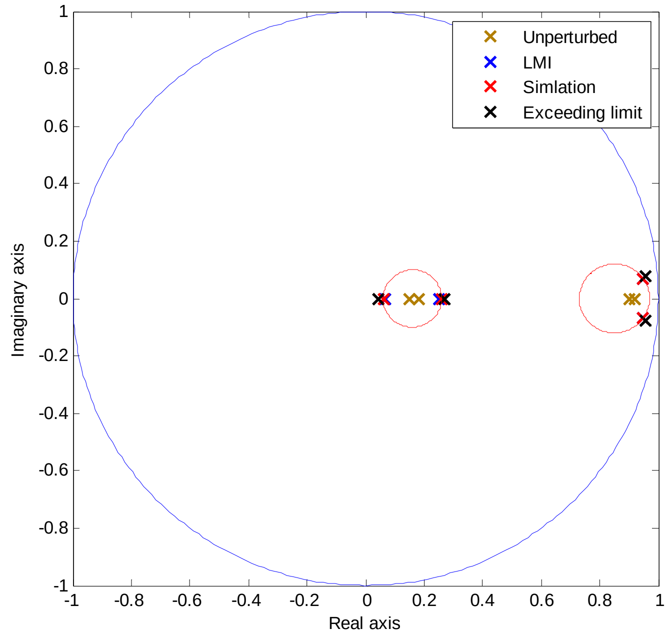

Figure 7.3-6 Controller and observer eigenvalue positions of all four cases

7.4 Conclusion

In this chapter, a performance analysis procedure for a resilient full-order dynamic feedback controller has been presented for discrete-time linear systems. By defining controller and observer gain regions, perturbation bounds allowed in both controller and observer gains are found. With this method, designers can evaluate the resilience degree of their dynamic controllers based on the design parameters chosen and adjust design parameters to fit appropriate design requirements. LMI techniques are used throughout the process.

CHAPTER 8

CONCLUSION AND FUTURE WORK

8.1 Summary

This dissertation has addressed the problems of robust and resilient control design for general performance criteria and performance analysis for uncertain systems with finite energy disturbances. LMI techniques are used throughout the design and analysis process. Simulation examples are illustrated showing the effectiveness of the proposed topics.

In Chapter 2, a robust and resilient state feedback controller design has been presented for a class of uncertain nonlinearities for general performance criteria. Uncertainties are allowed in both the center and the radius of the cone in which the nonlinearity resides as well as the feedback gain. In Chapter 3, a similar robust and resilient state feedback controller design problems in discrete-time has been presented. We have shown that a common framework for various performance criteria using linear matrix inequality techniques can be developed to solve the proposed controller design problem.

In Chapter 4 and Chapter 5, performance analysis procedures for a resilient state feedback controller have been presented for continuous-time and discrete-time linear systems. By defining controller eigenvalue regions, multiplicative and additive perturbation bounds allowed in controller gains are found. With this method, designers can evaluate the resilience degree of their controllers based on the design parameters chosen and adjust design parameters to fit appropriate design requirements.

In Chapter 6, a performance analysis procedure for a resilient full-order dynamic feedback controller has been presented for continuous-time linear systems. By defining controller and observer gain regions, perturbation bounds allowed in both controller and observer gains are found. With this method, designers can evaluate the resilience degree of their dynamic controllers based on the design parameters chosen and adjust design parameters to fit appropriate design requirements. Chapter 7 is the discrete-time counterpart of Chapter 6.

Most of the work above are presented or published in [35]-[43].

8.2 Future Work

For Chapter 2-3, the design can be extended to stochastic perturbations on the gain. Further analysis on the effect of the matrix perturbations bound versus scalar perturbations bound can be discussed. Multiplicative perturbations on the parameters should also be interesting.

For Chapter 4-7, the analysis methods can be extended to stochastic perturbations on the gain. Certain classes of nonlinear systems and systems with finite energy disturbances for general performance criteria can be considered. More complicated eigenvalue regions in the complex plane can be discussed associated with different system performance can also be discussed.

BIBLIOGRAPHY

[1] H.K. Khalil, Nonlinear Systems, 3rd. ed., Prentice Hall, 2001.

[2] G. C. Goodwin and K. S. Sin, "Adaptive Filtering Prediction and Control", Prentice-Hall, Englewood cliffs, NJ, 1984.

[3] K. Zhou and J. C. Doyle, "Essentials of Robust Control", Prentice-Hall, Englewood cliffs, NJ, 1997.

[4] A. Megretsky, *Power distribution approach in robust control*. Tech. Rep. TRITA / MAT – 92 –0027, Dept. of Math, Royal Inst. of Tech., S – 10044, Stokholm, Sweden, 1992.

[5] V. A. Yakubovich, *Nonconvex optimization problem: the infinite horizon linear quadratic control problem with quadratic constraints*. Syst. Contr. Lett.s, vol. 19, pp. 13 –22,1992.

[6] A. V. Savkin, and I. R. Petersen. Structured dissipativeness and absolute stability of nonlinear systems. Int. J. Contr., vol. 62, pp. 443 – 460, 1995.

[7] A. V. Savkin, and I. R. Petersen, *Robust state estimation for uncertain systems with averaged integral quadratic constraints*. Int. J. Contr., vol. 64, pp. 923 – 939, 1996.

[8] M. R. James, and I. R. Petersen, *Nonlinear state estimation for uncertain systems with an integral constraint*. Proceedings of Conference on Decision and Control, pp. 560 – 561, 1996.

[9] Karafyllis, I., Z. Jiang, "Control Lyapunov functionals and robust stabilization of nonlinear time-delay systems," IEEE Conference on Decision and Control, 2007, pp. 5312 - 5317.

[10] Y. Wei and Y. Lai, "Robust H_∞ guaranteed cost control for a class of nonlinear 2-D time delay discrete systems," Proc. of the International Conference on Computer and Automation Engineering, 2010, vol. 3, pp 39-53.

[11] L. Li, J. Zhao and G.M. Dimirovski, "Robust H_∞ control for a class of uncertain switched nonlinear systems using constructive approach," Proc. of the American Control Conference, 2008, pp. 5068 - 5073.

[12] W. Wang, S. Ma, J. Wang and S. Song, "Robust stability and stabilization for nonlinear uncertain discrete-time descriptor switched systems," Proc. of the Chinese Control and Decision Conference, 2012, pp. 4025-4030.

[13] S. Ye, Y. Zhang, C. A. Rabbath, X. Wang, Y. Li, "An LMI approach to mixed $H1/H_\infty$ robust fault-tolerant control design with uncertainties," Proc. of the American Control Conference, 2009, pp. 5540 - 5545.

[14] Y. Li, D. Yang, “Robust H_∞ control for a class of nonlinear singular system with uncertain parameters”, Journal of Systems Engineering and Electronics, 2009, vol. 20, issue 1, pp 136-140.

[15] X. Fu, X. Liu, M. Hou and Y. Li, “Robust non-fragile control for non-linear singular discrete systems with time-delay,” World Congress on Intelligent Control and Automation, 2012, pp. 1139-1143.

[16] Z. Yin, Q. Wu, X. Chang, S. Lun “H∞ robust fault tolerant control for a class of nonlinear systems with uncertainties and time-varying delays”, Proc. of the Chinese Control and Decision Conference, 2010, pp 2223-2228.

[17] H. Zhang, Q. Fang, X. Wang, Y. Li, C. Wu, “Non-fragile guaranteed-cost robust H_∞ control for a class of nonlinear networked control systems with long time-delay”, Proc. of the International Conference on Intelligent Computation Technology and Automation, 2010, vol.2 ,pp 784-787.

[18] Y. Zheng, G. M. Dimirocski, Y. Jing and M. Yang, “Discrete-time sliding mode control of nonlinear systems,” American Control Conference, 2007, pp. 3825-3830.

[19] M. ElBsat and E. E. Yaz, “Mixed criteria control design with finite-time boundedness and H_∞ property for a class of discrete-time nonlinear systems”, Proc. of 50th IEEE Conference on Decision and Control and European Control Conference, 2011, pp. 3520 - 3525.

[20] X. Wang, E. E. Yaz, S. Schneider and Y. I. Yaz, “H_2/H_∞ control of discrete-time nonlinear systems using the SDRE approach,” Proc. of the 4th Annual Dynamic Systems and Control Conference, 2011, DSCC2011-5935, 8 pp.

[21] L. H. Keel and S. P. Bhattacharyya, “Robust, fragile, or optimal?” IEEE Trans. on Automat. Control, vol. 42, 1997, pp. 1098–1105.

[22] P. Dorato, “Non-fragile controller design: An overview”, Proc. of American Control Conference, Philadelphia, PA, 1998, vol.5, pp. 2829–2831.

[23] M. M. Haddad and J. R. Corrado, “Robust resilient dynamic controllers for systems with parametric uncertainty and controller gain variations”, Proc. of American Control Conference, Philadelphia, PA, 1998, vol.5, pp. 2837–2841.

[24] A. Jadbabaie, C. T. Abdallah, D. Famularo, and P. Dorato. “Robust, non-fragile and optimal controller design via linear matrix inequalities”, Proc. of American Control Conference, Philadelphia, PA, 1998, vol.5, pp. 2842–2846.

[25] D. Peaucelle, D. Arzelier and C. Farges “LMI results for Resilient state-feedback with H_∞ performance”, in IEEE Conference on Decision and Control, Nassau, Bahamas, 2004, Vol.1, pp. 400 – 405.

[26] E.E. Yaz, C. S. Jeong, Y. I. Yaz and A. Bahakeem, "Resilient design of discrete-time observers with general criteria using LMIs", Journal of Mathematical and Computer Modeling, vol.42, 2005, pp. 931-938.

[27] E. E. Yaz, C. S. Jeong, and Y. I. Yaz, “An LMI approach to discrete-time observer design with stochastic resilience”, Journal of Mathematical and Computer Modeling, vol. 188, 2006, pp. 246–255.

[28] C. G. Rieger, K. L. Moore and T. L. Baldwin, “Resilient control systems: A multi-agent dynamic systems perspective”, IEEE Intl. Conf. on Electro/Information Technology, Rapid City, SD, 2013, pp. 1–16.

[29] H. Zhang, Q. Fang, X. Wang, Y. Li, C. Wu, “Non-fragile guaranteed-cost robust H_∞ control for a class of nonlinear networked control systems with long time-delay”, Proc. of the Int. Conference on Intelligent Computation Technology and Automation, Changsha, China, 2010, vol.2 , pp. 784–787.

[30] C. G. Rieger, “Notional examples and benchmark aspects of a resilient control system”, 3rd Intl. Symposium on Resilient Control Systems, Idaho Falls, ID, 2010, pp. 64–71.

[31] X. Jin, A. Ray and R. M. Edwards, “Integrated robust and resilient control of nuclear power plants for operational safety and high performance”, IEEE Transactions on Nuclear Science, 2010, vol. 57 , issue 2, pp. 807–817.

[32] Y. Hu, J. Li, and L. E. Holloway, “Resilient control for serial manufacturing networks with advance notice of disruptions”, IEEE Transactions on Systems, Man, and Cybernetics: Systems, 2013, vol. 43 , issue 1, pp. 98–114.

[33] M. N. ElBsat, “Finite-time control and estimation of nonlinear systems with disturbance attenuation”, doctoral dissertation, Marquette Univ., Milwaukee, WI, 2012.

[34] S. Boyd, L. ElGhaoui, E. Feron, and V. Balakrishnan, “Linear Matrix Inequalities In System and Control Theory”, SIAM Studies in Applied Mathematics, SIAM, Philadelphia, 1994.

[35] F. Feng, C.S. Jeong, E.E. Yaz, and Y.I. Yaz, “Discrete time state feedback controller design for conic nonlinear systems with general criteria,” Proc. of IASTED Int. Conf. on Identification, Control and Applications, 2009, pp. 94 – 97.

[36] C. S. Jeong, F. Feng, E. E. Yaz, Y. I. Yaz, “Robust and Resilient Optimal Controller Design for a Class of Nonlinear Systems with General Criteria”, Proceedings of American Control Conference, 2010, pp. 6363 – 6368.

[37] F. Feng, C. S. Jeong, E. E. Yaz, S. C. Schneider and Y. I. Yaz, “Robust controller design with general criteria for uncertain conic nonlinear systems with disturbances”, Proc. of American Control Conference, 2013, pp. 5889-5894.

[38] F. Feng, W. A. Baker, Jr., E. E. Yaz, and S. C. Schneider, “Design of Resilient General Criteria Controllers for Nonlinear Systems with Uncertainties”, Proc. of the IASTED International Conference on Intelligent Systems and Control, 2013, pp. 238-245.

[39] F. Feng, E. E. Yaz, S. C. Schneider and Y. I. Yaz, “Discrete-Time Robust Controller Design for a Class of Nonlinear Systems with Uncertainties”, IEEE Conference on Decision and Control, 2013, pp. 1119-1124.

[40] F. Feng, E. E. Yaz, S. C. Schneider and Y. I. Yaz, “Discrete-Time Resilient Controller Design with General Criteria for A Class of Uncertain Nonlinear Systems”, Proc. of American Control Conference, 2014, pp. 4268 - 4273.

[41] F. Feng, S. C. Schneider and E. E. Yaz, “Performance Analysis of Resilient Dynamic Feedback H2 Controllers for Discrete-time Systems”, Proc. of European Control Conference, Linz, Austria, 2015, pp. 2003-2008.

[42] F. Feng, J. L. Bonniwell, S. C. Schneider and E. E. Yaz, “Performance Analysis of Resilient Dynamic Feedback H2 Controllers”, IEEE Multi-Conference on Systems and Control, Sydney, Australia, 2015, pp. 1404-1409.

[43] F. Feng, S. C. Schneider and E. E. Yaz, “Analysis of Performance Resilience for Discrete-time Systems with Both Multiplicative and Additive Control Gain Perturbations”, Dynamic Systems and Control Conference, 2016, to be published.